TrkB and ERK signaling in the mechanism of NMDA receptor-blocking antidepressants

Iina Annala

University of Helsinki

Faculty of Pharmacy

Division of Pharmacology and Pharmacotherapy

April 2021

HELSINGIN YLIOPISTO
HELSINGFORS UNIVERSITET
UNIVERSITY OF HELSINKI

Tiedekunta – Fakultet – Faculty Faculty of Pharmacy		Koulutusohjelma – Utbildingsprogram – Degree Programme Master of Science in Pharmacy
Tekijä – Författare – Author Annala Iina Maria Josefiina		
Työn nimi – Arbetets titel – Title TrkB and ERK signaling in the mechanism of NMDA receptor-blocking antidepressants		
Oppiaine/Opintosuunta – Läroämne/Studieinriktning – Subject/Study track Pharmacology		
Työn laji – Arbetets art – Level Pro gradu	Aika – Datum – Month and year 04/2021	Sivumäärä – Sidoantal – Number of pages Manuscript: 24; Annex 1: 6, Annex 2: 39

Tiivistelmä – Referat – Abstract

Subanesthetic-dose ketamine, an N-methyl-D-aspartate receptor (NMDAR) blocker, exerts rapid antidepressant effects that sustain long after its elimination from the body. The precise mechanism remains unknown, but regulation of TrkB (tropomyosin receptor kinase B), ERK (extracellular-regulated kinase 1 and 2), GSK3β (glycogen synthase kinase 3β) and mTOR (mammalian target of rapamycin) signaling within the prefrontal cortex (PFC) have been deemed important for its antidepressant-like effects in rodents. In addition, activation of α-amino-3-hydroxy-5-methyl-4-isoxazolepropionic acid receptors (AMPARs) is thought to be an important step in its mechanism. Nitrous oxide (N_2O), another NMDAR antagonist and a putative rapid-acting antidepressant, regulates the same molecular pathways as ketamine in the rodent PFC. The fast pharmacokinetics of N_2O have been exploited to show that markers of neuronal excitation, including phosphorylation of ERK, are upregulated in the PFC during its acute pharmacological effects (NMDAR blockade), while regulation of TrkB, GSK3β and P70S6K emerges only upon N_2O withdrawal. In the first part of this study, we investigated the N_2O-induced biochemical changes associated with neuronal excitation and BDNF-TrkB signaling in the PFC and further, the requirement for AMPAR activation in inducing them. We focused on the effects seen after the acute pharmacological effects of N_2O. N_2O (65% for 20 min) was administered to adult male C57BL/6 mice with or without pretreatment with AMPAR antagonist (NBQX, 10 mg/kg) and PFC samples were collected 15 minutes after stopping N_2O delivery. Within this time N_2O is expected to be completely eliminated. The brain samples were analyzed using western blot, enzyme-linked immunosorbent assay and quantitative reverse transcription PCR. We observed that N_2O increased levels of phosphorylated TrkB, GSK3β and P70S6K, and these effects were not attenuated by NBQX pretreatment. At the same time, we observed a decrease in the levels of phosphorylated ERK, which was attenuated in mice that received NBQX prior to N_2O. Tissue levels of BDNF protein or messenger RNA (exon IV) were not different between control and experimental groups. These results indicate that the mechanism of N_2O is associated with TrkB and ERK signaling that are regulated independently of each other. It appears that AMPAR activation is not required for TrkB signaling, although it might play a role in ERK signaling. Further, N_2O-induced TrkB phosphorylation in the PFC is not associated with changes in total levels of BDNF. In the second part of the study, we aimed to search for new ketamine-like NMDAR blockers with antidepressant potential. Ketamine was used as a query compound for in silico substructure search to find commercial ketamine analogs. The retrieved ketamine analogs were filtered by their computed ADMET properties and then further screened virtually by docking them to the pore region of NMDAR complex (protein data bank code: 4TLM), around the predicted binding site of ketamine. Finally, we sought to study if selected ketamine analogs could elicit ketamine-like effects on TrkB and ERK signaling in mouse primary cortical neurons. However, we did not proceed to test the analogs since ketamine (positive control) did not show any effects on TrkB or ERK phosphorylation in our culture. Overall, this study advances the understanding of the mechanism of N_2O, possibly giving new insight of the antidepressant mechanisms of NMDAR-blocking agents more generally. Additionally, we found promising ketamine analogs that await experimental testing.

Avainsanat – Nyckelord – Keywords
Nitrous oxide, ketamine, NMDA receptor blocker, AMPA receptor, TrkB, ERK, rapid-acting antidepressants

Ohjaaja tai ohjaajat – Handledare – Supervisor or supervisors
Tomi Rantamäki, Henri Xhaard

Säilytyspaikka – Förvaringställe – Where deposited

Helsingin yliopiston kirjasto, Helsingfors universitets bibliotek, Helsinki University Library

Muita tietoja – Övriga uppgifter – Additional information

HELSINGIN YLIOPISTO
HELSINGFORS UNIVERSITET
UNIVERSITY OF HELSINKI

Tiedekunta – Fakultet – Faculty Farmasian tiedekunta		Koulutusohjelma – Utbildingsprogram – Degree Programme Proviisorin koulutusohjelma
Tekijä – Författare – Author Annala Iina Maria Josefiina		
Työn nimi – Arbetets titel – Title TrkB- ja ERK-signalointi NMDA-reseptoria salpaavien masennuslääkkeiden mekanismissa		
Oppiaine/Opintosuunta – Läroämne/Studieinriktning – Subject/Study track Farmakologia		
Työn laji – Arbetets art – Level Pro gradu	Aika – Datum – Month and year 04/2021	Sivumäärä – Sidoantal – Number of pages Käsikirjoitus: 24, Liite 1: 6, Liite 2: 39

Tiivistelmä – Referat – Abstract

Subanesteettinen annos ketamiinia, N-metyyli-D-aspartaatti (NMDA)-reseptorin salpaajaa, lievittää masennuksen oireita nopeasti, ja vaikutus kestää kauan sen elimistöstä poistumisen jälkeen. Vaikka tarkka mekanismi ei ole vielä selvillä, on TrkB (tropomyosiinireseptorikinaasi B), ERK (solunulkoisen signaalin säätelemä kinaasi 1 ja 2), GSK3β (glykogeenisyntaasikinaasi 3β) ja mTOR (engl. mammalian target of rapamycin)-signaloinnin säätely etuaivokuorella yhdistetty ketamiinin masennuslääkkeenkaltaisiin vaikutuksiin jyrsijöillä. Lisäksi α-amino-3-hydroksi-5-metyyli-4-isoksatsolipropionihappo (AMPA)-reseptorien aktivaation ajatellaan olevan tärkeä osa sen mekanismia. Typpioksiduuli (N_2O), joka niin ikään on NMDA-reseptorin antagonisti ja otaksuttu nopeavaikutteinen masennuslääke, säätelee samoja molekulaarisia signalointireittejä jyrsijöiden etuaivokuorella kuin ketamiini. Typpioksiduulin nopeaa farmakokinetiikkaa hyödyntämällä on huomattu, että sen akuuttien farmakologisten vaikutusten (NMDA-reseptorin salpauksen) aikana havaitaan lisääntynyt ERK:n fosforylaatio ja muita hermosolujen eksitaatioon liitettyjä signalointimuutoksia, kun taas TrkB:n, GSK3β:n ja P70S6K:n fosforylaation säätely ilmenee vasta typpioksiduulin eliminaation jälkeen. Tämän tutkimuksen ensimmäisessä osassa tutkimme typpioksiduulin aiheuttamia hermosolujen eksitaatioon ja BDNF-TrkB signalointiin liittyviä biokemiallisia muutoksia etuaivokuorella, ja lisäksi, AMPA-reseptorien aktivaation roolia näiden aikaansaamisessa. Keskityimme muutoksiin, jotka nähdään typpioksiduulin akuuttien farmakologisten vaikutusten jälkeen. Aikuisille C57BL/6-linjan uroshiirille annosteltiin 65% typpioksiduulia 20 minuutin ajan sen jälkeen, kun ne olivat saaneet injektiona joko AMPA-reseptorin salpaajaa (NBQX, 10 mg/kg) tai kontrolliliuosta (fysiologista suolaliuosta). Etuaivokuoren näytteet kerättiin 15 minuuttia typpioksiduulin annon lopettamisen jälkeen, jolloin sen oletetaan eliminoituneen elimistöstä kokonaan. Näytteet analysoitiin käyttäen western blot, ELISA (engl. enzyme-linked immunosorbent assay) ja RT-qPCR (kvantitatiivinen käänteistranskriptaasi PCR) menetelmiä. Havaitsimme, että typpioksiduuli lisäsi TrkB:n, GSK3β:n ja P70S6K:n fosforylaatiotasoja riippumatta siitä, olivatko eläimet saaneet ennen typpioksiduulia NBQX- vai suolaliuos-injektion. Samanaikaisesti ERK:n fosforylaatiossa nähtiin typpioksiduulin annon jälkeen väheneminen, joka oli heikentynyt eläimillä, jotka saivat NBQX:ää ennen typpioksiduulia. BDNF-proteiinin tai sen lähetti-RNA:n (eksoni IV) kudostasoissa ei havaittu muutoksia ryhmien välillä. Tulokset viittaavat siihen, että typpioksiduulin aikaansaama TrkB:n ja ERK:n säätely on toisistaan riippumatonta. AMPA-reseptorin aktivaatio ei näytä vaikuttavan TrkB-signalointiin, vaikka se saattaa säädellä ERK-signalointia. Lisäksi TrkB:n lisääntynyt fosforylaatio typpioksiduulin annon jälkeen tapahtuu ilman, että BDNF:n kudostasot nousevat. Tutkimuksen toisessa osassa tavoitteena oli etsiä ketamiininkaltaisia NMDA-reseptorin salpaajia, joilla on potentiaalisia masennuslääkevaikutuksia. Löytääksemme kaupallisia ketamiinianalogeja, suoritimme tietokoneavusteisesti osarakennehaun ketamiinin rakenteeseen perustuen. Löydetyt ketamiinianalogit suodatettiin niiden laskennallisten ADMET-ominaisuuksien perusteella, jonka jälkeen suoritettiin virtuaalinen seulonta telakoimalla yhdisteet NMDA-reseptorikompleksiin (protein data bank-koodi: 4TLM) ionikanavan alueelle, ketamiinin ennustetun sitoutumispaikan läheisyyteen. Lopuksi pyrimme selvittämään, saavatko valitut ketamiinianalogit aikaan ketamiininkaltaisia vaikutuksia TrkB- ja ERK- signalointiin primaarisessa hermosoluviljelmässä. Emme kuitenkaan edenneet testaamaan ketamiinianalogeja, sillä ketamiini (positiivinen kontrolli) ei vaikuttanut TrkB:n tai ERK:n fosforylaatioon meidän viljelmässämme. Kaiken kaikkiaan tämä tutkimus edistää ymmärrystä typpioksiduulin mekanismista, joka mahdollisesti valottaa myös yleisemmin NMDA-reseptoria salpaavien masennuslääkkeiden mekanismia. Lisäksi löysimme lupaavia ketamiinianalogeja, jotka odottavat kokeellista testausta.

Avainsanat – Nyckelord – Keywords
Typpioksiduuli, ketamiini, NMDA-reseptorin salpaaja, AMPA-reseptori, TrkB, ERK, nopeavaikutteiset masennuslääkkeet

Ohjaaja tai ohjaajat – Handledare – Supervisor or supervisors
Tomi Rantamäki, Henri Xhaard

Säilytyspaikka – Förvaringställe – Where deposited

Helsingin yliopiston kirjasto, Helsingfors universitets bibliotek, Helsinki University Library

Muita tietoja – Övriga uppgifter – Additional information

TABLE OF CONTENTS

TrkB and ERK signaling in the mechanism of NMDA receptor-blocking antidepressants

Iina Annala

Laboratory of Neurotherapeutics, Division of Pharmacology and Pharmacotherapy, Faculty of Pharmacy, University of Helsinki, Finland
Division of Pharmaceutical Chemistry and Technology, Faculty of Pharmacy, University of Helsinki, Finland
Corresponding author: Iina Annala, iina.annala@helsinki.fi, Viikinkaari 5, P.O. Box 56, Helsinki, Finland

Introduction

N-methyl-D-aspartate receptor (NMDAR) blocker ketamine, an intravenous anesthetic developed in the 1960's (Domino et al., 1965), was first demonstrated by Berman et al. (2000) to rapidly relieve symptoms of major depression when administered at subanesthetic dose. This has subsequently been replicated by numerous studies (Marcantoni et al., 2020). Robust antidepressant effects emerging within hours after a single ketamine infusion stand out from the delayed effects of classical antidepressants. Notably, the acute actions of ketamine are short-lived (elimination half-life in humans is 2-4 hours) (Peltoniemi et al., 2016) but its antidepressant effects are most prominent 24 hours after drug delivery, and they sustain for approximately one week (Marcantoni et al., 2020). It is suggested that the transient pharmacological effects of ketamine provoke long-lasting alterations in brain function, which underlies the sustained amelioration of depressive symptoms (Gould et al., 2019). However, the precise mechanism remains debated.

Preclinical studies investigating the antidepressant mechanism of ketamine have largely focused on prefrontal cortex (PFC), an area implicated in the pathophysiology of depression (Duman and Aghajanian, 2012). The determinant for ketamine's sustained antidepressant-like effects is suggested to be increased excitatory synaptic drive on pyramidal neurons in the PFC, which is accomplished by generation of new synaptic spines (spinogenesis) and long-term potentiation (LTP)-like increase in strength of the synapses (Gould et al., 2019). It is thought that the acute pharmacological effects of ketamine trigger these structural and functional synaptic changes by engaging endogenous mechanisms of neuroplasticity. BDNF (brain-derived neurotrophic factor) and its receptor TrkB (tropomyosin receptor kinase B) are critical regulators of synaptic plasticity (Park and Poo, 2013) and implicated in ketamine's antidepressant effects (Autry et al., 2011; Liu et al., 2012; Lepack et al., 2014). Upon BDNF binding, TrkB gets phosphorylated on multiple tyrosine residues that couple to diverse biochemical pathways inside the cell. Various intracellular events implicated in plasticity processes have been deemed important for the mechanism of ketamine, one of these being activation of extracellular signal-regulated kinases 1 and 2 (ERK1/2, or simply ERK) (Réus et al., 2014; Li et al., 2010). Another signaling event implicated in mechanisms of plasticity and ketamine is inhibition of GSK3β (glycogen synthase kinase 3β) (Beurel et al., 2011, 2016). Further, activation of mTORC1 (mammalian target of rapamycin complex 1) and its downstream targets such as P70S6K are considered critical for synthesis of proteins that are required for lasting synaptic changes that ketamine induces (Li et al., 2010). Stimulation of α-amino-3-hydroxy-5-methyl-4-isoxazolepropionic acid receptors (AMPARs), ionotropic non-NMDA glutamate receptors that mediate fast excitatory neurotransmission in the brain, is also held crucial for ketamine's mechanism. Specifically, pretreatment with AMPAR antagonist abolishes ketamine's antidepressant-like behavioral effects in rodents (Maeng et al., 2008), and blocks ketamine-induced stimulation of critical signaling pathways (Li et al., 2010).

Disinhibition hypothesis of ketamine's antidepressant mechanism relies on the discovery that ketamine at subanesthetic doses increases extracellular glutamate levels in the PFC (Moghaddam et al., 1997). It is thought that low-dose ketamine preferentially antagonizes NMDARs expressed on inhibitory

interneurons, causing decreased inhibitory tone and thus disinhibition of pyramidal neurons, which leads to their increased excitation and glutamate bursting (Homayoun and Moghaddam, 2007). Glutamate could then activate postsynaptic AMPARs on pyramidal neurons, which is suggested to cause release of BDNF that activates TrkB-signaling and stimulates intracellular cascades that eventually bring about synaptic changes (Zanos and Gould, 2018). The ketamine-induced disinhibitory effect and requirement for PFC activation in triggering the rapid antidepressant effects are supported by recent studies (Fuchikami et al., 2015; Hare et al., 2019; Gerhard et al., 2020; Ali et al., 2020). However, it has also been proposed that pertinent to ketamine's antidepressant effects is activation of homeostatic plasticity processes via blockade of postsynaptic NMDARs on pyramidal neurons (Autry et al., 2011; Miller et al., 2014). The importance of NMDAR blockade for triggering ketamine's antidepressant actions has also been questioned recently by the finding that ketamine's metabolite (2R,6R)-hydroxynorketamine, which does not have affinity for NMDAR, showed antidepressant-like effects in preclinical tests (Zanos et al., 2016).

Another NMDAR antagonist, nitrous oxide (N_2O; "laughing gas"), alleviated depressive symptoms with similar time profile as ketamine in a clinical pilot trial (Nagele et al., 2015), giving strong support for NMDAR-dependent mechanism of ketamine's antidepressant effects. Our group has found that N_2O regulates same signaling pathways that have been linked to ketamine's antidepressant effects in mouse PFC (Kohtala et al., 2019a). The very fast pharmacokinetics of N_2O, which is administered by inhalation and eliminated unchanged within minutes via respiration, was exploited to demonstrate intriguing temporal profile of the molecular alterations. It was found that during N_2O administration (i.e. NMDAR blockade), biological markers of neuronal activation, such as increased levels of phosphorylated (activated) form of ERK and upregulated expression of immediate-early genes (IEGs) like *c-fos*, are seen in PFC, which is suggestive of ongoing cortical excitation that is also associated with the acute effects of subanesthetic ketamine (Fuchikami et al., 2015; Ali et al., 2020). During this time, activity (phosphorylation) of TrkB, GSK3β and P70S6K is not regulated, but instead, increases in their phosphorylation levels emerge soon upon N_2O withdrawal, when the drug has been eliminated from the body (Kohtala et al., 2019a). Notably, these signaling effects coincide with slow-wave activity (SWA) seen on electroencephalography (EEG), which is also gradually seen after a bolus of subanesthetic ketamine (Kohtala et al., 2019a). We hypothesize that the brain state associated with SWA and TrkB signaling is an adaptive response to the preceding cortical excitation, and represents a physiologically meaningful step associated with ongoing plasticity processes (Rantamäki and Kohtala, 2020). Thus we figure that the ability to induce this state as an adaptive response is critical for rapid antidepressant effects.

By virtue of the similarities in the effects of N_2O and ketamine, we anticipate that they share a common mechanism, where NMDAR antagonism triggers intrinsic plasticity processes and associated signaling cascades, which lead to rapid and sustained antidepressant effects. This study has two parts. In the first part, we aimed to investigate the adaptive N_2O-induced molecular changes associated with antidepressant effects and further, the requirement for AMPAR activation in inducing them. To achieve this, we administered N_2O to adult male mice with or without pretreatment with an AMPAR antagonist, and studied excitation- and BDNF-TrkB signaling-associated biochemical changes using western blot, enzyme-linked immunosorbent assay (ELISA) and quantitative reverse transcription polymerase chain reaction (RT-qPCR), in PFC samples taken 15 minutes after termination of N_2O exposure. Within this time window, it is expected that N_2O has been completely eliminated from the brain and rest of the body. In the second part, our aim was to search for ketamine-like NMDAR blockers with antidepressant potential. To achieve this, we utilized ligand- and structure-based in silico methods to find ketamine analogs, whose NMDAR binding ability was predicted by virtual docking. Finally, we sought to study if selected ketamine analogs could elicit ketamine-like antidepressant-relevant signaling effects in vitro. To this end, we attempted to characterize ketamine's effects on TrkB and ERK phosphorylation in primary neuronal culture.

Materials and methods

In vivo experiment

Animals: Adult (10-12 weeks old) male C57BL/6 mice (Envigo RMS, the Netherlands) weighing 26-34 grams were acclimated to the animal facility of University of Helsinki (Finland) three weeks before the experiments. Mice were housed in groups of three per cage under standard conditions (21°C, constant 12-h light/dark cycle, lights on at 6 a.m.) with food and water available *ad libitum*. The experiments were carried out according to the guidelines of the Society for Neuroscience and were approved by the County Administrative Board of Southern Finland (License: ESAVI/10527/04.10.07/2014).

Pharmacological treatments: The experiment was carried out during the light phase between 9:00-12:00 a.m. Treatment-naïve mice were first given an injection of either 10 mg/kg NBQX (2,3-dihydroxy-6-nitro-7-sulphamoyl-benzo(F)quinoxaline; Tocris Bioscience, Bristol, UK; dissolved in saline) or isotonic saline (control) via intraperitoneal (i.p.) route. Ten minutes after the injection, 20-minute exposure to 65% N_2O (mixed with O_2) or sham (air) was achieved by placing the animals individually into anesthesia chambers of size 17 cm x 25 cm x 10 cm (width x length x height) filled with the respective gas mixtures (flow rate 5 l/min). The mice were allowed to move freely in the chambers. We used 18 mice that were randomly divided into three groups (n=6 per group). The sample sizes were estimated based on our past experience performing similar experiments (Kohtala et al., 2019a). Control group (saline+air) received an i.p. injection of isotonic saline followed by exposure to sham. Saline+N_2O group received an injection of isotonic saline followed by N_2O exposure. NBQX+N_2O group received an injection of NBQX (10 mg/kg) followed by N_2O exposure. After the 20-min sham or N_2O exposure, mice were placed individually to standard mouse cages, where they were allowed to move freely and breathe room air for 15 minutes. After the recovery period, the animals were euthanized by rapid cervical dislocation that was followed by decapitation. No anesthesia was used due to its potential confounding effects on the biochemical analyses of the brain samples (Kohtala et al., 2016).

Dissection and preparation of brain samples: Immediately after the decapitation, bilateral medial PFCs were dissected on a petri dish on top of dry ice and stored in –80°C. PFC samples were prepared for the biochemical analyses such that one side of the PFC was used for protein extraction for western blot and ELISA analyses, while the other side was used for RNA extraction for RT-qPCR analyses. Extraction of proteins: Samples were lysed in NP++ lysis buffer (137 mM NaCl, 20mM Tris, 1% NP-40, 10% glycerol, 48 mM NaF, H_2O, Pierce™ Phosphatase and Protease Inhibitor tablets [Thermo Fisher Scientific]) and homogenized using ultrasonication. After incubation on ice for ~15 min, the homogenates were centrifuged (16100 g, 15 min, 4°C) and protein containing supernatants collected. Total protein concentrations were determined using the DC™ protein assay (Bio-Rad), which is based on the well-documented Lowry protein assay (Lowry et al., 1951). The samples were stored in -80°C until further use (described below). Extraction of RNA: Samples were lysed and homogenized in Trizol (Thermo Fisher Scientific). After ~10 min incubation in room temperature, samples were mixed with chloroform and centrifuged (12000 g, 15 min, 4°C). The uppermost, RNA-containing phases were collected and precipitated with isopropanol. After 10 min incubation on ice, samples were centrifuged (12000 g, 10 min, 4°C), and the resulting pellets were washed twice with 75% ethanol (with 10 min centrifugation in 12000 g, 4°C between the washes). After that, RNA pellets were air-dried, dissolved in RNase-free water and incubated for 10 min in 60°C. The amount of total RNA was estimated using NanoDrop™ spectrophotometer (Thermo Fisher Scientific). The samples were stored in -80°C until further use (described below).

Primary cortical neuron culture and in vitro experiments

Primary neuronal culture: Cortical tissue from postnatal day 0 (P0) C57BL/6 mice were used for primary neuronal cultures. Four mouse pups were euthanized by decapitation. The brains were rapidly taken out and cortices dissected on phosphate buffered saline (PBS) containing petri dish placed on top of ice. The cortices were triturated with a 20G needle in L15 medium to dissociate the cells. The resulting suspension was centrifuged (160 g, 5 min, room temperature) to obtain a cell pellet that was collected and resuspended in NBM (Neurobasal Medium) with 10% Fetal Calf Serum. The new suspension was incubated on a petri dish (Thermo Fisher Scientific) in 37℃ to facilitate glial cell and debris separation from neurons (Sahu et al., 2019). After 30 minutes, the supernatant was collected and centrifuged (160 g, 5 min, room temperature). The pellet was collected, resuspended in NBM++ (NBM with 2% B27 Supplement, 1% Penicillin-Streptomycin and 1% L-Glutamine) and then allowed to settle for 2-3 min to sediment the debris. Finally, the supernatant was collected and neurons were counted using hemacytometer, after which 250 000 cells per well were plated to a poly-L-lysine pre-coated 24-well plate. Cells were maintained in 37℃, 5% CO_2 and 95% humidity for 14 days. Partial media change (NBM++) and checking of the morphology and fitness of the cells were performed twice a week.

Drug treatment and sample preparation: The experiment was done after 14 days in vitro (DIV14). To stimulate the neurons, wells were incubated with BDNF (20 ng/ml, dissolved in saline; n=6), ketamine (Ketalar®, Yliopiston apteekki, Helsinki; 500 nM, dissolved in saline; n=6) or isotonic saline (control, n=12) for 30 min. After the stimulation period, the drug-containing medium was aspirated, and the cells were lysed by adding of NP++ lysis buffer (137 mM NaCl, 20mM Tris, 1% NP-40, 10% glycerol, 48 mM NaF, H_2O, Pierce™ Phosphatase and Protease Inhibitor tablets [Thermo Fisher Scientific]) to the wells, followed by mechanical scraping. The suspensions were collected and centrifuged (16100 g, 15 min, 4℃) to obtain protein containing supernatants. Total protein concentrations of the supernatants were determined using DC™ protein assay (Bio-Rad) and stored in -80℃ until further analyzed using western blot (described below).

Biochemical analyses of the samples

Western blotting: Samples containing 40 µg (in vivo samples) or 17 µg (in vitro samples) of total protein were mixed with 2X Laemmli buffer (Bio-Rad) in 1:1 ratio, heated in 100℃ for 3 min and then loaded to SDS-PAGE (sodium dodecyl sulphate–polyacrylamide gel electrophoresis) gels (4-12% NuPAGE™, Thermo Fisher Scientific) with protein standard (Precision Plus Protein™ Dual Color Standards, Bio-Rad). Excess wells were loaded with 1X Laemmli buffer. Separation of proteins was conducted by running the gels in 180V for 1 h in running buffer (NuPAGE™ MOPS SDS, Thermo Fisher Scientific), after which the blots were transferred from the gel to methanol-immersed PVDF (polyvinylidene difluoride) membrane (300mA for 1 h, on ice) in transfer buffer (NuPAGE™, Thermo Fisher Scientific). Membranes were equilibrated in Tris-buffered saline (TBS) for 5 min in room temperature, blocked in 3% BSA/TBS-T (TBS-T [TBS/0,1% Tween20] containing 3% (m/V) bovine serum albumin [BSA]) for 60 min in room temperature, and then incubated overnight in 4℃ with the following primary antibodies diluted in 3% BSA/TBS-T: anti-p-TrkB^{Y816} (#4168, 1:1000, Cell Signaling Technology (CST)), anti-TrkB (#4603, 1:1000, CST), anti-p-GSK3β^{S9} (#9336, 1:1000, CST), anti-GSK3β (#9315, 1:1000, CST), anti-p-P70S6K$^{T421/S424}$ (#9204, 1:1000, CST), anti-P70S6K (#2708, 1:1000, CST), anti-p-p44/42MAPK$^{T202/Y204}$ (#9106, 1:1000, CST), anti-p44/42MAPK (#9102, 1:1000, CST) and anti-GAPDH (#2118, 1:1000, CST). After washing the membranes three times (15+10+10 min) with TBS-T, blots were incubated for 60 min with appropriate (anti-rabbit, anti-mouse or anti-goat; Bio-Rad) horseradish peroxidase-conjugated secondary antibodies (1:10000 in TBS-T with 5% non-fat dry milk) in room temperature. After washing with TBS-T (15+10+10 min) and TBS (10 min), the immunoreactive bands were visualized using enhanced chemiluminescence (ECL Plus™, Thermo Fisher Scientific) and ChemiDoc™ MP camera (Bio-Rad) to obtain digital images. After detection of each protein, the membranes were incubated (6 min; 60℃) in stripping solution (Tris 62.4mM, 2%

SDS, H_2O [Milli Q], 0,7% β-mercaptoethanol) and then washed in TBS (5 min) before next round of blocking and primary antibody treatment. Densitometric analysis of the chemiluminescent blots were quantified using ImageJ software (ImageJ 1.46v, National Institute of Health, USA). The density of blots representing each phospho-antibody were normalized to the density of blots of the respective total protein or GAPDH.

Enzyme-linked immunosorbent assay (ELISA): BDNF protein levels were analyzed using a commercially available BDNF ELISA kit (Quantikine® ELISA Kit, catalog #DBD00, R&D Systems Europe Ltd., Abingdon, UK) (Theilmann et al., 2020). The samples were acid-treated with 1 M HCl to pH 2-3, followed by neutralization to pH 7-8 with 1 M NaOH. The samples and BDNF standards (concentrations 0, 23,47, 94, 187, 375, 750 and 1500 pg/µl) were loaded as duplicates to a pre-blocked BDNF monoclonal antibody-coated 96-well ELISA-plate. The plate was incubated for 2 hours in room temperature in a shaker, then washed three times with provided washing buffer before addition of secondary antibody that was linked with biotin. The plate was incubated for 60 min in shaker, then washed three times before addition of streptavidin-horseradish peroxidase. After incubation for 20 min in a shaker (protected from light) and three washes with washing buffer, color reagents (hydrogen peroxide and chromogen) were added. The reaction was stopped using provided stop solution after a 20-min incubation in a shaker protected from light, and finally the plate was read for absorbance in 450 nm. The BDNF protein concentration was determined using standard curve method (standard curve shown in **S2 Fig**). Quantified BDNF protein levels were normalized against total protein concentration (determination of total protein described above) of each sample.

Quantitative reverse transcription polymerase chain reaction (RT-qPCR): Equal amounts of total RNA/DNA of the samples were loaded to well plate and treated with dsDNase (Thermo Fisher Scientific; incubation in +37℃ for 10 min) to digest residual DNA. Messenger RNA (mRNA) was reverse transcribed to complementary DNA (cDNA) by thermal cycling (10 min at +25℃, 30 min at +55℃, 5 min at +85℃) with Reverse Transcriptase mix including oligo(dT) and random hexamer primers (Maxima cDNA synthesis kit, Thermo Fisher Scientific). The amount of cDNA was quantified using real-time quantitative PCR. Primers used to amplify cDNAs of *c-fos, bdnf IV* and housekeeping genes *gapdh* and *β-actin* can be found from Supplementary Material **S1 Table**. DNA amplification reactions were run in triplicate with Maxima SYBRGreen qPCR Master Mix (Thermo Fisher Scientific) (45 cycles on LightCycler 480 system). Second derivative values from each sample were obtained using LightCycler 480 software (Roche). Relative quantification of template was performed as described previously using standard curve method (Kohtala et al., 2019a), with cDNA data from genes of interest being normalized to the geometric mean of *gapdh* and *β-actin* cDNA data determined from each sample.

In silico screening of ketamine analogs

Substructure search and filtering of compounds In order to find commercially available ketamine analogs, a substructure search was conducted by utilizing KNIME (Konstanz Information Miner) Analytics Platform (University of Konstanz, Zurich, Switzerland). The workflow compared the molecular structures of compounds in a virtual library to the molecular structure of ketamine, and retrieved those compounds that include ketamine (2-(2-chlorophenyl)-2-(methylamino)cyclohexan-1-one) as their substructure i.e. part of their overall molecular structure. Our compound library was downloaded 03.02.2019 from ZINC12 online database as SDF files. We used ZINC12 subset of clean drug-like compounds, which contains over 13 million commercially available compounds that follow Lipinski's rule of 5 and are devoid of reactive groups in their structure (Irwin et al., 2012). Aqueous solubility and the blood-brain-barrier (BBB) crossing ability of the retrieved output compounds (referred to as ketamine analogs in this paper) were computationally predicted by using ADMET Descriptor models in Discovery Studio (BIOVIA, version 2018). The ketamine analogs were filtered to only include those whose predicted BBB penetration ability was classified as "high" or "very high" by

the ADMET Blood Brain Barrier model. The compounds whose predicted water solubility was classified by the Aqueous solubility model as "very low, but possible" or lower were excluded.

Molecular docking The filtered ketamine analogs were further screened by virtually docking them to the three-dimensional (3D) structure of tetrameric NMDAR complex. The macromolecule used in the docking was the 3D crystal structure of the NMDAR complex (resolution 3.77 Å) consisting of two GluN1 subunits and two GluN2B subunits, which was obtained from Protein Data Bank (PDB; code 4TLM). The 4TLM was chosen because it was the best available tetrameric NMDAR complex that also has the pore-forming transmembrane domains (TMD) of the subunits at least partially resolved, which is important, because the region of interest in this study is the pore region of the NMDAR. Docking was accomplished using Glide software (Release 2018-4, Schrödinger LLC, USA) (Friesner et al., 2004). Before docking, the receptor complex was prepared using Maestro Protein Preparation Wizard (Release 2018-4, Schrödinger LLC, USA). Missing hydrogens were added, bond orders assigned, waters removed, hydrogen bonds optimized and energy minimized, disulfide bonds generated, ionization states generated in pH 7±2. Missing side chains or loops were not generated. Co-crystallized ligands were removed before grid calculations. Ketamine is known to bind inside the NMDAR pore, but the precise binding site is unknown. Therefore we first conducted blind docking of ketamine over the entire pore region to predict the binding site. Multiple grids (size 20 Å x 20 Å x 20 Å) were generated to cover the transmembrane region of the tetrameric protein. Ketamine's structure was prepared by LigPrep module in Maestro (Release 2018-4, Schrödinger LLC, USA): the structure was converted to 3D, energy minimized, stereoisomers and ring conformers generated, ionization in pH 7.4 accounted and salts removed. Then ketamine was docked to the created grids using Glide Standard Precision (SP)-mode with default settings and without adding any additional constraints. The protein structure was treated as rigid whereas ketamine was treated as flexible. The grid where ketamine obtained its best docking score (lowest docking score value in kcal/mol) was selected to be used in the docking of the filtered ketamine analogs found by the substructure search. Prior to docking, the analogs were prepared by LigPrep (converted to 3D, energy minimized, stereoisomers, ring conformers and tautomers generated, ionization in pH 7.4 accounted, salts removed). Docking was accomplished with the same settings as with ketamine. The docking scores were used as an outcome measure of the docking. Compounds were ranked according to their docking scores, such that the lower the docking score, the higher the priority number. The best-scoring commercially available compounds were selected and ordered as racemic mixtures from Ambinter.

Statistical analyses

Statistical analyses were performed and graphs prepared using Graphpad Prism 8.1.1 software (La Jolla CA, USA). Grubbs' test was used to determine outlier values, and upon detection of such values, they were excluded from the analyses. Results of in vivo studies with three study groups were analyzed using one-way analysis of variance (ANOVA) followed by a Tukey's post hoc test. Homogeneity of variances between group samples were confirmed using Levene's test in SPSS. The results of in vitro experiments with two study groups were analyzed using two-tailed independent t-test. Significance was assigned at $p \leq 0.05$. Details of statistical tests and *n* numbers for each experiment are given in **Table S2** in Supplementary Material.

Results

Effects of N_2O on TrkB and ERK signaling in the mouse PFC: role of AMPAR activation

In the first part of this study, we performed an in vivo experiment in mice to investigate the N_2O-induced molecular-level alterations in the PFC. The timeline of the experiment is shown in **Fig 1**. Twenty-minute exposure to 65% N_2O was chosen because it has been previously shown to induce changes in

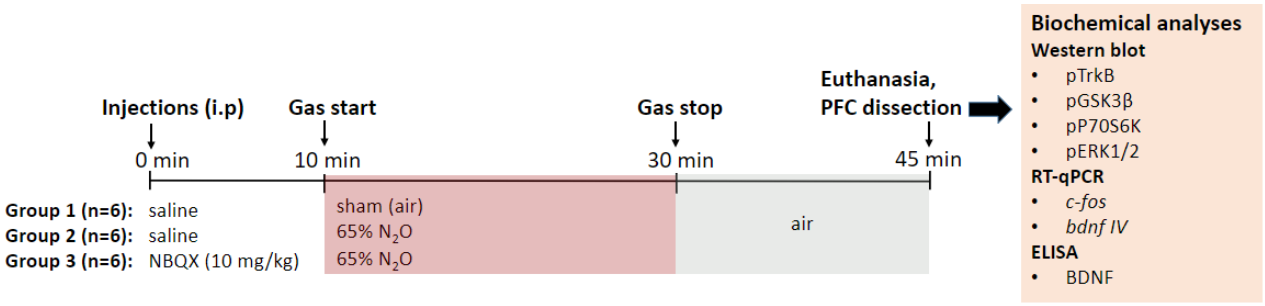

Fig 1. **Timeline of the in vivo experiment and biochemical analyses of the samples**. The mice received either NBQX (10 mg/kg) or saline via i.p. injection 10 minutes before being transferred into a chamber filled either with 65% N_2O mixed with O_2, or air (sham). After the 20 minute gas exposure, mice were shifted to recovery cages where they spent 15 minutes breathing room air. After the recovery period, the mice were euthanized, decapitated and their PFCs dissected for biochemical analyses. Abbreviations: i.p., intraperitoneal; PFC, prefrontal cortex; RT-qPCR, quantitative reverse transcription polymerase chain reaction; ELISA, enzyme-linked immunosorbent assay.

phosphorylation of plasticity-related proteins in the mouse PFC (Kohtala et al., 2019a). Because we wanted to focus on the adaptive effects that are seen after the acute pharmacological effects, we studied PFC samples that were taken 15 minutes after N_2O withdrawal. At this point, N_2O is expected to be eliminated from the brain and rest of the body. To study the role of AMPARs in triggering the molecular effects of N_2O, one group of mice was pretreated with a selective AMPAR antagonist, NBQX, before the start of N_2O treatment. To control effects of injection stress, other groups received injections of vehicle (saline). The NBQX pretreatment protocol (10 mg/kg i.p., 10 minutes before NMDAR blocker) has been previously used in experiments studying ketamine, where the molecular and behavioral changes associated with its antidepressant-like effects were shown to be blocked by NBQX (Li et al., 2010). We did not include a control group of mice receiving NBQX alone, since we have previously seen that it does not affect TrkB, GSK3β or P70S6K phosphorylation (Antila et al., 2017). The experiment only included male mice to allow comparison to previous studies with N_2O and ketamine.

Phosphorylation is a transient, reversible post-translational modification that occurs on specific residues of proteins and dynamically regulates their function. **Fig 2** shows the effects of N_2O on levels of phosphorylated TrkB, GSK3β and P70S6K ($pTrkB^{Y816}$, $pGSK3\beta^{S9}$ and $pP70S6K^{T421/S424}$, respectively), as measured by western blotting and normalized to total levels of the respective proteins. Of the many TrkB tyrosine residues that are associated with its activation, we measured phosphorylation of Y816, which is coupled to phospholipase γ (PLCγ) pathway (Minichiello et al., 2002) and regulated by antidepressants (Rantamäki et al., 2007). Compared to control, N_2O tend to increase $pTrkB^{Y816}$ in saline-pretreated mice, and a similar increase was also seen in NBQX-pretreated mice. However, one-way ANOVA did not detect statistically significant differences between the three groups ($F(2,15)=3,16$, $p=0,0713$). Phosphorylation of GSK3β at serine-9 residue, that is associated with its inhibition and facilitated by LTP-inducing stimuli (Bradley et al., 2012), was statistically significantly different between the groups ($F(2,15)=9,73$, $p=0,0019$). $pGSK3\beta^{S9}$ was increased in saline+N_2O ($p=0,0031$) as well as NBQX+N_2O ($p=0,0068$) groups when compared to control, without any significant difference between saline+N_2O and NBQX+N_2O treatments ($p=0,922$). $pP70S6K^{T421/S424}$ (activated P70S6K), which promotes protein translation, was also statistically significantly different between the groups ($F(2,13)=12,37$, $p=0,0010$). Compared to control, N_2O treatment increased $pP70S6K^{T421/S424}$ in saline-pretreated ($p=0,0051$) as well as NBQX-pretreated ($p=0,0012$) mice without significant difference between saline+N_2O and NBQX+N_2O groups ($p=0,802$). Analogous differences between the groups were observed when normalization of $pTrkB^{Y816}$, $pGSK3\beta^{S9}$ or $pP70S6K^{T421/S424}$ levels was done to GAPDH (glyceraldehyde 3-phosphate dehydrogenase; housekeeping protein) (**S2 Fig)**.

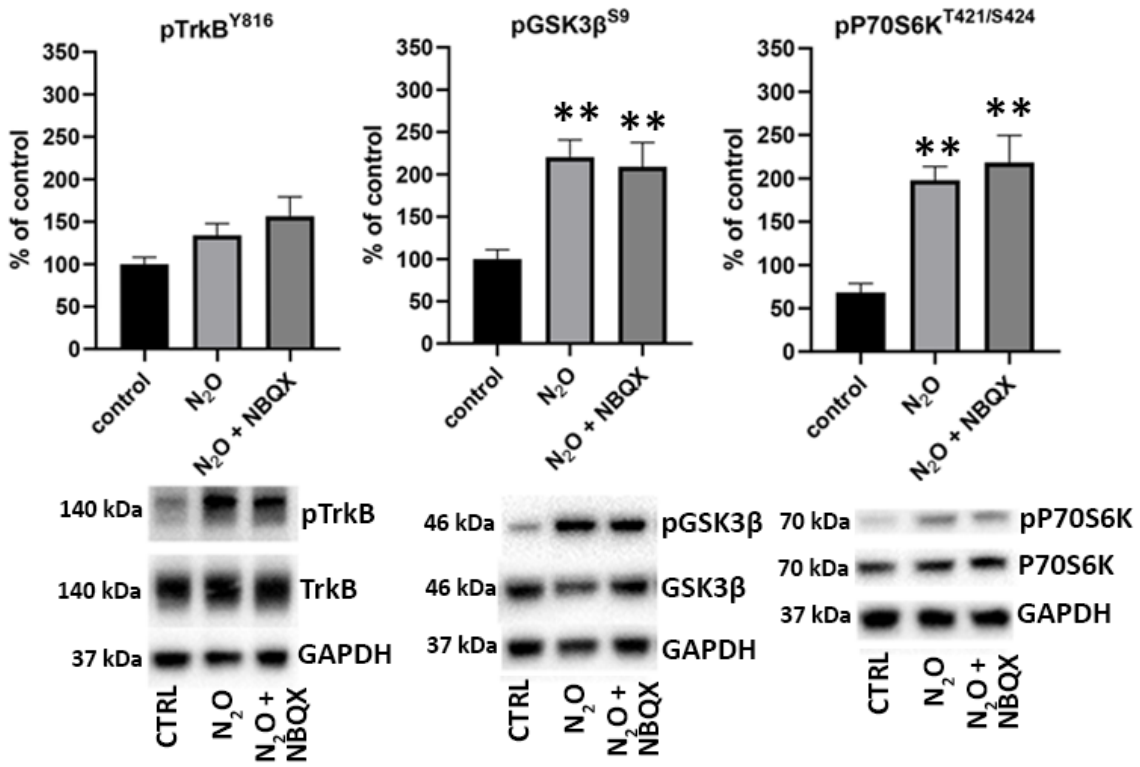

Fig 2. **NBQX pretreatment does not attenuate N_2O-induced increases in phosphorylation of TrkB^{Y816}, GSK3β^{S9} and P70S6K$^{T421/S424}$ in the mouse PFC.** Phosphorylated proteins are normalized to their respective total proteins. Representative western blots cropped from complete immunoblots are also shown. Data are means ± S.E.M expressed as percentual change of control value. *≤ 0.05, **≤0.01, ***≤ 0.001 compared to control group (for statistical analyses, p-values and *n* numbers, see S2 Table).

Activating phosphorylation of two ERK isoforms, ERK1 (pERK1$^{T202/Y204}$) and ERK2 (pERK2$^{T185/Y187}$), is associated with regulation of plasticity-related genes. The pathway that activates ERK isoforms can be stimulated by glutamate (Vanhoutte et al., 1999) and also by TrkB receptor (Park and Poo, 2013). We have previously shown that phosphorylation of ERK is increased during the acute effects of N_2O, at a time when TrkB^{Y816} phosphorylation was unaltered (Kohtala et al., 2019a). In this study, pERK was measured from the samples taken after the acute effects. The two ERK isoforms were similarly regulated and combined for quantitative analysis of western blots. We observed a significant difference between the groups when pERK levels were normalized to GAPDH ($F(2,14)=3,84$, $p=0,0467$) **(Fig 3A).** The phosphorylation of ERK in saline+N_2O treated mice was statistically significantly decreased when compared to control ($p=0,0374$). By contrast, there was no significant difference in pERK levels between NBQX+N_2O and control group ($p=0,381$) **(Fig 3A)**. The difference between saline+N_2O and NBQX+N_2O groups remained, however, statistically insignificant ($p=0,337$). When pERK levels were normalized to total ERK, there were no significant differences between the three groups ($F(2,15)=0,92$, $p=0,4168$).

Increased neuronal activity and particularly glutamatergic neurotransmission rapidly stimulates expression of IEGs, and thus their mRNA levels can be used as markers of recent neuronal excitation (Okuno, 2011). N_2O has been shown to raise levels of multiple activity-induced IEG transcripts, with increased *c-fos* mRNA levels detected already at 30 minutes after beginning of continuous N_2O administration (Kohtala et al., 2019a). In this study, *c-fos* mRNA levels were measured 35 minutes after start of N_2O exposure (20-minute N_2O treatment followed by 15-minute recovery period) by using RT-qPCR. Levels of *c-fos* were increased by N_2O in saline- and NBQX-pretreated mice when compared to control, but the changes did not reach statistical significance ($F(2,14)=2,13$, $p=0,1561$) **(Fig 3B).**

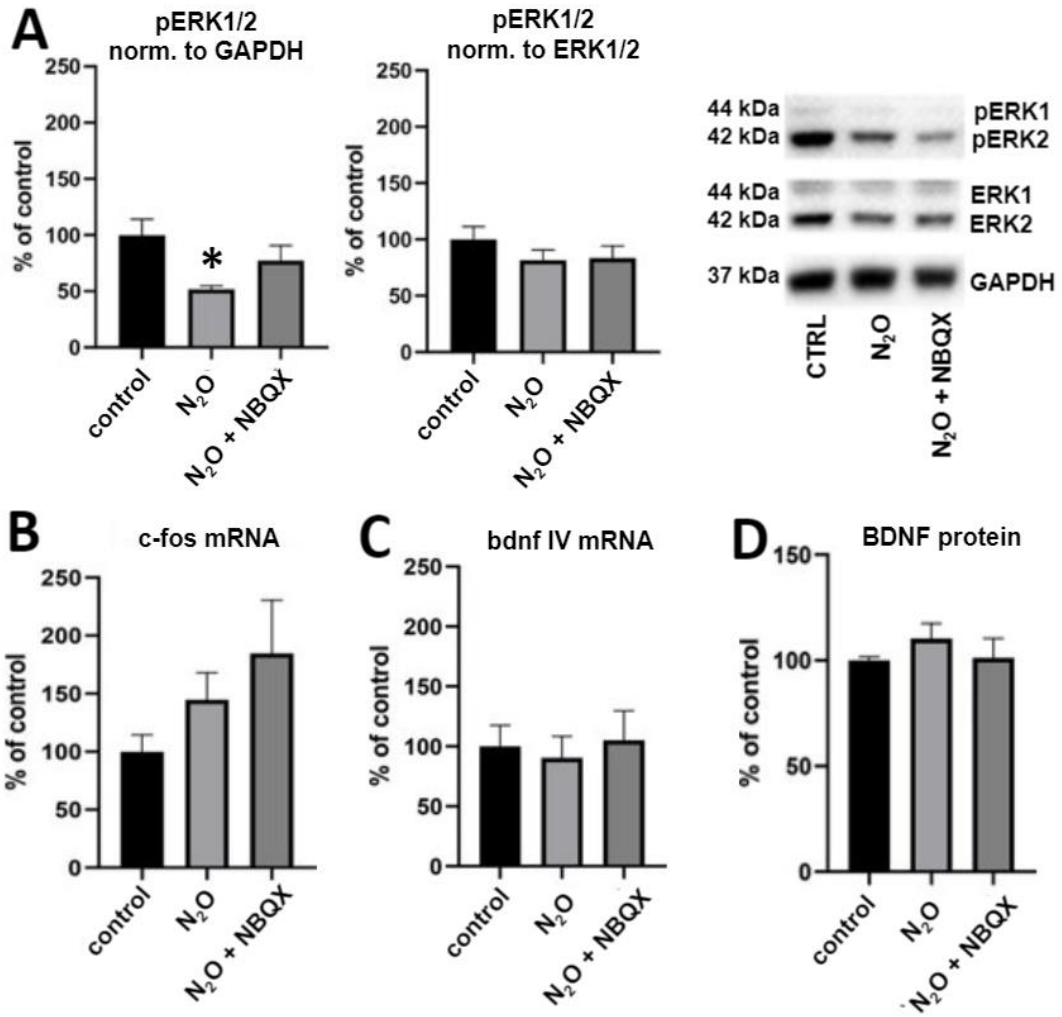

Fig 3. Effects of N_2O on markers of neuronal activity and BDNF expression in mouse PFC. A) Phosphorylation of ERK (pERK1$^{T202/Y204}$ and pERK2$^{T185/Y187}$ analyzed together) normalized (norm.) to either GAPDH or total ERK1/2. Representative western blots cropped from complete immunoblots are also shown. **B)** *c-fos* mRNA levels. Results are normalized to geometric mean of *β-actin* and *gapdh* mRNA. **C)** *Bdnf IV* mRNA levels. Results are normalized to geometric mean of *β-actin* and *gapdh* mRNA. **D)** BDNF protein levels. Results are normalized to total protein levels. Data are means ± S.E.M expressed as percentual change of control value. *≤ 0.05, **≤ 0.01, ***≤ 0.001 compared to control group (for statistical analyses, p-values and *n* numbers, see S2 Table).

BDNF is an endogenous ligand for TrkB. Its expression and release can be induced by neuronal activity (Park and Poo, 2013). Given that N_2O treatment increased TrkB phosphorylation, we wanted to measure if BDNF expression was changed at gene and/or protein level in the same samples. Of many bdnf transcripts that eventually code for the same BDNF protein, we measured exon IV-containing bdnf mRNA (*bdnf IV*), which is induced by depolarization. *Bdnf IV* mRNA levels were comparable to control in saline+N_2O and NBQX+N_2O groups, as measured by RT-qPCR ($F(2,14)=0,14$, $p=0,8700$) **(Fig 3C).** Next, the effects of N_2O on PFC levels of BDNF protein were determined by using BDNF ELISA. This method detects both mature and pro-BDNF forms, albeit the levels of the pro-form are extremely low in the adult mouse brain (Park and Poo, 2013). BDNF protein levels were not different from control in saline+N_2O or NBQX+N_2O groups ($F(2,15)=0,67$, $p=0,5253$) **(Fig 3D).**

Virtual screening of ketamine-like compounds: docking of ketamine analogs to NMDAR

Because two NMDAR antagonists, ketamine and N_2O, elicit rapid antidepressant effects in humans, NMDAR seems to be a promising target for antidepressants. In the second part of this study, we aimed to find new NMDAR blocking compounds with antidepressant potential. To achieve this, we took ketamine's structure as a starting point and utilized in silico methods to find ketamine analogs. The compounds were virtually screened by docking them around the predicted binding site of ketamine in the NMDAR pore region, in order to prioritize those with the best docking scores for experimental testing. The scheme showing the workflow of our in silico study is depicted in **Fig 4A**.

In order to find ketamine analogs, we conducted a virtual substructure search. The chosen ligand-based approach is fast and cost-effective, and relies on the principle that compounds with similar structures also have similar properties. The molecular structure of ketamine (2-(2-chlorophenyl)-2-(methylamino)cyclohexan-1-one) **(Fig 4B)** was used as a query, which was compared to the structures of compounds in a virtual library. Our library consisted of commercially available compounds whose structures were downloaded from ZINC12 database (Irwin et al., 2012). In order to limit the search to compounds that structurally resemble pharmaceuticals, we chose a ZINC12 subset of "clean drug-like compounds" that follow the Lipinski's rule of 5 (molecular weight ≤ 500 Da, log P ≤ 5, hydrogen bond donors ≤ 5, hydrogen bond acceptors ≤ 10) and do not contain reactive groups. The substructure search screened over 13 million compounds present in our library and retrieved 144 molecules that had ketamine's structure as their substructure i.e. incorporated as a part of their overall molecular structure.

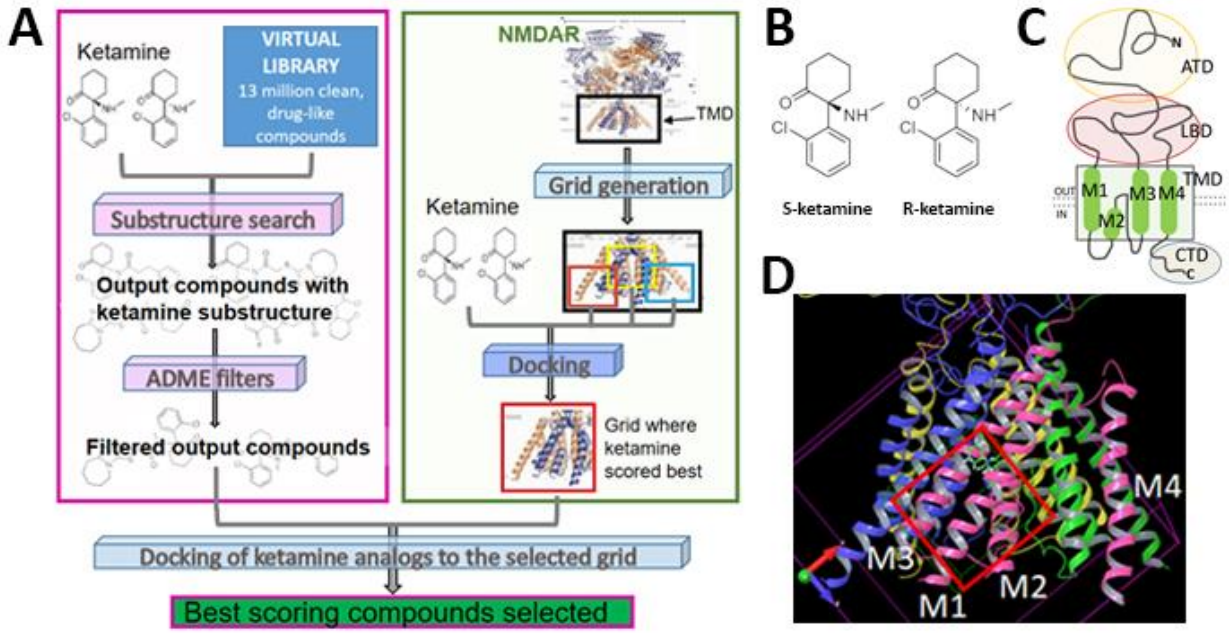

Fig 4. **Ketamine analogs were virtually searched and docked to the predicted binding site of ketamine in the transmembrane region of the NMDAR. A)** Scheme depicting the workflow of the in silico experiment, that combined ligand- and structure-based methods to find ketamine analogs and subsequently dock them to the region in an NMDAR complex where ketamine obtained its best docking score. **B)** Molecular structures of ketamine enantiomers. **C)** Simplified scheme showing the modular structure of a GluN subunit. The four helices (M1-M4) comprising the TMD are indicated. ATD, amino-terminal domain; LBD, ligand-binding domain; TMD, transmembrane domain; CTD, carboxy-terminal domain. **D)** The GluN1/GluN2B NMDAR complex 4TLM with S-ketamine docked to its pore region, which is formed by TMDs of the subunits. The shown binding pose of ketamine represents the one that obtained the best docking score. This best-scoring binding site is located in the TMD region of GluN1 subunit (shown in pink) in between its helices M1, M2 and M3 (labeled in the picture). The grid that spans this region (indicated in the picture as a red square that corresponds to a facet of the cube-shaped grid, showing the location of the grid relative to the TMD) was used in the docking of the ketamine analogs.

Because the aimed site of action of NMDAR blockers is in the central nervous system, in silico predictions of blood-brain barrier (BBB) crossing ability were computed for the retrieved compounds based on their chemical structure. The compounds were filtered to only include those whose predicted BBB penetration ability was classified as high or very high by the ADMET Blood-Brain Barrier model. To further minimize potential issues related to pharmacokinetics, aqueous solubility was predicted using ADMET Aqueous Solubility model, and the compounds with very low predicted solubility were excluded. Altogether, 132 compounds fulfilled these criteria.

The 3D structure of NMDAR was used to perform further screening of the filtered ketamine analogs by docking method. Molecular docking is a structure-based in silico method that can be used to predict interactions between a macromolecule (receptor) and a small molecule (Friesner et al., 2004). The predicted binding poses, where each pose corresponds to a specific conformation, location and orientation of the small molecule relative to the protein complex, are scored. In the present study, docking was employed to put the ketamine analogs in a rank order to prioritize those with the best scores for subsequent experimental testing. The objective was to dock the compounds to the same region where ketamine binds. The 3D crystal structure of NMDAR complex that was used in this study consisted of two GluN1 subunits and two GluN2B subunits (PDB code: 4TLM), representing a receptor assembly to which ketamine has been experimentally shown to bind (Kotermanski and Johnson, 2009). The binding site of ketamine is inside the NMDAR ion channel pore (Johnson et al., 2015), which is formed by the transmembrane domains (TMDs) of the four subunits. The 4TLM was chosen because it was the best available 3D structure of the tetrameric NMDAR complex that also includes the TMDs of the subunits (Lee et al., 2014). **Fig 4C** schematically shows the structure of an NMDAR subunit and indicates the transmembrane helices that make up the TMD. The 4TLM presumably represents blocked conformation of NMDAR (Lee et al., 2014), which increases the probability that the receptor complex is in the correct conformation for channel blocker binding.

The precise binding site of ketamine within the NMDAR pore is not known (Johnson et al., 2015). NMDAR represented by 4TLM was co-crystallized with MK-801, another open channel NMDAR blocker that at least partially shares the binding site with ketamine, but the electron density suggested to be MK-801 could not be confirmed (Lee et al., 2014). Thus, in the absence of knowledge about the binding site of ketamine, it was computationally predicted. This was accomplished by "blind docking" of ketamine over the transmembrane region of the NMDAR complex. The protein complex was prepared using Maestro Protein Preparation Wizard before conducting grid-based docking in Glide. Multiple grids that each represent the shape and properties of a region of a rigid protein that it confines, were generated to span the entire transmembrane area of the NMDAR complex. Ketamine was prepared by Maestro LigPrep tool and then flexibly docked as separate stereoisomers to the individual grids using Glide standard precision (SP) mode. The docking scores of the predicted binding poses (lowest docking score value corresponds to the best score) of ketamine in different grids were compared. Ketamine obtained the best docking scores (-6,73 kcal/mol for R-ketamine; -6,51 kcal/mol for S-ketamine) between TMD helices M1, M2 and M3 of GluN1 subunit. **Fig 4D** shows the best-scoring binding pose for S-ketamine. The grid that spanned this region (one facet of the grid indicated as a red square in the figure) was used to dock the ketamine analogs in the next step.

To predict NMDAR binding ability of the ketamine analogs, they were first prepared by Maestro LigPrep tool (relevant protonation states, tautomers and ring conformers of the stereoisomers were generated) and then docked to the grid where ketamine obtained its best docking scores in the previous step. Docking was accomplished using Glide SP mode and ligands were treated as flexible. The compounds were ranked according to the docking scores of their best binding pose. The range of the docking scores from best to worst was from -7.32 to 12.18. Eight compounds whose at least one stereoisomer was among the best-scoring compounds and commercially available with sufficient quality were selected and ordered from a vendor as racemic mixtures for subsequent testing. Structures

Table 1. The eight ketamine analogs selected by their docking scores.

No.	Chemical structure	IUPAC name	ZINC code	Docking score	Properties
1	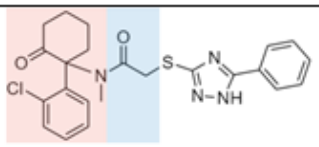	N-[1-(2-Chlorophenyl)-2-oxocyclohexyl]-N-methyl-2-[(5-phenyl-1H-1,2,4-triazol-3-yl)sulfanyl]acetamide	ZINC12749337	-7,01	MW: 455.0 cLogP: 4.71
2	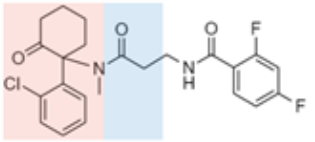	N-[1-(2-Chlorophenyl)-2-oxocyclohexyl]-3-[(2,4-difluorophenyl)formamido]-N-methylpropanamide	ZINC58147051	-6,81	MW: 448.9 cLogP: 4.24
3	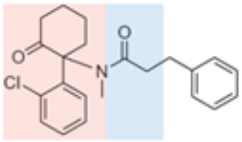	N-[1-(2-Chlorophenyl)-2-oxocyclohexyl]-N-methyl-3-phenylpropanamide	ZINC06509042	-6,54	MW: 369.9 cLogP: 4.77
4	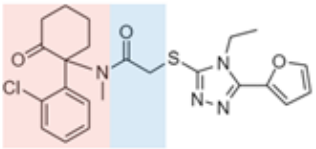	N-[1-(2-Chlorophenyl)-2-oxocyclohexyl]-2-[[4-ethyl-5-(furan-2-yl)-1,2,4-triazol-3-yl]sulfanyl]-N-methylacetamide	ZINC09513705	-6,33	MW: 473.0 cLogP: 4.80
5	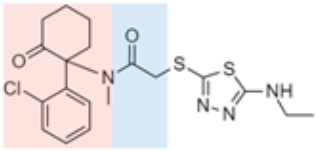	N-[1-(2-Chlorophenyl)-2-oxocyclohexyl]-2-[[5-(ethylamino)-1,3,4-thiadiazol-2-yl]sulfanyl]-N-methylacetamide	ZINC12749353	-6,19	MW: 439.0 cLogP: 4.21
6	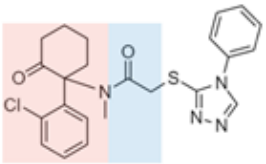	N-[1-(2-Chlorophenyl)-2-oxocyclohexyl]-N-methyl-2-[(4-phenyl-1,2,4-triazol-3-yl)sulfanyl]acetamide	ZINC09206744	-6,08	MW: 455.0 cLogP: 4.51
7	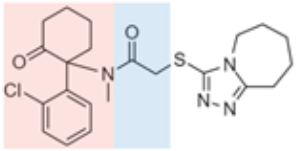	N-[1-(2-Chlorophenyl)-2-oxocyclohexyl]-N-methyl-2-(6,7,8,9-tetrahydro-5H-[1,2,4]triazolo[4,3-a]azepin-3-ylsulfanyl)acetamide	ZINC09594508	-5,66	MW: 447.0 cLogP: 4.25
8	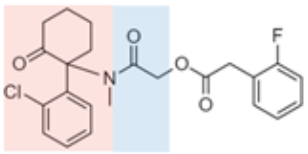	{[1-(2-Chlorophenyl)-2-oxocyclohexyl](methyl)carbamoyl}methyl 2-(2-fluorophenyl)acetate	ZINC09634536	-5,63	MW: 431.9 cLogP: 4.06

The molecular structures are shown (chirality omitted) with the part that corresponds to the ketamine substructure highlighted with red background. The structure highlighted with blue background shows the common bridging part that all compounds had incorporated in between the ketamine substructure and the additional aromatic ring-containing side chain. Docking scores (kcal/mol) and ZINC codes for the best-scoring enantiomers are shown. Molecular weight (MW) and calculated logP (cLogP) are given.

of the selected compounds are shown in **Table 1** along with their docking scores. All compounds incorporate ketamine (N-[1-(2-chlorophenyl)-2-oxocyclohexyl]) as their substructure, as indicated with red background in the structures. None of the compounds included any additional substituents in the chlorophenyl or oxocyclohexyl rings. By contrast, all compounds had a side chain attached to the nitrogen that was part of the secondary amine functionality in ketamine, by incorporating the nitrogen

to an amide structure. The resulting amide bond thus acts as a bridge between the original ketamine structure and the additional, aromatic ring-containing moiety whose size and nature varies between different compounds.

Primary neuronal culture for testing effects on TrkB and ERK signaling: trial with ketamine

We next sought to test whether the analogs share similar properties with ketamine in vitro. Ketamine has been shown to stimulate BDNF release and ERK phosphorylation in primary cortical neurons, which is suggested to reflect its actions in the cortex in vivo (Lepack et al., 2016). Given the importance of BDNF-TrkB and ERK signaling for the antidepressant effects, we wanted to test if ketamine could stimulate phosphorylation of ERK and BDNF receptor TrkB^{Y816} (PLCγ docking site) in our primary neuronal culture, with an endeavor to test the ability of the ketamine analogs to elicit ketamine-like effects in similar culture, potentially being predictive of antidepressant-like effects.

The dissociated primary neuronal culture was established from cortical cells of P0 mice. **Fig 5A** depicts the timeline of the in vitro experiment. Drug treatments were done on DIV14, when neurons have developed dendritic arborizations and form synaptic connections (Lesuisse and Martin 2002). The ability of BDNF to activate TrkB is developmentally regulated, and also affected by maturation of neurons in vitro (Di Lieto et al., 2012; Zhou et al., 2011). To test if TrkB signaling could be elicited in our culture by BDNF, subset of wells were treated with BDNF for 30 minutes at concentration of 20 ng/ml, which has previously elicited robust TrkB activation in cultured neurons at corresponding

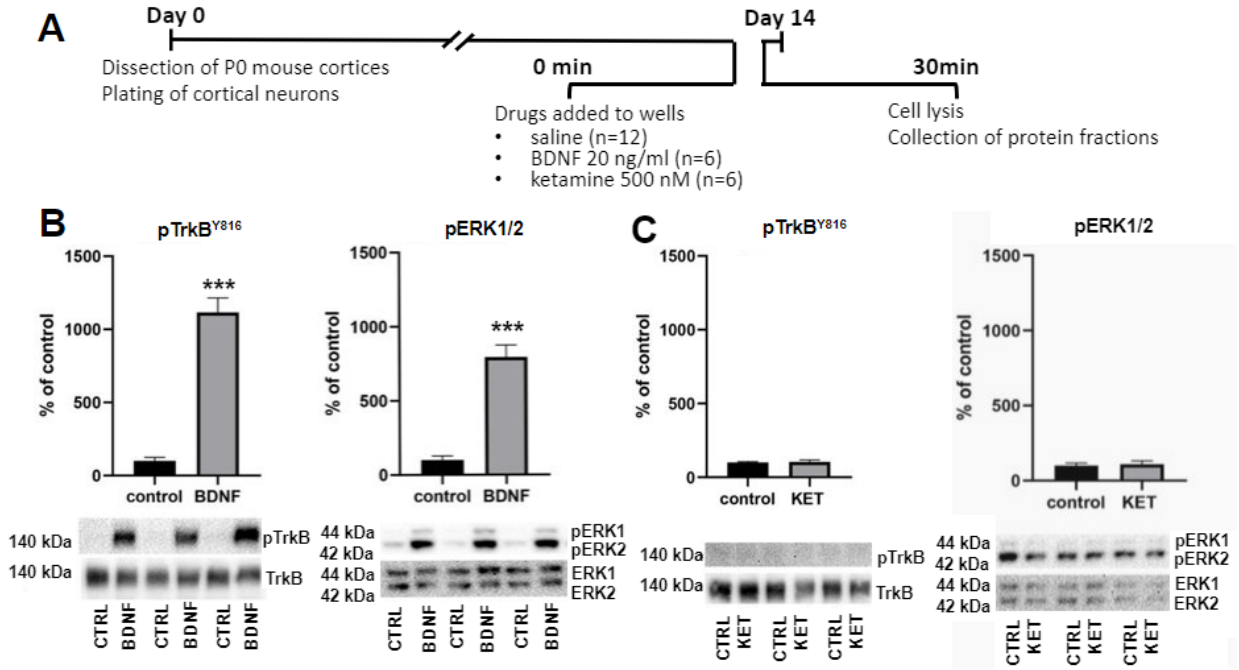

Fig 5. Ketamine did not increase TrkB or ERK phosphorylation in a primary neuronal culture, although BDNF showed robust effects. A) Timeline showing the establishment of the primary neuronal culture and schedule of drug stimulation experiment **B)** BDNF showed robust effects on phosphorylation of TrkB^{Y816} and ERK. **C)** Ketamine (KET) did not show effects on TrkB^{Y816} or ERK phosphorylation. Data are means (± S.E.M). Phosphorylated proteins are normalized to their respective total proteins. ERK1 and ERK2 were combined for quantitative analysis. Representative western blots cropped from complete immunoblots are shown below the graphs. *≤ 0.05, **≤ 0.01, ***≤ 0.001 (for statistical analyses, p-values and *n* numbers, see S2 Table).

developmental stage (Rantamäki et al., 2011). Accordingly, we saw a robust increase in pTrkB^{Y816} ($t(10)=10,01$, $p<0,0001$) as well as pERK ($t(10)=8.07$, $p<0,0001$) in cells treated with BDNF **(Fig 5B)**. To test the effects of ketamine on other subset of wells on the same plate, we used 30-minute incubation at ketamine concentration of 500 nM, which has been reported to cause robust increase on pERK and cause BDNF release (Lepack et al., 2016). Levels of pTrkB^{Y816} ($t(10)=0,30$, $p=0,768$) and pERK ($t(10)=0,31$, $p=0,7624$) were however unaltered by ketamine treatment **(Fig 5C)**. In the absence of positive results with ketamine, we did not proceed to test the ketamine analogs in this system.

Discussion

N_2O-induced TrkB and ERK signaling are uncoupled and differentially regulated by AMPARs

In order to gain better understanding of the mechanism of N_2O, an NMDAR-blocking putative rapid-acting antidepressant, the aim of the first part of this study was to investigate its effects in mice. Specifically, we examined biochemical changes in the PFC at a time point when N_2O has been eliminated from the brain to focus on the adaptive effects that emerge after its acute pharmacological actions. We observed that N_2O treatment increased phosphorylation of TrkB^{Y816}, GSK3β^{S9} and P70S6K$^{T421/S424}$, in concordance with previous studies (Kohtala et al., 2019a), indicating that the plasticity processes these signaling molecules promote are turned on during this time. The relative increases in the phosphorylated forms were similar when normalization was performed to either total levels of the respective proteins or to GAPDH. At the same time, levels of phosphorylated ERK were not different between control and N_2O-treated group, when normalization was done to total ERK. However, when pERK levels were normalized to GAPDH, we observed statistically significantly decreased levels of phosphorylated ERK in N_2O-treated group. The effect of normalization on pERK indicates that total ERK levels were also decreased by N_2O treatment, which should be further studied, although it is possible that this finding represents a technical artifact. Nonetheless, the results suggest that TrkB^{Y816} and ERK phosphorylation are uncoupled after N_2O cessation at a time which has shown to coincide with SWA seen in EEG (Kohtala et al., 2019a). Levels of pERK are increased during the acute effects of N_2O (Kohtala et al., 2019a), so the downregulation of pERK after N_2O elimination could be interpreted as a homeostatic response to its preceding upregulation. Similar course of acute TrkB-independent pERK upregulation followed by its downregulation in 30 minutes is seen after convulsions caused by electrical shock (Hansen et al., 2007), which supposedly causes glutamate release as a result of a brief depolarizing effect (Reid and Stewart, 1997). Moreover, convulsions caused chemically by flurothyl are followed by SWA with coincident TrkB phosphorylation, further corroborating our hypothesis that different treatments that cause brief cortical activation can induce homeostatic co-regulation of ERK, TrkB and SWA. Furthermore, interesting parallels can be drawn between these findings and physiological sleep, which is essential for plasticity. Levels of pERK are low during SWA-dominated non-rapid eye movement sleep, which is homeostatically regulated such that it increases in proportion to prior duration of waking, during which neuronal activity and pERK levels are high (Mikhail et al., 2017; Vyazovskiy et al., 2009). Curiously, TrkB^{Y816} phosphorylation with uncoupled pERK co-occurring with SWA is also observed during medetomidine-induced anesthesia (Kohtala et al., 2019a). Future studies should elucidate the mechanisms behind these phenomena and their significance to plasticity as well as antidepressant effects.

Pretreatment with selective AMPAR antagonist NBQX did not have an effect on N_2O-induced increases in pTrkB^{Y816}, pGSK3β^{S9} and pP70S6K$^{T421/S424}$ levels. This finding indicates that AMPAR activation is not required for these N_2O-induced effects, and thus they do not appear to be triggered by AMPAR activation. By contrast, NBQX pretreatment decreased the magnitude of N_2O-induced downregulation of GAPDH-normalized pERK. This could be interpreted to reflect attenuated AMPAR-mediated upregulation of pERK during the acute effects of N_2O. Indeed, ERK can be activated by AMPAR stimulation (Mao et al., 2004; Tian and Feig, 2006). This suggests that AMPARs may play a role in N_2O-induced ERK regulation. However, the difference in pERK between saline and NBQX-pretreated groups was not significant, and interpretation of the result is hindered by the lack of control group

receiving NBQX alone. Hence, this finding needs confirmation in subsequent experiments, that should also study brain samples taken during acute effects N_2O and associated pERK upregulation. Limitation of the present study is that we used one, fixed NBQX dose level. Effects of NBQX at other dose levels should also be investigated in the future. Pharmacokinetic studies measuring brain concentrations of NBQX at different times after the injection would help in determining the optimal dosing and timing of its administration prior to NMDAR blocker.

Li et al. (2010) demonstrated that the same NBQX dose that was used in this study blocked ketamine-induced antidepressant-like behavioral response and facilitation of ERK, AKT (upstream of GSK3β), mTOR and P70S6K phosphorylation in the PFC. Thus, it has been inferred that AMPAR activation is required to launch the entire cascade of molecular signaling events deemed essential for ketamine's antidepressant effects. This contrasts with our present findings that NBQX did not affect N_2O-induced facilitation of pTrkB, pGSK3β or pP70S6K, although did have an effect on pERK. Different NMDAR binding properties of N_2O and ketamine could underlie the observed difference on their AMPAR dependency. At resting membrane potential, NMDARs are blocked by endogenous Mg^{2+} ions. To permit ion flow through NMDARs upon agonist binding, Mg^{2+} block must be removed by depolarization, which is mainly achieved through AMPAR activation. Ketamine is a use-dependent blocker that binds to NMDAR channel pore, which is only accessible when NMDAR channel is open and the Mg^{2+} block removed (Johnson et al., 2015). High level of AMPAR blockade might reduce excitation in neurons to the extent that the threshold level of depolarization needed to relieve Mg^{2+} block from NMDARs would not be reached, and thus NMDAR activation would be indirectly inhibited by AMPAR antagonist. Indeed, although NBQX is selective for AMPARs in vitro, it reduced NMDAR function in vivo with increasing doses (Mathiesen et al., 1998). Hence, AMPAR blockade could implicitly prevent ketamine's binding to NMDARs. This would be expected to block all the steps in the cascade that NMDAR antagonism would trigger, including those that do not directly depend on AMPAR activation. In order to elucidate this ambiguity, effects of NBQX on NMDAR currents should be studied in the presence of physiological Mg^{2+}, both alone and in combination with ketamine, at concentrations that are relevant to antidepressant studies. In contrast to ketamine, N_2O is a noncompetitive NMDAR antagonist that does not require NMDAR activation to bind (Mennerick et al., 1998). Because NBQX would not be expected to indirectly limit binding of N_2O to NMDARs, it should only block those steps in the cascade that directly require AMPAR activation, which makes N_2O more suitable for studying the role of AMPARs in the mechanism of NMDAR blockers. This study suggests that by regulating ERK, but not TrkB, GSK3β, P70S6K signaling, AMPARs may regulate part of the overall mechanism triggered by NMDAR blockade, and thus be necessary, but not sufficient for antidepressant effects.

BDNF is an endogenous ligand for TrkB. Total PFC tissue levels of *bdnf IV*, the bdnf mRNA that is most dynamically induced by neuronal activity, or BDNF protein, were not altered by N_2O at the time of measuring. Thus, the increase in $pTrkB^{Y816}$ is not associated with change in total BDNF levels. To activate TrkB, BDNF must be released from intracellular storages, which occurs upon neuronal depolarization (Park and Poo, 2013). While exocytosis of BDNF vesicles upon neuronal activation is supposed to be immediate, increased levels of pTrkB are not seen during the acute N_2O-induced excitatory effects, but only after they fade (Kohtala et al., 2019a). Further, we did not observe any attenuation of N_2O-induced increase in pTrkB levels when animals were pretreated with NBQX. Thus, the role of depolarization-dependent BDNF release in the activation of TrkB by N_2O is inconclusive. Upon activation by BDNF, TrkB undergoes phosphorylation within multiple intracellular tyrosine residues, including autophosphorylation sites Y705/6 as well as Y515 and Y816, that act as docking sites for adaptor proteins that set off complex downstream pathways. In this study, we measured TrkB phosphorylation at Y816, which activates PLCγ pathway that has been shown to be particularly important for synaptic plasticity (Minichiello et al., 2002). Interestingly, classical antidepressants increase TrkB phosphorylation at Y816 but leave Y515 unaffected, which has been associated with transactivation of TrkB independently of BDNF (Rantamäki et al., 2007, 2011). TrkB phosphorylation

at Y515 is associated with activation of ERK pathway. We did not measure pTrkB at 515 in this study, but given the uncoupling of ERK and $TrkB^{Y816}$ phosphorylation, independent regulation of Y816 and Y515 by N_2O could be speculated, although pERK is also dynamically regulated by feedback loops and phosphatases downstream of Y515 (Murphy and Blenis, 2006). Notably, phosphorylation of $GSK3\beta^{S9}$ and $P70S6K^{T421/S424}$ is stimulated by AKT pathway that is also activated by Y515. Although GSK3β and P70S6K are regulated with a similar time-profile with TrkB, the causal relationship between these phenomena has not been established. The transactivation mechanism and the role of BDNF in N_2O-induced TrkB activation should be investigated in future studies, for example by using animals with conditional knockout of BDNF gene. Notably, although ketamine has been shown to cause rapid activity-dependent BDNF release in culture (Lepack et al., 2014), and cause rapid increases in BDNF protein levels in the cortex (Autry et al., 2011), studies have failed to see acute increases (30 min after ketamine administration) in TrkB phosphorylation in the cortex (Autry et al., 2011; Kohtala et al., 2019b). It remains to be investigated if ketamine induces TrkB phosphorylation at later time point, coinciding with peak SWA (i.e. 60 min after ketamine administration), similar to N_2O (Kohtala et al., 2019a).

Ketamine causes glutamate release in the PFC, which is explained by its preferential inhibition of NMDARs on inhibitory interneurons, which causes disinhibition of pyramidal neurons and thus their increased excitation (Homayon and Moghaddam, 1997; Moghaddam et al., 2007). Evidence for disinhibitory effects of N_2O is provided by an in vitro study, where N_2O conferred disinhibition on network-driven spike firing in hippocampal circuits (Nagashima et al., 2005). Effects of N_2O on PFC glutamate levels have not been directly studied, but increased excitation and/or glutamatergic neurotransmission is indicated by upregulation of a set of activity-induced IEGs such as *c-fos* (Kohtala et al., 2019a). In the present study, upregulation of *c-fos* did not reach significant level, and *bdnf IV* levels remained unaltered, which could be related to the time point of measuring. Nonetheless, *c-fos* tended to be increased. The trend-level increase in *c-fos* was also observed in the NBQX-pretreated group, and it could be speculated that *c-fos* is induced by some other stimulus than AMPAR activation. Expression of *c-fos* is induced by multiple stimuli, one of the strongest being NMDAR activation (Morgan and Curran, 1991). Importantly, released glutamate could, besides AMPARs, bind to unblocked synaptic NMDARs on pyramidal neurons. Ketamine at antidepressant-relevant doses likely leaves >50% NMDARs unblocked, and N_2O causes only partial (<70%) NMDAR inhibition even at 80% N_2O (Zorumski et al., 2015). As discussed above, it is unclear whether NBQX indirectly elicited any impairing effect on NMDAR-mediated signaling at the dose applied in this study. Activation of synaptic NMDARs initiates many Ca^{2+} -dependent pathways that critically regulate plasticity. The mechanism of N_2O and ketamine could involve an intricate, dose-dependent balance between NMDAR inhibition and activation in different cell types. Furthermore, synaptic and extrasynaptic NMDAR pools in pyramidal neurons can evoke opposite effects (Hardingham and Bading, 2011), and it has been proposed that inhibition of extrasynaptic NMDAR-driven homeostatic brake on synaptic protein synthesis could underlie the synaptogenic or potentiating effects of ketamine (Miller er al., 2014; Autry et al., 2011). Use- and voltage-dependent nature of ketamine's NMDAR binding modifies its selectivity towards different cell populations, NMDAR subtypes and NMDAR pools through its complex dependency on agonist and coagonist presentation, cellular activity (depolarization) levels and local concentrations of endogenous modulators including Mg^{2+} (Kotermanski and Johnson, 2009; Zorumski et al., 2015). By contrast, binding of N_2O to NMDAR is not use-dependent and only weakly voltage-dependent (Mennerick et al., 1998), with unstudied selectivity towards different NMDAR subunits. The different properties of N_2O and ketamine would be expected to lead to different balance between NMDAR inhibition and activation. However, similarities in their effects suggest that the result is comparable.

The mechanisms proposed to underlie the antidepressant effects of ketamine are shown in **Fig 6A**. **Fig 6B** shows a modified NMDAR-dependent hypothesis that we propose based on our studies with N_2O. Most importantly, this version adds a temporal dimension by separating the effects to two phases. First phase represents the acute pharmacological effects, including NMDAR blockade, assumed glutamate

release, activation of AMPARs and ERK signaling, as well as possible stimulation of synaptic NMDARs and its downstream effects. Second phase is seen soon after drug elimination and represents early adaptive response triggered by the acute effects, including TrkB, GSK3β and mTOR signaling with concurrent SWA seen in EEG. Notably, ERK signaling is uncoupled to TrkB activation. The pertinent signaling events during the two phases and the mechanism that links them to each other remains to be investigated. NMDAR blockade in different cell types and receptor pools could contribute to triggering the adaptive response. This study indicates that TrkB (as well as GSK3β and P70S6K) signaling is independent of AMPAR and ERK signaling, which are associated with the acute effects. The role of BDNF on activation of TrkB remains an open question. Further studies are needed to confirm and extend the findings of the present study and to test our speculative hypothesis. Importantly, subsequent experiments should also include female animals. Investigations on time-dependent effects of ketamine would elucidate if our proposed hypothesis also applies to its mechanism, although ketamine's metabolites could influence this course. Overall, N_2O and ketamine may have unique properties that affect their mechanisms, but the outcome seems to be similar because they both have shown antidepressant effects in humans. This makes NMDAR an attractive target for developing new antidepressants.

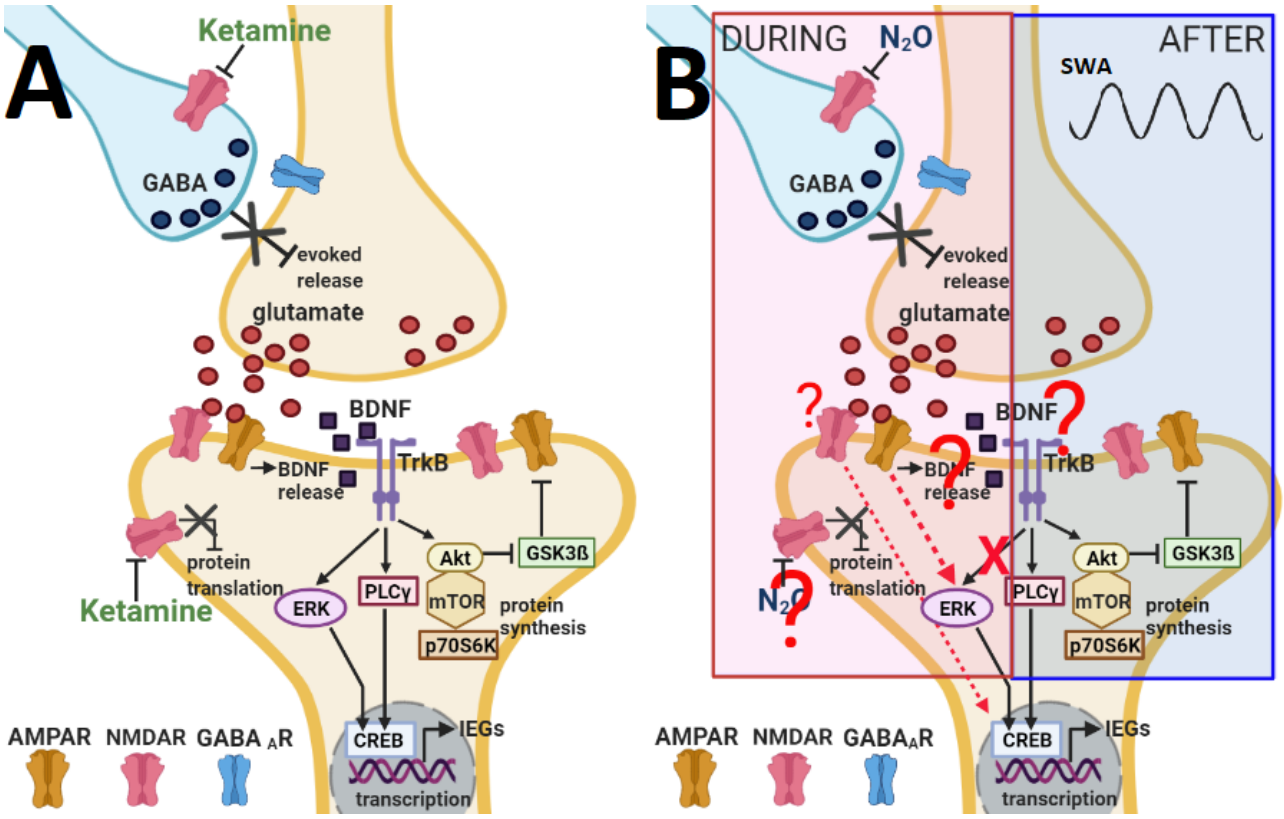

Fig 6. Hypotheses of NMDAR-triggered antidepressant mechanisms. A. Scheme showing NMDAR-dependent hypotheses that have been proposed to explain ketamine's mechanism. Inhibition of NMDARs on GABAergic neurons is hypothesized to cause disinhibition and result in glutamate bursting, which causes BDNF release and activation of TrkB signaling cascades in the postsynaptic cell. In addition, inhibition of extrasynaptic NMDARs in pyramidal neurons is proposed to lead to de-suppression of local protein synthesis. **B.** Our modified NMDAR-dependent hypothesis based on studies with N_2O. Steps in ketamine-based hypotheses that are questioned or proposed to be added and/or revised, are indicated in the scheme with red marks. Importantly, a temporal dimension to the mechanism is added: left side of the synapse picture shows the effects seen during the acute NMDAR blockade, and the right side shows the effects seen after the acute effects have faded, when slow-wave activity (SWA) dominates in electroencephalogram.

In silico screening of ketamine analogs and in vitro experiment with ketamine

The second aim of this study was to find new ketamine-like NMDAR blockers with antidepressant potential. In order to find ketamine analogs, ketamine's structure was taken as a starting point and used to carry out a substructure search. Inherent to this method is that the resulting output compounds will be bigger than the starting molecule, because they will have additional substituents incorporated into the query structure. The increased molecular weight could have pharmacokinetic issues. However, ketamine is a relatively small molecule (molecular weight 238 Da) and thus can be classified as lead-like (200-350 Da) and even fragment-like (120-250 Da) compound (Irwin et al., 2012), making it eligible for a strategy like this. We restricted our search to compounds with molecular weights under 500 Da. Despite this, some compounds with very hydrophobic side chains might present solubility issues, although those with very low predicted water solubility were excluded. All the output compounds were predicted to have a good BBB penetration ability, which is an essential property for drugs whose aimed site of action is central.

All the ketamine analogs we found had a structure where a side chain had been added to ketamine's secondary amine nitrogen via an amide bond. While there are few structure-activity relationship studies on ketamine and other open-channel NMDAR blockers, protonated amine and its hydrogen bonding and/or ionic interactions with the receptor are deemed important (Kroemer et al., 1998). Incorporation of the nitrogen atom, which is part of the secondary amine of ketamine, into a tertiary amide structure in the output compounds abolishes the nitrogen's proton affinity (it does not ionize in physiological pH) as well as hydrogen bond acceptor and donor properties. This would be expected to affect NMDAR affinity. Further, bulky side chains could hinder the binding of compounds to the NMDAR pore, whose size is restricted. Despite these concerns, the most promising analogs obtained better docking scores than ketamine, when they were docked to the same region of the NMDAR. These results are encouraging, but they should be interpreted with caution. Because the NMDAR structure lacked a resolved ligand bound in the pore region, accuracy of our docking procedure could not be validated by self-docking of such ligand to compare the crystallized binding pose to that predicted by docking. Furthermore, although the 4TLM was the best available TMD-containing structure, the pore region was still of relatively low resolution and partially unresolved. Particularly unfortunate was that the residues in the pore loop region of M2 that have been associated with binding of some channel blockers (Kashiwagi et al., 2002) were not resolved in 4TLM. Therefore, detailed inspection of binding poses and interactions of ketamine and the ketamine analogs with the receptor was not conducted. The region where the ketamine analogs were docked was dictated by the best-scoring pose of ketamine. However, the best score was not substantially superior to those of other poses, which brings into question if it represented the real binding site of ketamine. For these reasons, the result of this docking experiment should be interpreted as a rough prediction of the propensity of the compounds to bind NMDAR. Absolute docking scores of the ketamine analogs were not of interest, but instead, relative scores were used to rank the compounds to prioritize the ones with the best score for experimental testing.

The aim of this study was to find compounds with antidepressant potential. Notably, not all NMDAR blockers are antidepressants (Gould et al., 2019). The relationship between different clinical effects and varying pharmacodynamic properties, including NMDAR affinity, binding kinetics, voltage-dependency and trapping, is not clear. As a consequence, these characteristics are not useful in predicting antidepressant effects. Instead, we chose to take an experimental approach where we would measure the ability of the compounds to facilitate BDNF-TrkB and ERK signaling in vitro. These actions have been implicated in rapid antidepressant effects in vivo, and were shown by Lepack et al. (2016) to be regulated by ketamine also in neuronal culture. Our endeavor was to set up a primary cortical neuron culture and use ketamine as a positive control, in order to subsequently test if the ketamine analogs could mimic its effects, with a premise that similar effects in culture would be predictive of antidepressant effects in vivo. However, ketamine did not show any effects in our system. The same concentration of ketamine that provoked BDNF release in the study of Lepack et al. (2016)

did not increase pTrkB^{Y816} levels in the present study. Exogenous BDNF did show a robust effect, and therefore, pTrkB^{Y816} should correlate with BDNF release in our system. Lepack et al. (2016) also reported an increase in pERK levels after ketamine incubation, which was hypothesized to be downstream of TrkB, but notably, could also be stimulated by enhanced glutamatergic activity (Vanhoutte et al., 1999). In the present study, pERK levels were robustly increased after BDNF incubation, but unaltered after ketamine treatment. Various factors in the culture could contribute to the negative results and differences between this and the previous study. The effects of ketamine are hypothesized to be activity-dependent, triggered by inhibition of tonically firing GABAergic neurons. To see such effect in dissociated neuronal culture, spontaneous network activity with proper excitatory and inhibitory neuron function and connections are required. This could be affected by variability in the cultures, that could stem from differences in dissection, plating and culturing. Furthermore, many aspects of ketamine's mechanism, including NMDAR expression and BDNF-TrkB signaling are developmentally regulated. Importantly, GABA is a depolarizing neurotransmitter early in the development, but turns into hyperpolarizing during maturation of neurons in vivo as well as in culture (Ben-Ari et al., 2007). Developmental processes in vitro can be affected by different culturing conditions (Lesuisse and Martin, 2002), and further, we used P0 neurons and stimulated them on DIV14, whereas Lepack et al. (2016) stimulated embryonic day 18 neurons at DIV10. Species-specific factors could also contribute to different results, as we used neurons from mouse, whereas the previous study used rats.

Because the positive control ketamine did not show effects, our experimental system was not applicable to test the ketamine analogs. The experiment should be repeated with possible refinements in the culture, such as using a protocol that is more similar with the one used by Lepack et al. (2016). We stimulated the cells with only single ketamine concentration. However, other concentrations should be tested as well. Although this method could prove to be an ingenious tool to predict in vivo antidepressant effects, ketamine's mechanism is complex, and it may be that it cannot be recapitulated in a dissociated neuronal culture. Particularly, our overarching hypothesis is that TrkB-signaling in intact, mature brain is associated with a brain state characterized by SWA, which occurs only after elimination of ketamine. It remains unexplored if the time-dependent effects and the relationship between BDNF, TrkB and ERK signaling could be studied in the culture, possibly by inclusion of drug washout. Alternative methods to test the ketamine analogs should be sought. Although not directly predictive of antidepressant effects, electrophysiological studies measuring the ability of the compounds to inhibit NMDAR currents should be conducted. However, these experiments could not be performed in this study because of the lack of appropriate facilities. Additional in silico screens could be conducted in the future with different approaches to find more diverse molecules to be tested. The compounds found in this study are limited to commercially available structures with ketamine incorporated in the molecular framework. Ligand-based pharmacophore modeling could be utilized to discover novel compounds that share steric and electrostatic features with known NMDAR blockers but have varying molecular structures. Structure-based in silico methods could substantially aid in discovering novel NMDAR blockers, once NMDAR structures with more completely resolved TMD regions become available.

Conclusions

This study advances understanding of the mechanism of N_2O, which possibly gives new insight of the antidepressant mechanisms of NMDAR blockers more generally. Additionally, we found promising ketamine analogs that await experimental testing.

Acknowledgements

I want to express my gratitude for Tomi Rantamäki and Henri Xhaard for supervising this Master's thesis. I kindly thank Marko Rosenholm for instructing me in lab work, and Loic Dreano for helping me with the in silico experiments.

Supporting information

Supplementary material (Annex 1) includes Figures S1-S2 and Tables S1-S2.

References

Ali F, Gerhard DM, Sweasy K, Pothula S, Pittenger C, Duman RS, et al. Ketamine disinhibits dendrites and enhances calcium signals in prefrontal dendritic spines. Nat Commun 11: 72-019-13809-8, 2020

Antila H, Ryazantseva M, Popova D, Sipilä P, Guirado R, Kohtala S, et al. Isoflurane produces antidepressant effects and induces TrkB signaling in rodents. Sci Rep 7: 7811-017-08166-9, 2017

Autry AE, Adachi M, Nosyreva E, Na ES, Los MF, Cheng PF, et al. NMDA receptor blockade at rest triggers rapid behavioural antidepressant responses. Nature 475: 91-95, 2011

Ben-Ari Y, Gaiarsa JL, Tyzio R, Khazipov R. GABA: a pioneer transmitter that excites immature neurons and generates primitive oscillations. Physiol Rev 87: 1215-1284, 2007

Berman RM, Cappiello A, Anand A, Oren DA, Heninger GR, Charney DS, et al. Antidepressant effects of ketamine in depressed patients. Biol Psychiatry 47: 351-354, 2000

Beurel E, Grieco SF, Amadei C, Downey K, Jope RS. Ketamine-induced inhibition of glycogen synthase kinase-3 contributes to the augmentation of alpha-amino-3-hydroxy-5-methylisoxazole-4-propionic acid (AMPA) receptor signaling. Bipolar Disord 18: 473-480, 2016

Beurel E, Song L, Jope RS. Inhibition of glycogen synthase kinase-3 is necessary for the rapid antidepressant effect of ketamine in mice. Mol Psychiatry 16: 1068-1070, 2011

Bradley CA, Peineau S, Taghibiglou C, Nicolas CS, Whitcomb DJ, Bortolotto ZA, et al. A pivotal role of GSK-3 in synaptic plasticity. Front Mol Neurosci 5: 13, 2012

Di Lieto A, Rantamäki T, Vesa L, Yanpallewar S, Antila H, Lindholm J, et al. The responsiveness of TrkB to BDNF and antidepressant drugs is differentially regulated during mouse development. PLoS One 7: e32869, 2012

Domino EF, Chodoff P, Corssen G. Pharmacologic Effects of Ci-581, a New Dissociative Anesthetic, in Man. Clin Pharmacol Ther 6: 279-291, 1965

Duman RS, Aghajanian GK. Synaptic dysfunction in depression: potential therapeutic targets. Science 338: 68-72, 2012

Friesner RA, Banks JL, Murphy RB, Halgren TA, Klicic JJ, Mainz DT, et al. Glide: a new approach for rapid, accurate docking and scoring. 1. Method and assessment of docking accuracy. J Med Chem 47: 1739-1749, 2004

Fuchikami M, Thomas A, Liu R, Wohleb ES, Land BB, DiLeone RJ, et al. Optogenetic stimulation of infralimbic PFC reproduces ketamine's rapid and sustained antidepressant actions. Proc Natl Acad Sci U S A 112: 8106-8111, 2015

Gerhard DM, Pothula S, Liu RJ, Wu M, Li XY, Girgenti MJ, et al. GABA interneurons are the cellular trigger for ketamine's rapid antidepressant actions. J Clin Invest 130: 1336-1349, 2020

Gould TD, Zarate CA,Jr, Thompson SM. Molecular Pharmacology and Neurobiology of Rapid-Acting Antidepressants. Annu Rev Pharmacol Toxicol 59: 213-236, 2019

Hansen HH, Rantamäki TP, Larsen MH, Woldbye DP, Mikkelsen JD, Castrén EH. Rapid activation of the extracellular signal-regulated kinase 1/2 (ERK1/2) signaling pathway by electroconvulsive shock in the rat prefrontal cortex is not associated with TrkB neurotrophin receptor activation. Cell Mol Neurobiol 27: 585-594, 2007

Hardingham GE, Bading H. Synaptic versus extrasynaptic NMDA receptor signalling: implications for neurodegenerative disorders. Nat Rev Neurosci 11: 682-696, 2010

Hare BD, Shinohara R, Liu RJ, Pothula S, DiLeone RJ, Duman RS. Optogenetic stimulation of medial prefrontal cortex Drd1 neurons produces rapid and long-lasting antidepressant effects. Nat Commun 10: 223-018-08168-9, 2019

Homayoun H, Moghaddam B. NMDA receptor hypofunction produces opposite effects on prefrontal cortex interneurons and pyramidal neurons. J Neurosci 27: 11496-11500, 2007

Irwin JJ, Sterling T, Mysinger MM, Bolstad ES, Coleman RG. ZINC: a free tool to discover chemistry for biology. J Chem Inf Model 52: 1757-1768, 2012

Johnson JW, Glasgow NG, Povysheva NV. Recent insights into the mode of action of memantine and ketamine. Curr Opin Pharmacol 20: 54-63, 2015

Kashiwagi K, Masuko T, Nguyen CD, Kuno T, Tanaka I, Igarashi K, et al. Channel blockers acting at N-methyl-D-aspartate receptors: differential effects of mutations in the vestibule and ion channel pore. Mol Pharmacol 61: 533-545, 2002

Kohtala S, Theilmann W, Rosenholm M, Penna L, Karabulut G, Uusitalo S, et al. Cortical Excitability and Activation of TrkB Signaling During Rebound Slow Oscillations Are Critical for Rapid Antidepressant Responses. Mol Neurobiol 56: 4163-4174, 2019a

Kohtala S, Theilmann W, Rosenholm M, Müller HK, Kiuru P, Wegener G, et al. Ketamine-induced regulation of TrkB-GSK3β signaling is accompanied by slow EEG oscillations and sedation but is independent of hydroxynorketamine metabolites. Neuropharmacology 157: 107684, 2019b

Kohtala S, Theilmann W, Suomi T, Wigren HK, Porkka-Heiskanen T, Elo LL, et al. Brief Isoflurane Anesthesia Produces Prominent Phosphoproteomic Changes in the Adult Mouse Hippocampus. ACS Chem Neurosci 7: 749-756, 2016

Kotermanski SE, Johnson JW. Mg2+ imparts NMDA receptor subtype selectivity to the Alzheimer's drug memantine. J Neurosci 29: 2774-2779, 2009

Kroemer RT, Koutsilieri E, Hecht P, Liedl KR, Riederer P, Kornhuber J. Quantitative analysis of the structural requirements for blockade of the N-methyl-D-aspartate receptor at the phencyclidine binding site. J Med Chem 41: 393-400, 1998

Lee CH, Lu W, Michel JC, Goehring A, Du J, Song X, et al. NMDA receptor structures reveal subunit arrangement and pore architecture. Nature 511: 191-197, 2014

Lepack AE, Bang E, Lee B, Dwyer JM, Duman RS. Fast-acting antidepressants rapidly stimulate ERK signaling and BDNF release in primary neuronal cultures. Neuropharmacology 111: 242-25, 2016

Lepack AE, Fuchikami M, Dwyer JM, Banasr M, Duman RS. BDNF release is required for the behavioral actions of ketamine. Int J Neuropsychopharmacol 18: 10.1093/ijnp/pyu033, 2014

Lesuisse C, Martin LJ. Long-term culture of mouse cortical neurons as a model for neuronal development, aging, and death. J Neurobiol 51: 9-23, 2002

Li N, Lee B, Liu RJ, Banasr M, Dwyer JM, Iwata M, et al. mTOR-dependent synapse formation underlies the rapid antidepressant effects of NMDA antagonists. Science 329: 959-964, 2010

Liu RJ, Lee FS, Li XY, Bambico F, Duman RS, Aghajanian GK. Brain-derived neurotrophic factor Val66Met allele impairs basal and ketamine-stimulated synaptogenesis in prefrontal cortex. Biol Psychiatry 71: 996-1005, 2012

Lowry OH, Rosebrough NJ, Farr AL, Randall RJ. Protein measurement with the Folin phenol reagent. J Biol Chem 193: 265-275, 1951

Maeng S, Zarate CA,Jr, Du J, Schloesser RJ, McCammon J, Chen G, et al. Cellular mechanisms underlying the antidepressant effects of ketamine: role of alpha-amino-3-hydroxy-5-methylisoxazole-4-propionic acid receptors. Biol Psychiatry 63: 349-352, 2008

Mao L, Tang Q, Samdani S, Liu Z, Wang JQ. Regulation of MAPK/ERK phosphorylation via ionotropic glutamate receptors in cultured rat striatal neurons. Eur J Neurosci 19: 1207-1216, 2004

Marcantoni WS, Akoumba BS, Wassef M, Mayrand J, Lai H, Richard-Devantoy S, et al. A systematic review and meta-analysis of the efficacy of intravenous ketamine infusion for treatment resistant depression: January 2009 - January 2019. J Affect Disord 277: 831-841, 2020

Mathiesen C, Varming T, Jensen LH. In vivo and in vitro evaluation of AMPA receptor antagonists in rat hippocampal neurones and cultured mouse cortical neurones. Eur J Pharmacol 353: 159-167, 1998

Mennerick S, Jevtovic-Todorovic V, Todorovic SM, Shen W, Olney JW, Zorumski CF. Effect of nitrous oxide on excitatory and inhibitory synaptic transmission in hippocampal cultures. J Neurosci 18: 9716-9726, 1998

Mikhail C, Vaucher A, Jimenez S, Tafti M. ERK signaling pathway regulates sleep duration through activity-induced gene expression during wakefulness. 10: eaai9219.doi: 10.1126/scisignal.aai9219, 2017

Miller OH, Yang L, Wang CC, Hargroder EA, Zhang Y, Delpire E, et al. GluN2B-containing NMDA receptors regulate depression-like behavior and are critical for the rapid antidepressant actions of ketamine. Elife 3: e03581, 2014

Minichiello L, Calella AM, Medina DL, Bonhoeffer T, Klein R, Korte M. Mechanism of TrkB-mediated hippocampal long-term potentiation. Neuron 36: 121-137, 2002

Moghaddam B, Adams B, Verma A, Daly D. Activation of glutamatergic neurotransmission by ketamine: a novel step in the pathway from NMDA receptor blockade to dopaminergic and cognitive disruptions associated with the prefrontal cortex. J Neurosci 17: 2921-2927, 1997

Morgan JI, Curran T. Stimulus-transcription coupling in the nervous system: involvement of the inducible proto-oncogenes fos and jun. Annu Rev Neurosci 14: 421-451, 1991

Murphy LO, Blenis J. MAPK signal specificity: the right place at the right time. Trends Biochem Sci 31: 268-275, 2006

Nagashima K, Zorumski CF, Izumi Y. Nitrous oxide (laughing gas) facilitates excitability in rat hippocampal slices through gamma-aminobutyric acid A receptor-mediated disinhibition. Anesthesiology 102: 230-234, 2005

Nagele P, Duma A, Kopec M, Gebara MA, Parsoei A, Walker M, et al. Nitrous Oxide for Treatment-Resistant Major Depression: A Proof-of-Concept Trial. Biol Psychiatry 78: 10-18, 2015

Okuno H. Regulation and function of immediate-early genes in the brain: beyond neuronal activity markers. Neurosci Res 69: 175-186, 2011

Park H, Poo MM. Neurotrophin regulation of neural circuit development and function. Nat Rev Neurosci 14: 7-23, 2013

Peltoniemi MA, Hagelberg NM, Olkkola KT, Saari TI. Ketamine: A Review of Clinical Pharmacokinetics and Pharmacodynamics in Anesthesia and Pain Therapy. Clin Pharmacokinet 55: 1059-1077, 2016

Rantamäki T, Hendolin P, Kankaanpää A, Mijatovic J, Piepponen P, Domenici E, et al. Pharmacologically diverse antidepressants rapidly activate brain-derived neurotrophic factor receptor TrkB and induce phospholipase-Cgamma signaling pathways in mouse brain. Neuropsychopharmacology 32: 2152-2162, 2007

Rantamäki T, Kohtala S. Encoding, Consolidation, and Renormalization in Depression: Synaptic Homeostasis, Plasticity, and Sleep Integrate Rapid Antidepressant Effects. Pharmacol Rev 72: 439-465, 2020

Rantamäki T, Vesa L, Antila H, Di Lieto A, Tammela P, Schmitt A, et al. Antidepressant drugs transactivate TrkB neurotrophin receptors in the adult rodent brain independently of BDNF and monoamine transporter blockade. PLoS One 6: e20567, 2011

Reid IC, Stewart CA. Seizures, memory and synaptic plasticity. Seizure 6: 351-359, 1997

Réus GZ, Vieira FG, Abelaira HM, Michels M, Tomaz DB, dos Santos MA, et al. MAPK signaling correlates with the antidepressant effects of ketamine. J Psychiatr Res 55: 15-21, 2014

Sahu MP, Nikkilä O, Lågas S, Kolehmainen S, Castrén E. Culturing primary neurons from rat hippocampus and cortex. Neuronal Signal 3: NS20180207, 2019

Theilmann W, Rosenholm M, Hampel P, Löscher W, Rantamäki T. Lack of antidepressant effects of burst-suppressing isoflurane anesthesia in adult male Wistar outbred rats subjected to chronic mild stress. PLoS One 15: e0235046, 2020

Tian X, Feig LA. Age-dependent participation of Ras-GRF proteins in coupling calcium-permeable AMPA glutamate receptors to Ras/Erk signaling in cortical neurons. J Biol Chem 281: 7578-7582, 2006

Vanhoutte P, Barnier JV, Guibert B, Pagès C, Besson MJ, Hipskind RA, et al. Glutamate induces phosphorylation of Elk-1 and CREB, along with c-fos activation, via an extracellular signal-regulated kinase-dependent pathway in brain slices. Mol Cell Biol 19: 136-146, 1999

Vyazovskiy VV, Olcese U, Lazimy YM, Faraguna U, Esser SK, Williams JC, et al. Cortical firing and sleep homeostasis. Neuron 63: 865-878, 2009

Zanos P, Gould TD. Mechanisms of ketamine action as an antidepressant. Mol Psychiatry 23: 801-811, 2018

Zanos P, Moaddel R, Morris PJ, Georgiou P, Fischell J, Elmer GI, et al. NMDAR inhibition-independent antidepressant actions of ketamine metabolites. Nature 533: 481-486, 2016

Zhou X, Xiao H, Wang H. Developmental changes of TrkB signaling in response to exogenous brain-derived neurotrophic factor in primary cortical neurons. J Neurochem 119: 1205-1216, 2011

Zorumski CF, Nagele P, Mennerick S, Conway CR. Treatment-Resistant Major Depression: Rationale for NMDA Receptors as Targets and Nitrous Oxide as Therapy. Front Psychiatry 6: 172, 2015

ANNEX 1: Supplementary Material

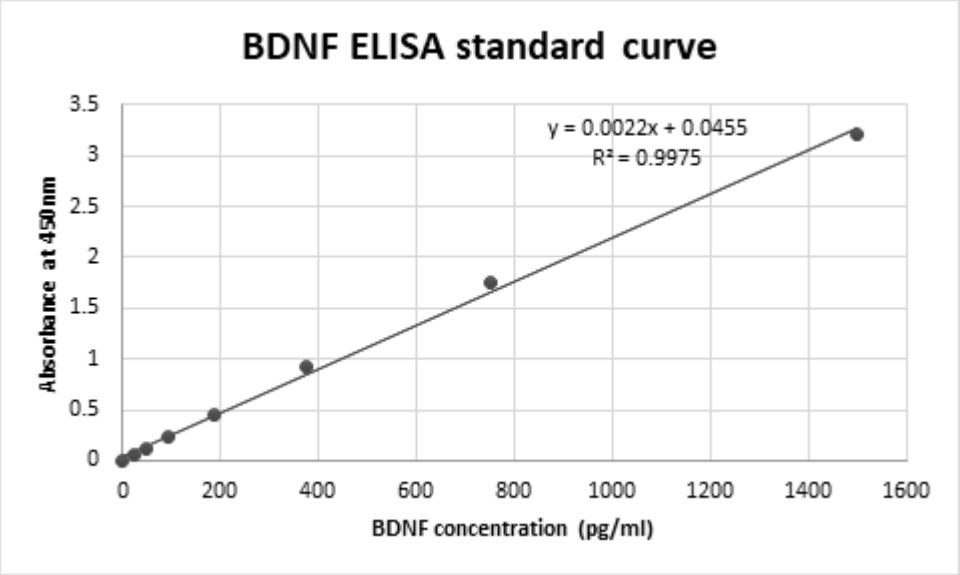

Fig S1. Standard curve for BDNF protein as determined using ELISA. Curve was established for BDNF standard concentrations (eight serially diluted samples ranging 0-1500 pg/ml) and their measured absorbances. The curve was used for calculation of BDNF concentrations present in our samples. Absorbances of all samples fell into the linear range of the standard curve.

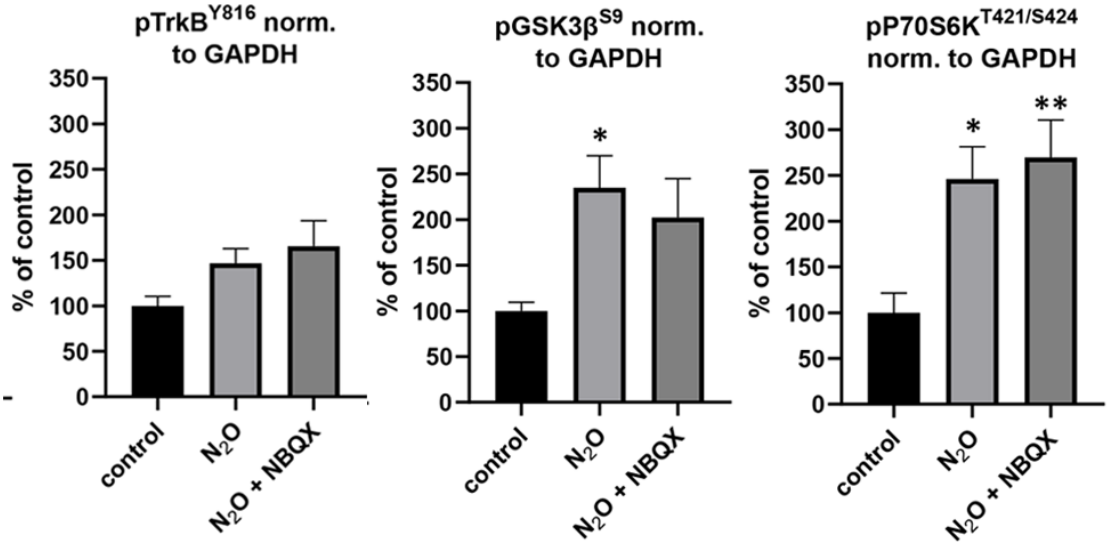

Fig S2. pTrkB, pGSK3b and pP70S6K levels normalized to GAPDH. NBQX pretreatment does not prevent N_2O-induced increases in phosphorylation of TrkB^{Y816}, GSK3β^{S9} and P70S6K$^{T421/S424}$ in the mouse PFC. Phosphorylated proteins are normalized to GAPDH. Representative western blots cropped from complete immunoblots are also shown. Data are means ± S.E.M expressed as percentual change of control value. *≤ 0.05, **≤0.01, ***≤ 0.001 compared to control group (for statistical analyses, p-values and *n* numbers, see Table S1).

Table S1. Primers used for quantitative RT-PCR.

Gene	**Forward primer**	**Reverse primer**
β-actin	GGCTGTATTCCCCTCCATCG	CCAGTTGGTAACAATGCCATGT
Bdnf IV	TGTTTACTTTGACAAGTAGTGACTGAA	ACCGAAGTATGAAATAACCATAGTAAG
c-fos	CGGGTTTCAACGCCGACTA	TTGGCACTAGAGACGGACAGA
Gapdh	GGTGAAGGTCGGTGTGAACGG	CATGTAGTTGAGGTCAATGAAGGG

Table S2. Statistical tests, p-values and n numbers of in vivo and in vitro experiments.

Figure	n	Significance	Statistical test
Figure 2			
pTrkB^{Y816} (normalized to total TrkB)	6, 6, 6	F(2,15) = 3,165, p=0,0713	One-way ANOVA
control vs N_2O		0,3163	Tukey's post hoc
control vs N_2O + NBQX		0,0602	Tukey's post hoc
N_2O vs N_2O + NBQX		0,5924	Tukey's post hoc
pGSK3β^{S9} (normalized to total GSK3β)	6, 6, 6	F(2,15)=9,735, p=0,0019	One-way ANOVA
control vs N_2O		0,0031	Tukey's post hoc
control vs N_2O + NBQX		0,0068	Tukey's post hoc
N_2O vs N_2O + NBQX		0,9216	Tukey's post hoc
pP70S6K$^{T421/S424}$ (normalized to total P70S6K)	5, 5, 6	F(2,13)=12,370, p=0,001	One-way ANOVA
control vs N_2O		0,0051	Tukey's post hoc
control vs N_2O + NBQX		0,0012	Tukey's post hoc
N_2O vs N_2O + NBQX		0,8021	Tukey's post hoc
Figure 3A			
pERK1/2 (normalized to total ERK1/2)	6, 6, 6	F(2,15)=0,928, p=0,4168	One-way ANOVA
control vs N_2O		0,4503	Tukey's post hoc
control vs N_2O + NBQX		0,5215	Tukey's post hoc
N_2O vs N_2O + NBQX		0,9914	Tukey's post hoc
pERK1/2 (normalized to GAPDH)	6, 5, 6	F(2,14)=3,845, p=0,0467	One-way ANOVA
control vs N_2O		0,0374	Tukey's post hoc
control vs N_2O + NBQX		0,3806	Tukey's post hoc
N_2O vs N_2O + NBQX		0,3374	Tukey's post hoc
Figure 3B			
c-fos	6, 6, 5	F(2,14)=2,127, p=0,1561	One-way ANOVA
control vs N_2O		0,5076	Tukey's post hoc
control vs N_2O + NBQX		0,1358	Tukey's post hoc
N_2O vs N_2O + NBQX		0,6072	Tukey's post hoc
Figure 3C			
bdnf IV	6, 6, 5	F(2,14)=0,1407, p=0,8700	One-way ANOVA
control vs N_2O		0,9348	Tukey's post hoc
control vs N_2O + NBQX		0,9817	Tukey's post hoc
N_2O vs N_2O + NBQX		0,8643	Tukey's post hoc
Figure 3D			
BDNF protein levels	6, 6, 6	F(2,15)=0,6723, p=0,5253	One-way ANOVA
control vs N_2O		0,5526	Tukey's post hoc
control vs N_2O + NBQX		0,9919	Tukey's post hoc
N_2O vs N_2O + NBQX		0,6256	Tukey's post hoc
Figure 5B			
pTrkB^{Y816}			
control vs BDNF	6, 6	t(10)=10,014, p<0,0001	Unpaired t-test
pERK1/2			
control vs BDNF	6, 6	t(10)=8.070, p<0,0001	Unpaired t-test
Figure 5C			
pTrkB^{Y816}	6, 6	t(10)=0,3032, p=0,768	Unpaired t-test
control vs KET			
pERK1/2	6, 6	t(10)=0,3107, p=0,7624	Unpaired t-test
control vs KET			
Figure S1			
pTrkB (normalized to GAPDH)	6, 6, 6	F(2,15)=2,983, p=0,0811	One-way ANOVA
control vs N_2O		0,2381	Tukey's post hoc
control vs N_2O + NBQX		0,0764	Tukey's post hoc

N_2O vs N_2O + NBQX		0,7833	Tukey's post hoc
pGSK3B (normalized to GAPDH)	6, 5, 5	F(2,13)=5,688,p=0,0168	One-way ANOVA
control vs N_2O		0,0181	Tukey's post hoc
control vs N_2O + NBQX		0,0742	Tukey's post hoc
N_2O vs N_2O + NBQX		0,7447	Tukey's post hoc
pP70S6K (normalized to GAPDH)	6, 6, 6	F(2,15)=7,479,p=0,0056	One-way ANOVA
control vs N_2O		0,0199	Tukey's post hoc
control vs N_2O + NBQX		0,0074	Tukey's post hoc
N_2O vs N_2O + NBQX		0,8745	Tukey's post hoc

ANNEX 2: PROV-002A Literature review

PROV-002A Literature review

NMDA RECEPTOR BLOCKADE AS A TRIGGER FOR RAPID AND SUSTAINED ANTIDEPRESSANT EFFECTS OF KETAMINE

Iina Annala

University of Helsinki

Faculty of Pharmacy

Division of Pharmacology and Pharmacotherapy

March 2021

TABLE OF CONTENTS

1 INTRODUCTION

Major depressive disorder (MDD) is a highly prevalent and seriously disabling mental health problem that affects 16% of the world population at some point of their lives (Malhi and Mann, 2018). Depression is the leading cause of death of suicide worldwide (Bachmann, 2018). In addition, it has very high societal costs. Estimated economic burden of MDD in Europe was 92 billion euros in the year 2010 (Olesen et al., 2012).

Most MDD patients have multiple depressive episodes during their lifetime (Malhi and Mann, 2018). Major depressive episode is characterized by low mood and/or anhedonia (loss of interest to, or inability to enjoy previously pleasurable activities) that persist for more than 2 weeks and cause functional impairment. Those hallmark symptoms are accompanied with other symptoms, that can be a subset of the following: fatigue, feelings of excessive guilt and/or worthlessness, difficulties to concentrate, change (either increase or decrease) in appetite, psychomotor activity or sleeping patterns and recurrent thoughts of self-harm. Depending on the number of symptoms and the level of impairment they cause, the episode can be categorized as mild, moderate or severe. If a patient has had at least one manic episode in addition to depressive episode, then a diagnosis of bipolar disorder instead of MDD is made.

Treatment of MDD includes pharmacotherapy with antidepressant drugs and psychotherapy, either alone or in combination (Malhi and Mann, 2018). However, the conventional antidepressant drugs that mainly affect monoaminergic (serotonergic, noradrenergic and dopaminergic) neurotransmission, suffer from major drawbacks. They require chronic treatment, and it takes 2-4 weeks on average to see any clinical benefit, which is a significant problem especially considering the high risk of suicide in MDD patients. Furthermore, substantial proportion (50-60%) of patients eventually fail to respond (response is usually defined in clinical contexts as 50% reduction in symptoms) to one or more treatment trials (Fava, 2003). In this case, MDD is classified as treatment resistant depression (TRD). Increasing number of failed antidepressant trials correlates

with poorer prognosis to respond to new treatment trial, and increases the risk for chronic depression.

In patients suffering from severe depression or TRD, electroconvulsive therapy (ECT) can be used, and it is in most cases very effective, with high response rates in TRD population (Payne and Prudic, 2009). In ECT, electric current leading into transient epileptiform activity in the brain is delivered under light anesthesia. In contrast to conventional pharmacotherapy, ECT acts faster, sometimes already after one treatment. However, ECT is unpractical and limited by resources, cognitive side-effects and disrepute among population. Thus, there has been a high unmet need for more effective and rapid-acting treatments.

In the year 2000, Berman et al. made a curious finding that ketamine, an anesthetic agent developed in 1960's, showed robust, rapid and relatively sustained amelioration of core symptoms of depression in TRD population after a single intravenous infusion given at subanesthetic dose (Berman et al., 2000). Since this finding that revolutionized the field of depression studies, ketamine has been a subject of numerous studies. Now, in 2021, there is no doubt of its clinical efficacy, but the neurobiological mechanisms behind ketamine's antidepressant effects are still debated and a topic of this review.

2 MAJOR DEPRESSIVE DISORDER

MDD is associated with disruption of brain circuitries that regulate mood, reward and executive function (Duman, 2014). Many interconnected brain regions have shown structural and functional abnormalities in clinical and preclinical studies. Among the most studied regions are prefrontal cortex (PFC) and hippocampus. Brain imaging studies have revealed decreased volumes of PFC and hippocampus in MDD patients, extent of which correlates to the length and severity of illness. Functional imaging studies have also

shown decreased activity and connectivity in the same regions. Conversely, other regions, such as amygdala, has demonstrated hypertrophy and increased activity. It has been hypothesized that circuit-specific atrophy or hypertrophy and altered reciprocal connections within and between PFC and other regions underlie the unbalanced emotional, cognitive and autonomic functions seen in MDD patients.

Post mortem studies of the brain of MDD patients have found decreases in neuronal cell body size and arborization as well as number of neurons and glial cells in PFC and hippocampus, indicating these alterations as cellular determinants underlying the macroscopic structural changes (Duman, 2014). Ultrastructural studies also indicate reduction in density of synapses. These observations are supported by preclinical findings from stress-based animal models. Animals exposed to chronic stress create a behavioral phenotype that mimics aspects of human MDD phenotype, such as anhedonia (Li et al., 2011). Furthermore, PFC and hippocampus of stressed animals show atrophic changes, that are characterized by decreased dendrite length and branching, decreases in density of spine synapses and loss of neurons and glial cells (Duman, 2014). Because of these similarities to human MDD, stress-based animal models are often used preclinically when studying MDD or antidepressant treatments.

MDD has a complex etiopathogenesis that acts at neurobiological and psychosocial levels (Malhi and Mann, 2018). Stress, especially during early life but also later on, is an important risk factor for MDD. Pathophysiological processes associated with the structural and functional abnormalities seen in depression include overactive hypothalamic-pituitary-adrenal axis, which is a central regulator of stress responses, as well as decreased neurotrophic support (Duman, 2014). Substantial focus has been on brain-derived neurotrophic factor (BDNF), which is a neurotrophic factor that exerts its trophic actions via binding to tropomyosin receptor kinase B (TrkB) receptor (Park and Poo, 2013). BDNF-TrkB signaling is critical for formation of neurons, synapses and neural circuits during development. However, BDNF is also important in more mature brain, as BDNF-TrkB signaling regulates synaptic efficacy and neuronal morphology and plays an important part in activity-dependent synaptic plasticity, especially long-term

potentiation (LTP). Decreased BDNF expression and/or its activity-dependent secretion make mice and humans more vulnerable to effects of stress (Duman and Monteggia, 2006). Lowered levels of BDNF have been observed in the cortex and hippocampus in animal models of stress, as well as in post mortem brain of human MDD patients. However, BDNF levels are increased in some brain regions, including amygdala and nucleus accumbens, whose activity is increased in MDD. Instead of global reduction in BDNF (or other neurotrophic factors) being directly causal to depression, MDD and changes in BDNF levels are associated with impaired neuroplasticity. Environmental as well as genetic risk factors, and disruptions to many physiological systems, including inflammatory, sex steroid or metabolic processes, could contribute to pathophysiology of depression by disrupting different aspects of plasticity on molecular and cellular level (Duman et al., 2016). Conversely, the present view is that antidepressants and other treatments for depression modulate neuroplasticity in an opposite way.

3 KETAMINE

3.1 Pharmacology and pharmacokinetics

Ketamine refers to (R,S)-ketamine, racemic mixture of two enantiomers, (S)- and (R)-ketamine. It is an arylcyclohexylamine that was developed in 1960's as an anesthetic agent derived from phencyclidine (PCP), another anesthetic with a similar core structure (McCarthy et al., 1965). The term "dissociative anesthetics" was coined to differentiate these two as a new class of agents whose actions were different from other known anesthetics (Domino et al., 1965; Corssen and Domino, 1966). Ketamine and PCP both have dose-dependent psychotropic actions, that have been attributed to their ability to act as use-dependent N-methyl-D-aspartate receptor (NMDAR) blockers (Lodge and Mercier, 2015). Ketamine as a less potent NMDAR-blocker is safer than PCP, that has been removed from the market. In addition to NMDARs, other pharmacological targets for ketamine have also been reported, including sigma, opioid, nicotine and

monoaminergic receptors as well as hyperpolarization-activated cyclic nucleotide-gated (HCN) channels (Zanos et al., 2018)

Anesthesia with amnesia occurs at 1-2 mg/kg intravenous bolus of ketamine (Zanos et al., 2018). During ketamine anesthesia, airway tone is preserved and minor elevations in blood pressure and heart rate can occur due to activation of sympathetic nervous system. Ketamine anesthesia is associated with a cataleptic, dissociative state. The patients do not lose consciousness and they appear awake with open eyes and preserved muscle tone, but are detached from the surroundings (Corssen and Domino, 1966). Already at subanesthetic doses, ketamine causes profound analgesia as well as psychotropic effects characterized by sensations of dissociation (altered perception of sensory stimuli, self and time) and schizophrenia-like psychotomimetic effects (such as hallucinations, unusual thought content).

Ketamine's actions start fast and are short-lived. After intravenous administration, it is rapidly distributed and taken up to the brain, after which it is eliminated with a half-life of 2-4 hours in humans (Zanos et al., 2018). Intravenous administration is the most common route used in clinical settings, although intramuscular, intranasal, sublingual and oral (bioavailability 15-29%) administration are also possible. Ketamine is heavily metabolized in the liver. The main enzymes responsible for its metabolism are cytochrome P450 (CYP) enzymes CYP2B6, CYP3A4 and CYP2A6. The major metabolic pathway is through N-demethylation to obtain S- and R-norketamine (NK), which are further hydroxylated on the cyclohexyl ring to obtain various hydroxynorketamine (HNK)-metabolites (primarily 2R,6R;2S,6S-HNK) or oxidized to dehydronorketamine (DHNK).

3.2 Clinical studies of ketamine as an antidepressant

The original, small double-blind study conducted by Berman et al. (2000) showed that a single intravenous 40-minute infusion of ketamine, at sub-anesthetic dose of 0.5 mg/kg relieves core symptoms of depression rapidly and that the effects sustain for days. This finding has subsequently been replicated in many randomized clinical studies with double-blind placebo-controlled or active comparator (midazolam) conditions (Zarate et al., 2006; Murrough et al., 2013). The results are consistent: depressive symptoms are relieved within 2 hours, reaching peak effect within 24 hours and maintaining the effects for a week on average. In addition to MDD patients, ketamine has also shown effect in patients with bipolar depression (Diazgranados et al., 2010a; Zarate et al., 2012) and remarkably, majority of all clinical trials have been conducted on TRD population. In addition to depressive symptoms, ketamine also relieves anhedonia (Lally et al., 2014) and it has been demonstrated to be effective in reducing suicidal ideation (Price et al., 2014; Diazgranados et al., 2010b). Repeated ketamine administration (i.v. administration two or three times a week) appears to maintain the response of those who respond or remit to the initial infusion and is generally well tolerated (Singh et al., 2016a). Although the intravenous route is the most commonly used administration route in antidepressant studies of ketamine, intranasal administration is also shown to be effective (Lapidus et al., 2014). The S-isomer of ketamine (esketamine) is also effective (Singh et al., 2016b; Canuso et al., 2018; Daly et al., 2018), and approved for use in the treatment of TRD as intranasal formulation. R-ketamine (arketamine) has also shown promising rapid and sustained antidepressant effects in an open-label pilot study (Leal et al., 2021).

Because antidepressant effects in clinical studies occur in the same dose-range that acutely causes transient dissociative and psychotomimetic effects, some studied have sought to study the correlations of these two. Some studies have found a correlation with acute dissociative effects (Luckenbaugh et al., 2014) or psychotomimetic (Sos et al., 2013) effects with ketamine's antidepressant efficacy, whereas others have not (Valentine et al., 2011). Thus, it is unknown if diminishing the acute psychotropic side effects could be attempted without compromising the antidepressant efficacy. Anesthetic doses are not considered antidepressive.

The acute dissociative and psychotomimetic effects of ketamine follow its plasma concentrations and thus are short-lasting, but the antidepressant effects of ketamine peak and sustain after ketamine (and its metabolites) have been eliminated from the blood and the brain. Clinical imaging study at the time of ketamine's peak antidepressant effects, 24 hours after administration, studied changes in brain connectivity and their relation to response to ketamine. Abnormal global brain connectivity within PFC observed in the brain of MDD patients was normalized in those who responded to the treatment, but not in non-responders, suggesting that this enhancement of connectivity could contribute to ketamine's efficacy as an antidepressant (Abdallah et al., 2017a).

4 ANTIDEPRESSANT MECHANISM OF KETAMINE

Exhaustive number of preclinical studies in rodents have demonstrated that ketamine at subanesthetic doses exerts antidepressant-like effects. It has been tested in naïve animals as well as many stress-based animal models of depression, using various behavioral tests thought to predict antidepressant-like effects. Interpretation of preclinical results on rodents is, however, hard because many often-used behavioral tests and animal models have poor translational validity. In addition, there is considerable variation in the subanesthetic doses that have been used, ranging from 2,5 mg/kg (Maeng et al., 2008) to 50 mg/kg (Miller et al. 2014). The most common dose in rats and mice seems to be 10 mg/kg via intraperitoneal injection. Estimating the dose that best corresponds to that used in human depression studies is hard, because it would require knowledge of the free drug concentration present in the extracellular space of the brain in humans and animals after administration of different doses (Khlestova et al., 2016). The time profile of the antidepressant-like behavioral responses in rodents is consistent with human studies because the effects emerge rapidly and sustain for days after its elimination (Polis et al., 2019). However, interpretation of the responses 30 min post-administration, which is an often-used time point in assessing rapid behavioral effects, could still be confounded by

pharmacological effects of ketamine and its metabolites, and the associated motor syndrome (hyperlocomotion, stereotypies and ataxia) that subanesthetic ketamine acutely causes (t½ in rodents is ~15 minutes).

Neurobiological studies on ketamine's mechanism of action have focused on its effects on PFC and hippocampus. Preclinical findings support the idea that acute, transient effects of ketamine engage endogenous mechanisms of synaptic plasticity (Gould et al., 2019). Activation of these intrinsic adaptive processes leads to long-lasting changes in the synaptic excitability and connections, which alters function and connections of the brain and is thought to underlie the amelioration of the depressive symptoms. The next chapters discuss what is known about the antidepressant mechanism of ketamine.

4.1 Synaptic potentiation and synaptogenesis

Increase in α-amino-3-hydroxy-5-methyl-4-isoxazolepropionic acid receptors (AMPAR)-mediated excitatory synaptic drive on pyramidal neurons in the PFC is a neurobiological change that is observed after ketamine has been eliminated (Gould et al., 2019). Thus, it is thought that this change underlies the sustained antidepressant-like effects. Consistent with involvement of increased AMPAR-mediated neurotransmission in the sustained effects of ketamine, NBQX, a selective AMPAR-blocker, can occlude ketamine's behavioral effects when it is given just before the forced swim test (FST; measures antidepressant-like response), 24 hours after ketamine (Koike and Chaki, 2014, Zanos et al., 2016). Pyramidal neurons receive excitatory input on their dendritic spines, that act as storage sites of synaptic strength. Generation of new spines (spinogenesis) can grow the number of functional synapses (synaptogenesis) between neurons, and it represents one way to increase excitatory drive. Another way is to regulate the strength of existing synapses, which can be accomplished by altering the number and/or conductance of AMPARs on the postsynaptic membrane. Long-term potentiation (LTP) or depression (LTD) represent mechanisms of synaptic plasticity that increase or decrease, respectively, synaptic strength in response to activity of a given synapse.

Functional synaptic changes are followed by structural alterations. The strength of the synapse correlates with the size and shape of the spine, with “mushroom-shaped” spines representing strong and stable synapses.

Single administration of ketamine (10 mg/kg) increases levels of pre- and postsynaptic proteins such and GluA1, PSD95 (post-synaptic density protein 95) and synapsin I in synaptosomal fractions of medial PFC (mPFC), which is indicative of synaptogenesis (Li et al. 2010). This is followed by increases in number and function of spine synapses in mPFC layer V in naïve animals. After 24 hours, spine density and especially mushroom-shaped spines were increased, accompanied by increased frequency and amplitude of 5-hydroxytryptamine and hypocretin-induced (representing corticocortical and thalamocortical synapses, respectively) excitatory postsynaptic currents (EPSCs) (Li et al. 2010). Similarly, other study found potentiated AMPAR-induced inward currents measured by intracellular recordings of ex vivo mPFC layer V/VI neurons 24 hours after 10 mg/kg ketamine (Björkholm et al., 2015). These ketamine-induced changes are relevant to treatment of MDD, because different stress models induce opposite effects on synaptic protein levels, spine density and synaptic function in the PFC, and a single ketamine injection is able to reverse these effects (Li et al., 2011, Moda-Sava et al., 2019, Dong et al., 2017). Longitudinal *in vivo* imaging of mPFC in awake, behaving animals revealed that ketamine increased spine formation in dendritic branch-specific fashion, partly reversing the stress-induced targeted spine loss, along with generation of *de novo* spines to new positions (Moda-Sava et al., 2019). Ketamine also reversed stress-induced decrease in ensemble function of PFC microcircuits. This reversing effect on functional connectivity as well as the antidepressant-like behavioral effects emerge already after 3 hours, whereas the increase in spine formation after ketamine injection emerges later, indicating that ketamine-induced increases in circuit function occur more rapidly, and the spine formation could be an activity-dependent consequence of this. The spine formation was required for sustained increase in the enhanced circuit function and antidepressant effects. The ketamine-induced spine restoration is transient, because the spines were spontaneously lost, which correlates with the timescale of the transient anti-depressant effects.

There are also signs of rapid ketamine-induced enhancement of AMPAR-mediated transmission in the hippocampus. *In vivo* extracellular electrophysiological recordings in pyramidal neurons of hippocampus CA3 area revealed increased firing activity in response to AMPA stimulation after intraperitoneal administration of subanesthetic ketamine dose (El Iskandrani et al. 2015). Hippocampal expression of AMPAR subunits GluA1 and GluA2 on cell membranes increased rapidly (Zhang et al., 2017; Nosyreva et al., 2013), as well as GluA1 phosphorylation at Ser845, which promotes GluA1 trafficking to membrane and increases conductance of GluA1-containing AMPARs (Zhang et al., 2017). Similarly, ketamine rapidly potentiates AMPAR-mediated field excitatory postsynaptic potentials (fEPSPs) in hippocampal slices (Zhang et al., 2016; Autry et al., 2011; Nosyreva et al., 2013), which was associated with increased GluA1 membrane insertion and phosphorylation of Ser845. Sustained synaptic changes in hippocampus *in vivo* are indicated by increases in synaptic protein levels of GluA1 and GluA2 measured 24 hours after ketamine administration (Zanos et al. 2016).

Corroborating the importance of synaptogenesis and/or potentiation of synapses for antidepressant effects, electroconvulsive shock (ECS), a preclinical correlate of ECT in humans, is associated with synaptic potentiation and rescue of stress-induced morphological changes in dendrites and spines in the cortex and hippocampus (Reid and Stewart, 1997; Maynard et al., 2018; Castrén and Hen, 2013). Traditional antidepressants also induce structural plasticity after chronic use (Castrén and Hen, 2013), although synaptogenic effects appear to be unique to rapid-acting agents (Duman et al., 2016).

4.2 Molecular signaling pathways underlying the synaptic and behavioral effects

4.2.1 Protein synthesis and role of mTORC1 and eEF2K

De novo synthesis of proteins is required for synaptogenesis and long-lasting changes in synaptic strength. Levels of synaptic proteins postsynaptic as well as presynaptic proteins

are increased after subanesthetic ketamine (Li et al., 2010; Zanos et al., 2016). Pretreatment with anisomycin, which inhibits protein translation, blocked the rapid and sustained behavioral effects of ketamine (Autry et al., 2011).

Mammalian target of rapamycin (mTOR) is a serine/threonine protein kinase that assembles to a multi-protein signaling complex mTORC1 (mTOR complex 1) which controls many major functions of the cells, including protein translation in neurons both at the level of soma and locally in dendrites (Hay and Sonenberg, 2004). mTORC1 regulates synthesis of many synaptic proteins by phosphorylating its two major downstream targets, 4E-BP1 and p70S6K, that critically control initiation and elongation phases of protein translation. Subanesthetic ketamine rapidly and transiently increases phosphorylation (activation) of mTOR and its downstream targets 4E-BP1 and p70S6K in PFC synaptosomal fractions (Li et al., 2010; Fukumoto et al., 2019; Carrier et al., 2013; Miller et al., 2014). Blocking mTORC1 activation with intracerebroventricular (ICV) or intra-PFC infusion of rapamycin blocks ketamine-induced sustained behavioral effects as well as increases in synaptic proteins and formation, maturation, and function of new spine synapses, indicating that mTORC1 activation is crucial for ketamine-induced synaptogenesis and antidepressant-like effects (Li et al. 2010; 2011).

Eukaryotic elongation factor 2 (eEF2) is a translation elongation factor important for local protein synthesis and implicated in ketamine's effects in the hippocampus (Sutton et al., 2007; Autry et al., 2011). Activity of eEF2 is regulated by Ca^{2+}/calmodulin-dependent eEF2 kinase (eEF2K; also known as CaMKIII). Phosphorylation of eEF2 at Thr56 by eEF2K renders eEF2 inactive, which suppresses protein synthesis. Ketamine has been shown to rapidly decrease eEF2 phosphorylation in hippocampus (Autry et al., 2011; Zanos et al., 2016; Gideons et al., 2014), which causes de-suppression of protein synthesis. Ketamine does not induce antidepressant-like behavioral effects in eEF2K knockout animals, which indicates that eEF2 is necessary for its effects (Nosyreva et al., 2013).

4.2.2 BDNF-TrkB signaling

BDNF and its receptor TrkB are implicated in antidepressant effects. Ketamine's antidepressant-like effects are not seen in conditional forebrain specific BDNF knockout mice (Autry et al., 2011). Rapid increases in hippocampal BDNF levels (Autry et al., 2011; Gideons et al., 2014; Garcia et al. 2008; Zhou et al., 2013) and activating phosphorylation of TrkB (Autry et al., 2011) has been seen, although others have only seen delayed (24 hours post-administration) increases in BDNF protein levels (Zanos et al., 2016). Some studies have also reported rapid increases in BDNF protein levels in the cortex (Autry et al., 2011; Zhou et al., 2013), although others have not (Zanos et al., 2016). Activity-dependent release of BDNF seems to be crucial for ketamine's effects, because mice with a mutation (Val66Met) that diminishes activity-dependent BDNF release do not show behavioral antisepressant-like responses or increases in spine number or function after ketamine administration, in contrast to wild-type animals (Liu et al., 2012). Indeed, ketamine-induced release of BDNF in mPFC is critical for its actions, because intra-mPFC infusion of BDNF function-blocking antibody abolished its effects (Lepack et al., 2014). Ketamine increased BDNF release *in vitro* in a primary cortical neuron culture (Lepack et al., 2014, 2016). However, TrkB activation has not been seen in the cortex *in vivo* (Autry et al., 2011; Kohtala et al., 2019). Upon activation, TrkB undergoes phosphorylation within specific tyrosine residues located in its intracellular domain, and these act as docking sites for downstream effectors that set forth intracellular cascades such as PI3K-AKT and ERK pathways. Low-dose ketamine increases phosphorylation of ERK1/2 (extracellular signal regulated kinase 1 and 2) as well as AKT (also known as protein kinase B). Pharmacological inhibition of ERK1/2 or AKT phosphorylation abolished ketamine's behavioral effects, as well as ketamine-induced activation of mTOR, p70S6K and 4EBP1 in the PFC (Li et al., 2010), indicating that ERK and AKT signaling are required for ketamine's effects. However, at present, the role of BDNF and TrkB in the mechanism of ketamine remains unknown.

BDNF is also strongly implicated in the effects of classical antidepressants as well as ECT. Chronic, but not acute, administration of conventional antidepressants from

different classes gradually increase expression of BDNF messenger RNA (mRNA) in the hippocampus and PFC (Duman and Monteggia, 2006). Indeed, BDNF-TrkB signaling is both required (antidepressant activity is abolished in BDNF or TrkB knockout animals) and seems to be sufficient (direct intracerebral or intraventricular administration of BDNF or overexpression of TrkB is antidepressive) for antidepressant-like effects in rodents. Chronic use of antidepressants has been associated with normalization of reduced hippocampal BDNF levels in human post mortem studies of MDD patients. Furthermore, ECS increases BDNF mRNA expression more robustly and with faster time course than conventional antidepressants, consistent with its superior efficacy and faster onset of action.

4.2.3 GSK3β

Glycogen synthase kinase-3 (GSK3), which has two isoforms, α and β, is a kinase with high number of substrates. Among its many functions, it has a role in neuroplasticity (Bradley et al., 2011). GSK3β is a constitutively active kinase which promotes AMPAR internalization and LTD, unless it is phosphorylated at its inhibitory residue Ser9. Phosphorylation of GSK3β at Ser9 is induced by LTP-inducing stimuli (Bradley et al., 2011), and by ketamine in PFC and hippocampus (Beurel et al., 2011). Regulation of GSK3β has been demonstrated to be necessary for ketamine's effects, because mice carrying a mutation that blocks phosphorylation of GSK3 isoforms at Ser9 (renders kinase maximally active) do not show antidepressant-like behavioral responses to ketamine (Beurel et al., 2011). In addition, ketamine's rapid increase in synaptosomal membrane levels of GluA1 in hippocampus and PFC required GSK3β Ser9 phosphorylation (Beurel et al., 2016). Similar to ketamine, acute ECS rapidly increases GSK3β Ser9 phosphorylation in the hippocampus and frontal cortex (Basar et al., 2013).

4.3 Cortical excitation and release of glutamate

Acute effects of ketamine on the brain are widespread but region-specific and dependent on the dose. Given the importance of PFC for antidepressant effects as well as higher-level cognitive processes, which are disturbed during acute effects of ketamine, effects of ketamine on this region are of particular interest. Clinically, brain imaging studies have observed that subanesthetic doses of ketamine acutely increase blood flow and metabolic activity in various brain regions, including prefrontal cortex, suggestive of increased neuronal activity (Maltbie et al., 2017; Långsjö et al., 2004; Vollenweider et al., 1997; Breier et al., 1997). Increased glutamate release in the PFC was implicated in a clinical study that measured glutamate-glutamine cycling after ketamine administration by using 13-carbon magnetic resonance spectroscopy (^{13}C-MRS) (Abdallah et al., 2018). These clinical findings are corroborated by preclinical studies that indicate that subanesthetic, in contrast to anesthetic, doses of ketamine cause overall activation of the brain. In rodents, subanesthetic ketamine causes distinct pattern of regional activation of the brain, as shown by neuroanatomically selective increase in [^{14}C]-2-deoxyglucose uptake, including limbic cortical regions such as PFC and anterior cingulate cortex (ACC) (Miyamoto et al., 2000; Duncan et al., 1998). Subanesthetic, but not anesthetic, dose of ketamine acutely increases extracellular glutamate as measured by microdialysis (Moghaddam et al., 1997) and increases glutamate cycling as measured by ex vivo ^{1}H-[^{13}C]-nuclear magnetic resonance spectroscopy, which indicates its increased release (Chowdhury et al., 2017), in the PFC. Expression of immediate-early gene *c-fos*, which is a commonly used biological marker of neuronal activity, is upregulated after ketamine in the mPFC (Duncan et al., 1998; Fuchikami et al., 2015). Recent studies using calcium imaging techniques showed enhanced activity in the mPFC acutely after subanesthetic ketamine (Hare et al., 2020, Ali et al., 2020), which is indicative of increased excitation. High-frequency gamma oscillations on cortical electroencephalography are increased acutely after low-dose ketamine which also indicates altered balance between inhibition and excitation (Zanos et al., 2016). Gamma oscillations are thought to rely on fast excitatory neurotransmission, which is accomplished through AMPARs, because selective AMPAR antagonist NBQX blocks ketamine-induced gamma oscillations. NBQX pretreatment blocked ketamine-induced antidepressant-like behavioral effects of

ketamine, which indicates that activation of AMPARs is important for induction of ketamine's effects (Autry et al. 2011, Zanos et al. 2016, Zhou et al. 2013). NBQX pretreatment also prevented activation of biochemical pathways, including mTOR, ERK and AKT signaling, that have been deemed essential for ketamine's effects in the PFC, indicating that their facilitation by ketamine is activity-dependent (Li et al. 2010). This is supported by finding that NBQX blocked ketamine-induced BDNF release as well as ERK phosphorylation in primary cortical neuron culture (Lepack et al., 2014).

Activation of specific regions, cell types, circuits or projections could be important for triggering the antidepressant actions, whereas others might be irrelevant or contribute to side effects. Neuronal silencing pharmacologically with $GABA_A$ agonist muscimol in infralimbic, but not prelimbic PFC before systemic administration of ketamine in rats occluded its sustained anti-depressant like effects (Fuchikami et al., 2015). Chemogenetic silencing of *Drd1*-expressing subpopulation of PFC pyramidal neurons during ketamine administration blocked ketamine's sustained antidepressant effects (Hare et al., 2019). This was not seen when *Drd2*-expressing subpopulation with different connections was silenced, indicating that activation of specific circuits is necessary for antidepressant effects of ketamine, whereas activation of others is dispensable. Furthermore, the antidepressant-like effects of ketamine were also occluded if only projections from PFC *Drd1*-expressing neurons to basolateral amygdala (BLA) were silenced, indicating that PFC-BLA connections, which play a role in emotional regulation, is important for ketamine's antidepressant effects. Moreover, optogenetic activation of infralimbic cortex (Fuchikami et al., 2015) or mPFC *Drd1* neurons (or only their BLA projections) (Hare et al. 2019) replicated ketamine's antidepressant-like effects, indicating that activation of these regions or circuits seems not only to be necessary, but also sufficient for ketamine's effects.

Increased levels of other neurotransmitters than glutamate have also been detected after ketamine using microdialysis. Subanesthetic ketamine increases extracellular dopamine, serotonin and noradrenaline levels in PFC (Moghaddam et al., 1997; Ago et al., 2019; Tarrés-Gatius et al., 2020). Some of these effects could be secondary to increased

glutamate release, because AMPAR blocker abolished some of the effects. Contribution of these neurotransmitters in triggering the plasticity mechanisms that lead to antidepressant effects is unknown, although role of dopamine and serotonin and activation of their receptors have been implicated by some studies to be necessary for ketamine's sustained antidepressant-like effects (Hare et al., 2019; Fukumoto et al., 2014, 2016, 2018).

Similar to ketamine, ECT (and ECS) is associated with transient, wide-spread activation of the brain. ECS causes cortical depolarization by essentially forcing activity into groups of cortical neurons, that then fire simultaneously and cause propagation of seizure-like activity to other brain regions (Singh and Kar, 2017). This epileptiform activity is associated with increased metabolic activity and release neurotransmitters, including glutamate (Singh and Kar, 2017; Reid and Stewart, 1997). In the case of ECS, the regions of the brain that get activated depend on the site of electrode placement as well as the seizure that is induced as a result of the initial electrical activation (Singh and Kar, 2017). The similarities between acute effects of ECT and ketamine strengthen the view that brain activation is important in inducing rapid plasticity-related actions.

5 NMDAR BLOCKADE AS A MOLECULAR TRIGGER FOR ANTIDEPRESSANT EFFECTS

5.1 Structure, function and properties of NMDARs

NMDAR is a non-selective cation channel that is activated by glutamate, the primary excitatory transmitter of the brain (Traynelis et al., 2010). NMDARs along with AMPA and kainate receptors constitute the ionotropic group of glutamate receptors. Glutamate also signals through eight different metabotropic glutamate receptors (mGluR1-8), that are G-protein coupled receptors.

NMDARs consist of four subunits that together form a central ion channel pore (Traynelis et al. 2010). Seven NMDAR subunits have been identified: one GluN1 subunit with eight splice variants, four GluN2 subunits (2A-D) and two GluN3 subunits (3A-B). For a functional NMDAR, there must be two GluN1 subunits coupled with two GluN2 subunits or one GluN2 and one GluN3 subunit, although the latter combination is less common. NMDAR activation requires binding of glutamate to GluN2 and a coagonist glycine to GluN1. Upon agonist binding, conformational change occurs that opens the channel pore. At resting membrane potential NMDAR channels are blocked by endogenous Mg^{2+} ions, and ion flux through the channel will not occur unless the Mg^{2+} block is removed by cell depolarization. Thus, NMDARs are both ligand- and voltage-gated receptors. The depolarization is usually achieved by activation AMPARs, that typically colocalize in the synapses with NMDARs to form a functional synaptic unit. Upon activation, NMDAR lets Na^{+}, Ca^{2+} and K^{+} flow through the pore. This leads to excitation of the cell, which occurs with slower time scale than that achieved by AMPARs due to slower deactivation kinetics of NMDARs. Importantly, influx of Ca^{2+} activates many plasticity-related intracellular signaling cascades, including LTP and LTD, and as such, NMDAR activation is considered essential for learning and memory. Overactivation of NMDARs in pathophysiological conditions can result in excitotoxicity and neuronal death due to accumulation of Ca^{2+}.

In addition to synaptic NMDARs that can be found from post-synaptic densities, there are also extrasynaptic NMDARs (Traynelis et al., 2010). Extrasynaptic NMDARs usually consist of GluN2B-containing heterotetramers. These receptors are not activated by transient synaptic glutamate release, but instead are tonically activated by ambient glutamate levels that are present in the extracellular space (Miller et al., 2014) and can activate different downstream pathways and have opposite effects when compared to synaptic NMDARs (Hardingham and Bading, 2010). In the cortex, these receptors are involved in maintaining synaptic homeostasis by suppressing protein synthesis through mTOR signaling pathway (Miller et al., 2014). In addition, it has been proposed that there exists a separate population of NMDARs that specifically activate in response to spontaneous quantal glutamate release and take part in homeostatic plasticity by negatively regulating synaptic upregulation by suppressing local protein synthesis

(Atasoy et al., 2008; Sutton et al., 2006). Presynaptic NMDARs and their function is less studied, but they are found from specific axon terminals throughout the brain, including cortex and hippocampus, and are associated with regulation of plasticity (Bouvier et al., 2015).

NMDARs are distributed throughout the brain and expressed in pyramidal neurons as well as inhibitory interneurons (Traynelis et al., 2010) NMDAR subunits have distinct, developmentally regulated distribution patterns. GluN1 as an obligatory subunit is abundant throughout the development in all brain regions. Until early postnatal period, GluN2B is the only GluN2 isoform that is expressed. GluN2A expression peaks later in development and partly replaces GluN2B subunits in synaptic regions. GluN2B containing NMDARs shift to extrasynaptic sites, although they are still also found from synapses in the adult brain. GluN2A and GluN2B-containing NMDARs are the most ubiquitous NMDAR types in the cortex and hippocampus in the adult nervous system. GluN2C- and GluN2D-containing receptors are found in mature brain from thalamus, hippocampus and cortex, and they are especially found from interneurons. GluN3 subunit expression in adult brain is sparse.

Different subunit compositions endow NMDARs with different biophysical properties in terms of open probability, single channel conductance, deactivation kinetics and sensitivity to Mg^{2+}-block (Traynelis et al., 2010). For example, GluN2A-containing NMDARs have high conductance and rapid deactivation kinetics as opposed to GluN2B containing NMDARs, that have lower conductance and slower deactivation. GluN2C and GluN2D containing NMDARs have lower sensitivity to Mg^{2+} block than GluN2A or GluN2B-containing counterparts, which renders their activation less voltage-dependent. NMDARs can be modulated by other endogenous substances as well. Polyamines, neurosteroids, fatty acids, protons and Zn^{2+} ions can allosterically modify NMDAR properties with different efficacy depending on the subunit composition.

5.2 Interaction of ketamine with NMDARs

Ketamine is an uncompetitive NMDAR blocker. Ketamine's binding site resides inside the NMDAR channel pore, in a so-called PCP-binding site (Johnson et al. 2015). Binding of ketamine in occludes current flow through the channel and thus inhibits NMDAR function. Ketamine is an open-channel blocker, which means that it cannot enter or leave the binding site if the channel is closed. Thus, binding of ketamine requires activation of NMDARs, which renders it use-dependent. The channel can close around ketamine while it is bound, which prevents its exit from the channel, leaving it trapped. The degree of trapping a compound exhibits is affected by receptor binding kinetics, so that fast dissociation rate decreases the degree of trapping. Ketamine has fast/moderate binding kinetics and the degree of channels that retain ketamine trapped within is 86% in hyperpolarized membrane potentials (Mealing et al., 1999). As a positively charged molecule, ketamine's NMDAR blockade exhibits voltage dependence: it enters the channel more quickly, leaves it more slowly and inhibits the current flow more effectively when cell's membrane potential is more negative (Johnson et al., 2015). Its voltage-dependency is however modified by Mg^{2+}, which endogenously blocks NMDARs. The binding site of ketamine overlaps with the binding site of endogenous Mg^{2+}, so the Mg^{2+} block, which is also voltage-dependent, must be removed before ketamine can bind. Thus, initial depolarization is needed to relieve Mg^{2+} block and permit ketamine binding.

Ketamine's affinity towards NMDARs consisting of different subunits is similar when measured in the absence of Mg^{2+}, so it is considered non-subunit selective blocker. However, in the presence of Mg^{2+} íons that compete for the binding site, ketamine's half-inhibitory constant (IC50) is increased and subunit selectivity is brought about (Kotermanski and Johnson, 2009). The affinity of Mg^{2+} is lower for GluN1/GluN2C and GluN1/GluN2D containing receptors than for receptors comprised of GluN1/GluN2B or GluN1/GluN2D subunits, which indirectly affects ketamine's relative subtype selectivity, so that IC50 for GluN2C and GluN2D containing NMDARs is lower in the presence of Mg^{2+}. Thus, in physiological conditions, ketamine might have subunit-selective actions if its concentration is low, which might have functional implications.

5.3 Disinhibition hypothesis of ketamine's effects

The initial event that acts as a trigger that sets forth the biochemical cascade that leads to the antidepressant effects that sustain after ketamine's elimination is proposed to be NMDAR blockade. According to disinhibition hypothesis, subanesthetic doses of ketamine preferentially inhibit NMDARs in GABAergic interneurons, that normally inhibit and tune the action of excitatory pyramidal neurons in cortical and hippocampal circuits (Moghaddam et al., 1997; Homayoun and Moghaddam, 2007). Inhibitory interneurons are important in regulating the excitability and synchronic firing of pyramidal neurons. Preventing tonic firing of GABAergic neurons results in decreased inhibitory tone and thus disinhibition of pyramidal neurons, which drives balance towards their increased excitation. This is thought to result in increased firing of pyramidal neurons that release glutamate. It is hypothesized that the released glutamate could then induce activity-dependent plasticity via binding to AMPARs, which would lead to release of BDNF, that could then bind TrkB and activate its downstream cascades (Gould et al., 2019). This would result in mTOR-dependent synthesis of synaptic proteins that are needed for synaptogenesis and LTP-like strengthening of existing synapses. This hypothesis could explain how ketamine can induce glutamate release and activation of the cortex at low doses, although it would expected to decrease excitation because it is a blocker of excitatory glutamate receptor. Inverted U-shaped dose-response in PFC neuronal and metabolic activation (Hare et al., 2020; Duncan et al., 1998), glutamate levels and cycling (Moghaddam et al., 1997; Chowdhury et al., 2017) as well as induction of signaling pathways (Li et al., 2010) could be explained by increasing levels of blockade of postsynaptic NMDARs with increasing doses, which is supposed to counteract the excitatory effect caused by disinhibition.

Evidence for preferential inhibition in inhibitory neurons came originally from studies using another NMDAR blocker, MK-801, which was shown to decrease firing rate of fast-spiking inhibitory neurons while increasing firing rate of regular spiking pyramidal neurons (Homayon and Moghaddam, 2007). Recent studies with ketamine corroborate this finding. Low-dose ketamine decreases the frequency of spontaneous inhibitory post-

synaptic currents (sIPSCs) and increases frequency of spontaneous excitatory postsynaptic currents (eEPSC) in mPFC layer V slices *in vitro*, consistent with selective effect of low-dose ketamine on sIPSCs (Gerhard et al. 2020). In awake mice *in vivo*, low-dose ketamine acutely reduces Ca^{2+}-transients in dendrite-targeting somatostatin (SST)-expressing interneurons in mPFC, and simultaneously increases Ca^{2+}-transients in apical dendrite tuft spines (corresponding to synaptic activation), and somas (indicative of hyperactive firing) of pyramidal cells in the same region, which gives *in vivo* evidence for disinhibitory effects (Ali et al. 2020).

Reduction of excitability of *Gad1*-expressing neurons (GABAergic neurons) in mPFC by knocking down GluN2B selectively in them, resulted in baseline antidepressant effects that occluded ketamine's further antidepressant-like effects, which indicated that inhibition of GABAergic neurons is important for ketamine's antidepressant effects (Gerhard et al., 2020). There are many types of inhibitory GABAergic interneurons, which differ in their electrophysiological properties, synaptic connections, and morphology. They also inhibit different regions of pyramidal neurons, which renders them different functional roles. Although ketamine appears to inhibit many types of interneurons and cause general disinhibition, inhibition of different populations of GABAergic neurons could have differential consequences: disinhibition of discrete populations could result in antidepressant-like effects whereas others could contribute to side effects. Importance of inhibition of SST-expressing interneurons in PFC and subsequent disinhibition of pyramidal cells for triggering antidepressant-like effects was indicated by recent studies. They showed that decreasing the activity of SST neurons in mPFC by knocking down GluN2B specifically in these cells, was associated with ketamine-like disinhibition of PFC pyramidal cells *in vitro* (Gerhard et al., 2020) and *in vivo* (Ali et al., 2020), and the knockdown mice exhibited an antidepressant-like baseline effect in FST (Gerhard et al., 2020). Furhermore, ketamine's FST effects were occluded in these animals, which indicates that GluN2B inhibition in SST interneurons is necessary for triggering ketamine's effects, although it cannot be excluded that SST interneurons are required later, instead of as a triggering event. Knockdown of GluN2A, which was less abundantly expressed by SST neurons, did not result in baseline effect or occlusion of ketamine's antidepressant-like effects, indicating that GluN2B-containing NMDARs

are more important in controlling activity of SST interneurons and that inhibition of GluN2B in these cells is important for ketamine's effects (Gerhard et al., 2020)

.

Another type of GABAergic interneurons are parvalbumin (PV) expressing neurons, that are fast-spiking and inhibit perisomatic regions of pyramidal cells. Knocking down GluN2B receptors from parvalbumin (PV) expressing neurons in mPFC did not result in disinhibition *in vitro* or baseline effects in FST. However, ketamine's antidepressant effects in re-test FST were occluded, and might have a role in its mechanism (Gerhard et al., 2020). Global knockdown of obligatory NMDAR GLuN1 subunit for PV-interneurons did not result in baseline effect on NSF or block ketamine's response (Pozzi et al. 2014). Thus, the role of PV-experessing interneurons for ketamine's antidepressant effects remains elusive.

The reason for preferential inhibition of NMDARs on interneurons versus pyramidal neurons could be that NMDARs play a more important role in the excitation of interneurons than of pyramidal cells (Gould et al., 2019). Interneurons are tonic firing, which could result in more positive membrane potential and hence facilitate ketamine's access to these NMDARs. It could also be that interneurons have different NMDAR subunit composition than pyramidal neurons. GluN2C and GluN2D, which have reduced voltage-dependency, are expressed in interneurons (Monyer et al., 1994) and could render them more susceptible to block by ketamine because of their reduced sensitivity to Mg^{2+} block (Khlestova et al., 2016)

5.4 Other NMDAR-dependent hypotheses of ketamine's effects

Another hypothesis proposed for ketamine's antidepressant effects in the PFC considers that inhibition of extrasynaptic GluN2B-containing NMDARs present on pyramidal neurons would be important for ketamine's antidepressant effects (Miller et al., 2014). It

is proposed that ketamine as a use-dependent blocker preferentially binds to these receptors because they are tonically activated by ambient glutamate. Because of their role in maintaining synaptic homeostasis by suppressing protein synthesis, ketamine is thus supposed to regulate homeostatic synaptic plasticity by de-suppressing protein synthesis, which is suggested to result in global upregulation of synaptic strength and generation of new synapses. Importantly, this hypothesis does not take into account the requirement for activity for ketamine's effects. This hypothesis was strengthened by the finding that mice with cortex-specific GluN2B deletion in pyramidal cells showed a behavioral phenotype, including hyperlocomotion, and synaptic baseline effects that occluded ketamine's antidepressant-associated effects (Miller et al., 2014). However, Gerhard et al. (2020) used viral knock-down of GluN2B receptors in pyramidal cells of PFC, which did not cause any baseline effects on locomotor activity. Ketamine's sustained antidepressant effects were not blocked in these animals, indicating that direct inhibition of GluN2B-containing NMDARs in pyramidal cells of PFC is not sufficient to cause the antidepressant effects.

The effects of ketamine in the hippocampus have been proposed to rely on activation of homeostatic plasticity mechanisms by blocking postsynaptic NMDAR miniature EPSCs (mEPSCs) caused by spontaneous presynaptic glutamate release that occurs tonically without neuronal stimulation. NMDAR mEPSCs regulate dendritic protein synthesis and synaptic strength by suppressing local protein synthesis via activation of eEF2K (Sutton et al., 2006; 2007). Blocking mEPSCs selectively is possible *in vitro* when use-dependent blockers are incubated at rest, i.e. when neuronal firing is prevented (Nosyreva et al., 2013). When NMDAR mEPSCs were selectively inhibited by ketamine in hippocampal slices, decreased phosphorylation of eEF2 was observed, along with increased AMPAR responses, which was dependent on protein synthesis, BDNF and eEF2K. Although this study was conducted in the absence of Mg^{2+} ions, NMDAR mEPSCs have been later shown to be blocked by ketamine also under physiological Mg^{2+} concentration (Gideons et al., 2014). It was concluded that that this eEF2K-dependent rapid translation of BDNF in the hippocampus triggered by inhibition of NMDAR mEPSCs is the determinant of ketamine's antidepressant effects (Autry et al., 2011; Nosyreva et al., 2013). However, major drawback of this hypothesis is that resting conditions used in *in vitro* studies are

not physiological. Another study proposed that ketamine blocks presynaptic NMDARs in the hippocampus area CA3 (Zhang et al., 2017). It was hypothesized that the mechanism would involve NMDAR-dependent downregulation of presynaptic HCN channels, which would lead to facilitation of presynaptic glutamate release and postsynaptic changes in AMPARs (Zhang et al., 2017).

5.4 NMDAR-independent hypotheses of ketamine's effects

Both R- and S-ketamine have exerted sustained and long-lasting antidepressant effects when given separately at subanesthetic doses in various animal models and tests. S-ketamine has four-fold higher affinity to inhibit NMDAR receptors (Zanos et al., 2016) and it is also more potent in inducing anesthesia, psychotomimetic and rewarding effects in preclinical as well as clinical studies, which has been linked to NMDAR inhibition (Zanos et al., 2018; Yang et al., 2015). At doses that are relevant to preclinical antidepressant-like effects, S-ketamine causes activation pattern of PFC and other brain regions which is similar with racemic ketamine and associated with NMDAR inhibition, whereas R-ketamine at equimolar dose does not cause similar brain activation (Hare et al., 2020; Masaki et al., 2019). However, R-ketamine appears to be more potent in inducing antidepressant effects in preclinical studies, and further, to exert longer-lasting effects at equimolar dose (Zanos et al., 2016; Yang et al., 2015, 2017, 2018; Fukumoto et al., 2017). Thus, the NMDAR-dependent antidepressant mechanism of ketamine has been questioned. S- and R-ketamine both have other binding targets as well, with different relative potencies (Zanos et al., 2018), so it has been hypothesized that the trigger for antidepressant effects is not NMDAR, but instead another target, that R-ketamine binds with higher affinity than S-ketamine. However, the more potent antidepressant effects of R-ketamine remain to be confirmed in clinical studies where R- and S-ketamine as well as racemic ketamine would be directly compared. S- and R-ketamine have been shown regulate different intracellular cascades in preclinical studies (Yang et al., 2018), so it is possible that they both exert antidepressant actions but with different mechanisms.

It has also been proposed that the metabolites of ketamine are responsible for its antidepressant properties. Main metabolites of ketamine in human and rodents are 2S,6S-HNK and 2R,6R-HNK that form from S-ketamine and R-ketamine, respectively (Zanos et al., 2018). 2S,6S-HNK and 2R,6R-HNK do not have affinity for NMDARs when used as antidepressant-relevant doses (Zanos et al., 2016; Lumsden et al., 2019). Zanos et al. (2016) proposed that these HNK metabolites are essential for ketamine's sustained antidepressant actions, because chemical modification (deuteration) of ketamine's structure such that formation of 6-hydroxymetabolites *in vivo* was prevented, abolished its antidepressant-like effects 24 hours post-administration. They also showed that 2R,6R-HNK and 2S,6S-HNK exerted sustained antidepressant effects when administered separately to mice. 2R,6R-HNK was demonstrated to be more potent, which was proposed to explain the more potent effects of R-ketamine. Antidepressant effects of 2R,6R-HNK have been replicated by many studies in naïve animals as well as stress-based animal models of depression after systemic (Lumsden et al., 2019; Zanos et al., 2016; Fukumoto et al., 2019) or direct intra-mPFC or ICV (Zanos et al., 2018; Fukumoto et al., 2019) administration, although not all studies have seen effects (Yang et al., 2017; Shirayama et al., 2018; Yokoama et al., 2020). Because the antidepressant effects sustain after 2R,6R-HNK elimination, it is also proposed to cause adaptive synaptic changes, and NMDAR-independently regulate same biochemical pathways as ketamine (Zanos et al. 2016; Fukumoto et al. 2019), although the doses used in these studies is higher than what is achieved *in vivo* after ketamine injection. Regardless of the possible independent effects of R-HNK at higher doses (that remain to be investigated in humans), several studies imply that this metabolite is not necessary for antidepressant effects of R-ketamine. Yamaguchi et al. (2018) used CYP-inhibitors to demonstrate that preventing *in vivo* formation of HNK after R-ketamine administration did not abolish antidepressant actions. In addition, while ketamine is not metabolized in the brain, direct cerebral infusion of R-ketamine showed antidepressant-like effects (Shirayama and Hashimoto, 2017). Subsequently Zanos et al. have argued that while R-ketamine has antidepressant-like effects on its own, 2R,6R-HNK lowers antidepressant potency of R-ketamine and is thus partially responsible for its effects (Zanos et al., 2018). However, clinical studies are not concordant with this, as an inverse relationship has been found between HNK concentrations and antidepressant response (Farmer et al., 2020).

5.5 Antidepressant effects of other NMDAR blockers

Antidepressant properties of other NMDAR antagonists have been investigated in preclinical and clinical studies. Lanicemine (AZD6765) is a non-selective NMDAR open-channel blocker like ketamine, and exhibits similar NMDAR binding properties. It exhibits low affinity, rapid blocking kinetics, strong voltage-dependency and low trapping (Mealing et al., 1997; Mealing et al., 1999). It has been tested in clinical studies in MDD patients, where it demonstrated rapid effects and did not cause psychotomimetic or dissociative side effects, although the response was not as robust or sustained as that of ketamine (Zarate et al., 2013). In a later Phase IIb study, adjunctive repeated-dose lanicemine did not separate from placebo (Sanacora et al., 2017). Memantine, another open-channel NMDAR blocker with similar affinity and blocking kinetics with ketamine did not have effects in clinical studies with chronic oral treatment (Zarate et al. 2006; Smith et al. 2013). High-affinity blocker MK-801 that has very slow blocking and unblocking kinetics has exerted rapid, but not sustained antidepressant effects in animal models (Maeng et al. 2008; Autry et al. 2011; Zanos et al. 2016; Pozzi et al. 2014). Differences in NMDAR binding properties and/or kinetics could explain why these open-channel blockers do not exhibit ketamine-like robust effects.

Nitrous oxide is another NMDAR antagonist that is considered nonselective towards NMDAR subunits (although it has not been directly studied). In contrast to ketamine and other open channel blockers, nitrous oxide is not a use-dependent channel blocker, but a noncompetitive antagonist with little voltage-dependency (Mennerick et al., 1998). A small placebo-controlled pilot study with double-blind crossover design using one-hour inhalation of 50% nitrous oxide showed significantly improved antidepressant response rates in TRD patients when compared to placebo (50 % nitrogen gas over one hour) (Nagele et al., 2015). Significant improvement in symptoms of depression emerged within hours and sustained for at least 24 hours post-treatment, with subset of patients maintaining the response at 1 week post-treatment. Although the study had small number of patients (n=20), this result is encouraging.

Antidepressant potential of GluN2B-selective negative allosteric modulators, also referred to as noncompetitive antagonists in the literature although they do not cause complete block at saturating concentrations (Traynelis et al. 2010), has been studied in preclinical as well clinical studies. Ro25-6981, which is a prototypical GluN2B negative allosteric modulator, has shown rapid and sustained antidepressant effects in rodents, which was blocked by rapamycin (Li et al. 2010) as well NBQX (Maeng et al., 2008). In addition, it increased glutamate cycling (Chowdhury et al., 2017) as well as increased mTOR, ERK, and Akt signaling and levels of synaptic proteins (Li et al., 2010) in the PFC, similar to ketamine. Clinical trial on CP-101,606 (traxoprodil), another GluN2B-selective allosteric modulator showed promising antidepressant results in MDD patients (Preskorn et al., 2008). The response criteria were met in 60% of patients in a group that received traxoprodil infusion, compared to response rate of 20% in placebo group. The antidepressant effects lasted at least one week in 78% of treatment responders, although the onset of action was delayed (5 days). However, its development was stopped because of potential cardiac toxicity due to QTc prolongation (Henter et al., 2018). Clinical studies investigating antidepressant potential of orally administered GluN2B negative allosteric modulator CERC-301 (MK-0657) have failed to show significant effects in primary endpoint measures in MDD patients (Henter et al., 2018).

6 DISCUSSION

Clinical and preclinical studies have found that ketamine's mechanism of action is tied to endogenous plasticity processes. Because of the fast and robust effects of ketamine on structure and function in cortical neurons, it is probable that its NMDAR-dependent actions on glutamatergic system, which is the major neurotransmitter system in the brain, underlies these effects. NMDARs are associated with many forms of synaptic plasticity in different brain regions, including LTP, LTD and homeostatic plasticity. Ketamine is a use- and voltage-dependent NMDAR blocker, and it will bind to any open NMDAR

channels that have their Mg^{2+} block removed, regardless if they are present in pyramidal neurons or interneurons, or at presynaptic, postsynaptic, or extrasynaptic regions. Although ketamine is not intrinsically selective to any particular NMDAR type, its selectivity towards different cell populations, NMDAR subtypes and NMDAR pools is brought about through its complex dependency on agonist and coagonist presentation, cellular activity levels, frequency of NMDAR stimulation, and local concentrations of endogenous modulators, including Mg^{2+} and other ionic and non-ionic allosteric modulators. Depending on these factors and the free concentration of ketamine present in the extracellular space of the brain, some kind of balance between blockade of these different NMDARs throughout the brain is established, resulting in downstream effects that depend on the identity and functional role of the blocked NMDARs. Furthermore, ketamine causes glutamate release that could *activate* unblocked synaptic NMDARs, which could be very important for inducing plasticity-related changes. The interplay between inhibition and activation of NMDARs is likely complex, again stemming from the use- and voltage-dependent as well as trapping nature of ketamine's NMDAR blockade.

Disinhibition hypothesis considers preclinically and clinically demonstrated acute neuronal and metabolic activation as an essential aspect of the antidepressant mechanism. ECT is also associated with similar wide-spread activation of the brain, which underscores this as an important step for rapid antidepressant effects. Importantly, although ketamine-induced disinhibition and subsequent glutamate release might be widespread and general, disinhibition of distinct cell populations and/or activation of distinct circuits by inhibiting different inhibitory interneurons could have different consequences. The ketamine-induced glutamate release may cause secondary effects on other neurotransmitter systems, such as stimulate monoaminergic pathways, with the resultant activation of their respective receptors in their projection regions. These effects might modify the plastic changes in network function. Binding of ketamine enantiomers and metabolites to other targets than NMDARs with varying affinities might contribute to ketamine's effects depending on ketamine dose and extent of metabolism. Some of these wide-spread effects might be relevant to rapid and sustained antidepressant effects, whereas others might be related to side effects. Dissection of ketamine's mechanisms

could inform if some side effects of ketamine could be controlled without compromising the antidepressant efficacy, and if new, even more effective rapid-acting antidepressants devoid of psychotomimetic or dissociative effects could be developed.

Other NMDAR blockers or antagonists have not proven to exhibit ketamine-like robust, rapid and sustained antidepressant effects. This could be related to differences in NMDAR blocking characteristics. Although open channel blockers like memantine and lanicemine have roughly similar binding properties with ketamine, slight differences in binding kinetics, voltage-dependency and trapping could result in different balance between inhibition and activation of NMDARs on different cell types and/or receptor pools, which would result in different outcome. Because this is highly dependent on dose, more rigorous studies on dose-dependency of the effects should be conducted. Curiously, nitrous oxide, which is not an open-channel blocker, has shown very promising antidepressant effects. It is also notable that ketamine and nitrous oxide are both dissociative anesthetics depending on dose (although surgical anesthesia is not possible to achieve with nitrous oxide alone in normobaric conditions), whereas memantine, which does not show antidepressant effects, is not an anesthetic and instead used for treatment of Alzheimer's disease. This demonstrates how NMDAR antagonists with different properties can elicit very different clinical effects, although pharmacokinetic differences as well as other pharmacological targets of these agents could also contribute to these differences. GluN2B selective negative allosteric modulators likely result in different overall effects when compared to open channel blockers, but given that GluN2B receptors are implicated in ketamine's antidepressant effects, these agents could have antidepressant actions with improved side-effect profile.

7 REFERENCES

Abdallah CG, Averill LA, Collins KA, Geha P, Schwartz J, Averill C, DeWilde KE, Wong E, Anticevic A, Tang CY, Iosifescu DV, Charney DS, Murrough JW: Ketamine Treatment and

Global Brain Connectivity in Major Depression. Neuropsychopharmacology 42: 1210-1219, 2017

Abdallah CG, De Feyter HM, Averill LA, Jiang L, Averill CL, Chowdhury GMI, Purohit P, de Graaf RA, Esterlis I, Juchem C, Pittman BP, Krystal JH, Rothman DL, Sanacora G, Mason GF: The effects of ketamine on prefrontal glutamate neurotransmission in healthy and depressed subjects. Neuropsychopharmacology 43: 2154-2160, 2018

Ago Y, Tanabe W, Higuchi M, Tsukada S, Tanaka T, Yamaguchi T, Igarashi H, Yokoyama R, Seiriki K, Kasai A, Nakazawa T, Nakagawa S, Hashimoto K, Hashimoto H: (R)-Ketamine Induces a Greater Increase in Prefrontal 5-HT Release Than (S)-Ketamine and Ketamine Metabolites via an AMPA Receptor-Independent Mechanism. Int J Neuropsychopharmacol 22: 665-674, 2019

Ali F, Gerhard DM, Sweasy K, Pothula S, Pittenger C, Duman RS, Kwan AC: Ketamine disinhibits dendrites and enhances calcium signals in prefrontal dendritic spines. Nat Commun 11: 72-019-13809-8, 2020

Atasoy D, Ertunc M, Moulder KL, Blackwell J, Chung C, Su J, Kavalali ET: Spontaneous and evoked glutamate release activates two populations of NMDA receptors with limited overlap. J Neurosci 28: 10151-10166, 2008

Autry AE, Adachi M, Nosyreva E, Na ES, Los MF, Cheng PF, Kavalali ET, Monteggia LM: NMDA receptor blockade at rest triggers rapid behavioural antidepressant responses. Nature 475: 91-95, 2011

Bachmann S: Epidemiology of Suicide and the Psychiatric Perspective. Int J Environ Res Public Health 15: 1425; doi:10.3390/ijerph15071425, 2018

Basar K, Eren-Kocak E, Ozdemir H, Ertugrul A: Effects of acute and chronic electroconvulsive shocks on glycogen synthase kinase 3β level and phosphorylation in mice. J ECT 29: 265-270, 2013

Berman RM, Cappiello A, Anand A, Oren DA, Heninger GR, Charney DS, Krystal JH: Antidepressant effects of ketamine in depressed patients. Biol Psychiatry 47: 351-354, 2000

Beurel E, Grieco SF, Amadei C, Downey K, Jope RS: Ketamine-induced inhibition of glycogen synthase kinase-3 contributes to the augmentation of alpha-amino-3-hydroxy-5-methylisoxazole-4-propionic acid (AMPA) receptor signaling. Bipolar Disord 18: 473-480, 2016

Beurel E, Song L, Jope RS: Inhibition of glycogen synthase kinase-3 is necessary for the rapid antidepressant effect of ketamine in mice. Mol Psychiatry 16: 1068-1070, 2011

Bjorkholm C, Jardemark K, Schilstrom B, Svensson TH: Ketamine-like effects of a combination of olanzapine and fluoxetine on AMPA and NMDA receptor-mediated transmission in the medial prefrontal cortex of the rat. Eur Neuropsychopharmacol 25: 1842-1847, 2015

Bouvier G, Bidoret C, Casado M, Paoletti P: Presynaptic NMDA receptors: Roles and rules. Neuroscience 311: 322-340, 2015

Bradley CA, Peineau S, Taghibiglou C, Nicolas CS, Whitcomb DJ, Bortolotto ZA, Kaang BK, Cho K, Wang YT, Collingridge GL: A pivotal role of GSK-3 in synaptic plasticity. Front Mol Neurosci 5: 13, 2012

Breier A, Malhotra AK, Pinals DA, Weisenfeld NI, Pickar D: Association of ketamine-induced psychosis with focal activation of the prefrontal cortex in healthy volunteers. Am J Psychiatry 154: 805-811, 1997

Canuso CM, Singh JB, Fedgchin M, Alphs L, Lane R, Lim P, Pinter C, Hough D, Sanacora G, Manji H, Drevets WC: Efficacy and Safety of Intranasal Esketamine for the Rapid Reduction of Symptoms of Depression and Suicidality in Patients at Imminent Risk for Suicide: Results of a Double-Blind, Randomized, Placebo-Controlled Study. Am J Psychiatry 175: 620-630, 2018

Carrier N, Kabbaj M: Sex differences in the antidepressant-like effects of ketamine. Neuropharmacology 70: 27-34, 2013

Castrén E, Hen R: Neuronal plasticity and antidepressant actions. Trends Neurosci 36: 259-267, 2013

Chowdhury GM, Zhang J, Thomas M, Banasr M, Ma X, Pittman B, Bristow L, Schaeffer E, Duman RS, Rothman DL, Behar KL, Sanacora G: Transiently increased glutamate cycling in rat PFC is associated with rapid onset of antidepressant-like effects. Mol Psychiatry 22: 120-126, 2017

Corssen G, Domino EF: Dissociative anesthesia: further pharmacologic studies and first clinical experience with the phencyclidine derivative CI-581. Anesth Analg 45: 29-40, 1966

Daly EJ, Singh JB, Fedgchin M, Cooper K, Lim P, Shelton RC, Thase ME, Winokur A, Van Nueten L, Manji H, Drevets WC: Efficacy and Safety of Intranasal Esketamine Adjunctive to Oral Antidepressant Therapy in Treatment-Resistant Depression: A Randomized Clinical Trial. JAMA Psychiatry 75: 139-148, 2018

Diazgranados N, Ibrahim L, Brutsche NE, Newberg A, Kronstein P, Khalife S, Kammerer WA, Quezado Z, Luckenbaugh DA, Salvadore G, Machado-Vieira R, Manji HK, Zarate CA,Jr: A randomized add-on trial of an N-methyl-D-aspartate antagonist in treatment-resistant bipolar depression. Arch Gen Psychiatry 67: 793-802, 2010

DiazGranados N, Ibrahim LA, Brutsche NE, Ameli R, Henter ID, Luckenbaugh DA, Machado-Vieira R, Zarate CA,Jr: Rapid resolution of suicidal ideation after a single infusion of an N-methyl-D-aspartate antagonist in patients with treatment-resistant major depressive disorder. J Clin Psychiatry 71: 1605-1611, 2010

Domino EF, Chodoff P, Corssen G: Pharmacologic Effects of Ci-581, a New Dissociative Anesthetic, in Man. Clin Pharmacol Ther 6: 279-291, 1965

Dong C, Zhang JC, Yao W, Ren Q, Ma M, Yang C, Chaki S, Hashimoto K: Rapid and Sustained Antidepressant Action of the mGlu2/3 Receptor Antagonist MGS0039 in the Social Defeat Stress Model: Comparison with Ketamine. Int J Neuropsychopharmacol 20: 228-236, 2017

Duman RS: Pathophysiology of depression and innovative treatments: remodeling glutamatergic synaptic connections. Dialogues Clin Neurosci 16: 11-27, 2014

Duman RS, Aghajanian GK, Sanacora G, Krystal JH: Synaptic plasticity and depression: new insights from stress and rapid-acting antidepressants. Nat Med 22: 238-249, 2016

Duman RS, Monteggia LM: A neurotrophic model for stress-related mood disorders. Biol Psychiatry 59: 1116-1127, 2006

Duncan GE, Moy SS, Knapp DJ, Mueller RA, Breese GR: Metabolic mapping of the rat brain after subanesthetic doses of ketamine: potential relevance to schizophrenia. Brain Res 787: 181-190, 1998

El Iskandrani KS, Oosterhof CA, El Mansari M, Blier P: Impact of subanesthetic doses of ketamine on AMPA-mediated responses in rats: An in vivo electrophysiological study on monoaminergic and glutamatergic neurons. J Psychopharmacol 29: 792-801, 2015

Espinosa F, Kavalali ET: NMDA receptor activation by spontaneous glutamatergic neurotransmission. J Neurophysiol 101: 2290-2296, 2009

Farmer CA, Gilbert JR, Moaddel R, George J, Adeojo L, Lovett J, Nugent AC, Kadriu B, Yuan P, Gould TD, Park LT, Zarate CA,Jr: Ketamine metabolites, clinical response, and gamma power in a randomized, placebo-controlled, crossover trial for treatment-resistant major depression. Neuropsychopharmacology 45: 1398-1404, 2020

Fava M: Diagnosis and definition of treatment-resistant depression. Biol Psychiatry 53: 649-659, 2003

Fuchikami M, Thomas A, Liu R, Wohleb ES, Land BB, DiLeone RJ, Aghajanian GK, Duman RS: Optogenetic stimulation of infralimbic PFC reproduces ketamine's rapid and sustained antidepressant actions. Proc Natl Acad Sci U S A 112: 8106-8111, 2015

Fukumoto K, Fogaça MV, Liu RJ, Duman C, Kato T, Li XY, Duman RS: Activity-dependent brain-derived neurotrophic factor signaling is required for the antidepressant actions of (2R,6R)-hydroxynorketamine. Proc Natl Acad Sci U S A 116: 297-302, 2019

Fukumoto K, Iijima M, Chaki S: Serotonin-1A receptor stimulation mediates effects of a metabotropic glutamate 2/3 receptor antagonist, 2S-2-amino-2-(1S,2S-2-carboxycycloprop-1-yl)-3-(xanth-9-yl)propanoic acid (LY341495), and an N-methyl-D-aspartate receptor antagonist, ketamine, in the novelty-suppressed feeding test. Psychopharmacology (Berl) 231: 2291-2298, 2014

Fukumoto K, Iijima M, Chaki S: The Antidepressant Effects of an mGlu2/3 Receptor Antagonist and Ketamine Require AMPA Receptor Stimulation in the mPFC and Subsequent Activation of the 5-HT Neurons in the DRN. Neuropsychopharmacology 41: 1046-1056, 2016

Fukumoto K, Toki H, Iijima M, Hashihayata T, Yamaguchi JI, Hashimoto K, Chaki S: Antidepressant Potential of (R)-Ketamine in Rodent Models: Comparison with (S)-Ketamine. J Pharmacol Exp Ther 361: 9-16, 2017

Garcia LS, Comim CM, Valvassori SS, Reus GZ, Barbosa LM, Andreazza AC, Stertz L, Fries GR, Gavioli EC, Kapczinski F, Quevedo J: Acute administration of ketamine induces antidepressant-like effects in the forced swimming test and increases BDNF levels in the rat hippocampus. Prog Neuropsychopharmacol Biol Psychiatry 32: 140-144, 2008

Gerhard DM, Pothula S, Liu RJ, Wu M, Li XY, Girgenti MJ, Taylor SR, Duman CH, Delpire E, Picciotto M, Wohleb ES, Duman RS: GABA interneurons are the cellular trigger for ketamine's rapid antidepressant actions. J Clin Invest 130: 1336-1349, 2020

Gideons ES, Kavalali ET, Monteggia LM: Mechanisms underlying differential effectiveness of memantine and ketamine in rapid antidepressant responses. Proc Natl Acad Sci U S A 111: 8649-8654, 2014

Gould TD, Zarate CA,Jr, Thompson SM: Molecular Pharmacology and Neurobiology of Rapid-Acting Antidepressants. Annu Rev Pharmacol Toxicol 59: 213-236, 2019

Hardingham GE, Bading H: Synaptic versus extrasynaptic NMDA receptor signalling: implications for neurodegenerative disorders. Nat Rev Neurosci 11: 682-696, 2010

Hare BD, Pothula S, DiLeone RJ, Duman RS: Ketamine increases vmPFC activity: Effects of (R)- and (S)-stereoisomers and (2R,6R)-hydroxynorketamine metabolite. Neuropharmacology 166: 107947, 2020

Hare BD, Shinohara R, Liu RJ, Pothula S, DiLeone RJ, Duman RS: Optogenetic stimulation of medial prefrontal cortex Drd1 neurons produces rapid and long-lasting antidepressant effects. Nat Commun 10: 223-018-08168-9, 2019

Hay N, Sonenberg N: Upstream and downstream of mTOR. Genes Dev 18: 1926-1945, 2004

Henter ID, de Sousa RT, Zarate CA,Jr: Glutamatergic Modulators in Depression. Harv Rev Psychiatry 26: 307-319, 2018

Homayoun H, Moghaddam B: NMDA receptor hypofunction produces opposite effects on prefrontal cortex interneurons and pyramidal neurons. J Neurosci 27: 11496-11500, 2007

Johnson JW, Glasgow NG, Povysheva NV: Recent insights into the mode of action of memantine and ketamine. Curr Opin Pharmacol 20: 54-63, 2015

Khlestova E, Johnson JW, Krystal JH, Lisman J: The Role of GluN2C-Containing NMDA Receptors in Ketamine's Psychotogenic Action and in Schizophrenia Models. J Neurosci 36: 11151-11157, 2016

Koike H, Chaki S: Requirement of AMPA receptor stimulation for the sustained antidepressant activity of ketamine and LY341495 during the forced swim test in rats. Behav Brain Res 271: 111-115, 2014

Kotermanski SE, Johnson JW: Mg2+ imparts NMDA receptor subtype selectivity to the Alzheimer's drug memantine. J Neurosci 29: 2774-2779, 2009

Lally N, Nugent AC, Luckenbaugh DA, Ameli R, Roiser JP, Zarate CA: Anti-anhedonic effect of ketamine and its neural correlates in treatment-resistant bipolar depression. Transl Psychiatry 4: e469, 2014

Långsjö JW, Salmi E, Kaisti KK, Aalto S, Hinkka S, Aantaa R, Oikonen V, Viljanen T, Kurki T, Silvanto M, Scheinin H: Effects of subanesthetic ketamine on regional cerebral glucose metabolism in humans. Anesthesiology 100: 1065-1071, 2004

Lapidus KA, Levitch CF, Perez AM, Brallier JW, Parides MK, Soleimani L, Feder A, Iosifescu DV, Charney DS, Murrough JW: A randomized controlled trial of intranasal ketamine in major depressive disorder. Biol Psychiatry 76: 970-976, 2014

Leal GC, Bandeira ID, Correia-Melo FS, Telles M, Mello RP, Vieira F, Lima CS, Jesus-Nunes AP, Guerreiro-Costa LNF, Marback RF, Caliman-Fontes AT, Marques BLS, Bezerra MLO, Dias-Neto AL, Silva SS, Sampaio AS, Sanacora G, Turecki G, Loo C, Lacerda ALT, Quarantini LC: Intravenous arketamine for treatment-resistant depression: open-label pilot study. Eur Arch Psychiatry Clin Neurosci 271: 577-582, 2021

Lepack AE, Bang E, Lee B, Dwyer JM, Duman RS: Fast-acting antidepressants rapidly stimulate ERK signaling and BDNF release in primary neuronal cultures. Neuropharmacology 111: 242-252, 2016

Lepack AE, Fuchikami M, Dwyer JM, Banasr M, Duman RS: BDNF release is required for the behavioral actions of ketamine. Int J Neuropsychopharmacol 18: pyu033. doi: 10.1093/ijnp/pyu033, 2014

Li N, Lee B, Liu RJ, Banasr M, Dwyer JM, Iwata M, Li XY, Aghajanian G, Duman RS: mTOR-dependent synapse formation underlies the rapid antidepressant effects of NMDA antagonists. Science 329: 959-964, 2010

Li N, Liu RJ, Dwyer JM, Banasr M, Lee B, Son H, Li XY, Aghajanian G, Duman RS: Glutamate N-methyl-D-aspartate receptor antagonists rapidly reverse behavioral and synaptic deficits caused by chronic stress exposure. Biol Psychiatry 69: 754-761, 2011

Liu RJ, Lee FS, Li XY, Bambico F, Duman RS, Aghajanian GK: Brain-derived neurotrophic factor Val66Met allele impairs basal and ketamine-stimulated synaptogenesis in prefrontal cortex. Biol Psychiatry 71: 996-1005, 2012

Lodge D, Mercier MS: Ketamine and phencyclidine: the good, the bad and the unexpected. Br J Pharmacol 172: 4254-4276, 2015

Luckenbaugh DA, Niciu MJ, Ionescu DF, Nolan NM, Richards EM, Brutsche NE, Guevara S, Zarate CA: Do the dissociative side effects of ketamine mediate its antidepressant effects? J Affect Disord 159: 56-61, 2014

Lumsden EW, Troppoli TA, Myers SJ, Zanos P, Aracava Y, Kehr J, Lovett J, Kim S, Wang FH, Schmidt S, Jenne CE, Yuan P, Morris PJ, Thomas CJ, Zarate CA,Jr, Moaddel R, Traynelis SF, Pereira EFR, Thompson SM, Albuquerque EX, Gould TD: Antidepressant-relevant concentrations of the ketamine metabolite (2R,6R)-hydroxynorketamine do not block NMDA receptor function. Proc Natl Acad Sci U S A 116: 5160-5169, 2019

Maeng S, Zarate CA,Jr, Du J, Schloesser RJ, McCammon J, Chen G, Manji HK: Cellular mechanisms underlying the antidepressant effects of ketamine: role of alpha-amino-3-hydroxy-5-methylisoxazole-4-propionic acid receptors. Biol Psychiatry 63: 349-352, 2008

Malhi GS, Mann JJ: Depression. Lancet 392: 2299-2312, 2018

Maltbie EA, Kaundinya GS, Howell LL: Ketamine and pharmacological imaging: use of functional magnetic resonance imaging to evaluate mechanisms of action. Behav Pharmacol 28: 610-622, 2017

Masaki Y, Kashiwagi Y, Watabe H, Abe K: (R)- and (S)-ketamine induce differential fMRI responses in conscious rats. Synapse 73: e22126, 2019

Maynard KR, Hobbs JW, Rajpurohit SK, Martinowich K: Electroconvulsive seizures influence dendritic spine morphology and BDNF expression in a neuroendocrine model of depression. Brain Stimul 11: 856-859, 2018

Mccarthy DA, Chen G, Kaump DH, Ensor C: General Anesthetic and Other Pharmacological Properties of 2-(O-Chlorophenyl)-2-Methylamino Cyclohexanone Hcl (Ci-58l). J New Drugs 5: 21-33, 1965

Mealing GA, Lanthorn TH, Murray CL, Small DL, Morley P: Differences in degree of trapping of low-affinity uncompetitive N-methyl-D-aspartic acid receptor antagonists with similar kinetics of block. J Pharmacol Exp Ther 288: 204-210, 1999

Mealing GA, Lanthorn TH, Small DL, Black MA, Laferriere NB, Morley P: Antagonism of N-methyl-D-aspartate-evoked currents in rat cortical cultures by ARL 15896AR. J Pharmacol Exp Ther 281: 376-383, 1997

Mennerick S, Jevtovic-Todorovic V, Todorovic SM, Shen W, Olney JW, Zorumski CF: Effect of nitrous oxide on excitatory and inhibitory synaptic transmission in hippocampal cultures. J Neurosci 18: 9716-9726, 1998

Miller OH, Yang L, Wang CC, Hargroder EA, Zhang Y, Delpire E, Hall BJ: GluN2B-containing NMDA receptors regulate depression-like behavior and are critical for the rapid antidepressant actions of ketamine. Elife 3: e03581, 2014

Miyamoto S, Leipzig JN, Lieberman JA, Duncan GE: Effects of ketamine, MK-801, and amphetamine on regional brain 2-deoxyglucose uptake in freely moving mice. Neuropsychopharmacology 22: 400-412, 2000

Moda-Sava RN, Murdock MH, Parekh PK, Fetcho RN, Huang BS, Huynh TN, Witztum J, Shaver DC, Rosenthal DL, Alway EJ, Lopez K, Meng Y, Nellissen L, Grosenick L, Milner TA, Deisseroth K, Bito H, Kasai H, Liston C: Sustained rescue of prefrontal circuit dysfunction by antidepressant-induced spine formation. Science 364: eaat8078. doi: 10.1126/science.aat8078, 2019

Moghaddam B, Adams B, Verma A, Daly D: Activation of glutamatergic neurotransmission by ketamine: a novel step in the pathway from NMDA receptor blockade to dopaminergic and cognitive disruptions associated with the prefrontal cortex. J Neurosci 17: 2921-2927, 1997

Monyer H, Burnashev N, Laurie DJ, Sakmann B, Seeburg PH. Developmental and regional expression in the rat brain and functional properties of four NMDA receptors. Neuron 12: 529-540, 1994

Murrough JW, Iosifescu DV, Chang LC, Al Jurdi RK, Green CE, Perez AM, Iqbal S, Pillemer S, Foulkes A, Shah A, Charney DS, Mathew SJ: Antidepressant efficacy of ketamine in treatment-resistant major depression: a two-site randomized controlled trial. Am J Psychiatry 170: 1134-1142, 2013

Nagele P, Duma A, Kopec M, Gebara MA, Parsoei A, Walker M, Janski A, Panagopoulos VN, Cristancho P, Miller JP, Zorumski CF, Conway CR: Nitrous Oxide for Treatment-Resistant Major Depression: A Proof-of-Concept Trial. Biol Psychiatry 78: 10-18, 2015

Nosyreva E, Szabla K, Autry AE, Ryazanov AG, Monteggia LM, Kavalali ET: Acute suppression of spontaneous neurotransmission drives synaptic potentiation. J Neurosci 33: 6990-7002, 2013

Olesen J, Gustavsson A, Svensson M, Wittchen HU, Jonsson B, CDBE2010 study group, European Brain Council: The economic cost of brain disorders in Europe. Eur J Neurol 19: 155-162, 2012

Park H, Poo MM: Neurotrophin regulation of neural circuit development and function. Nat Rev Neurosci 14: 7-23, 2013

Polis AJ, Fitzgerald PJ, Hale PJ, Watson BO: Rodent ketamine depression-related research: Finding patterns in a literature of variability. Behav Brain Res 376: 112153, 2019

Pozzi L, Pollak Dorocic I, Wang X, Carlén M, Meletis K: Mice lacking NMDA receptors in parvalbumin neurons display normal depression-related behavior and response to antidepressant action of NMDAR antagonists. PLoS One 9: e83879, 2014

Preskorn SH, Baker B, Kolluri S, Menniti FS, Krams M, Landen JW: An innovative design to establish proof of concept of the antidepressant effects of the NR2B subunit selective N-methyl-D-aspartate antagonist, CP-101,606, in patients with treatment-refractory major depressive disorder. J Clin Psychopharmacol 28: 631-637, 2008

Price RB, Nock MK, Charney DS, Mathew SJ: Effects of intravenous ketamine on explicit and implicit measures of suicidality in treatment-resistant depression. Biol Psychiatry 66: 522-526, 2009

Sanacora G, Johnson MR, Khan A, Atkinson SD, Riesenberg RR, Schronen JP, Burke MA, Zajecka JM, Barra L, Su HL, Posener JA, Bui KH, Quirk MC, Piser TM, Mathew SJ, Pathak S: Adjunctive Lanicemine (AZD6765) in Patients with Major Depressive Disorder and History of Inadequate Response to Antidepressants: A Randomized, Placebo-Controlled Study. Neuropsychopharmacology 42: 844-853, 2017

Sanacora G, Smith MA, Pathak S, Su HL, Boeijinga PH, McCarthy DJ, Quirk MC: Lanicemine: a low-trapping NMDA channel blocker produces sustained antidepressant efficacy with minimal psychotomimetic adverse effects. Mol Psychiatry 19: 978-985, 2014

Shirayama Y, Hashimoto K: Lack of Antidepressant Effects of (2R,6R)-Hydroxynorketamine in a Rat Learned Helplessness Model: Comparison with (R)-Ketamine. Int J Neuropsychopharmacol 21: 84-88, 2018

Singh A, Kar SK: How Electroconvulsive Therapy Works?: Understanding the Neurobiological Mechanisms. Clin Psychopharmacol Neurosci 15: 210-221, 2017

Singh JB, Fedgchin M, Daly E, Xi L, Melman C, De Bruecker G, Tadic A, Sienaert P, Wiegand F, Manji H, Drevets WC, Van Nueten L: Intravenous Esketamine in Adult Treatment-Resistant Depression: A Double-Blind, Double-Randomization, Placebo-Controlled Study. Biol Psychiatry 80: 424-431, 2016

Singh JB, Fedgchin M, Daly EJ, De Boer P, Cooper K, Lim P, Pinter C, Murrough JW, Sanacora G, Shelton RC, Kurian B, Winokur A, Fava M, Manji H, Drevets WC, Van Nueten L: A Double-Blind, Randomized, Placebo-Controlled, Dose-Frequency Study of Intravenous Ketamine in Patients With Treatment-Resistant Depression. Am J Psychiatry 173: 816-826, 2016

Smith EG, Deligiannidis KM, Ulbricht CM, Landolin CS, Patel JK, Rothschild AJ: Antidepressant augmentation using the N-methyl-D-aspartate antagonist memantine: a randomized, double-blind, placebo-controlled trial. J Clin Psychiatry 74: 966-973, 2013

Sos P, Klirova M, Novak T, Kohutova B, Horacek J, Palenicek T: Relationship of ketamine's antidepressant and psychotomimetic effects in unipolar depression. Neuro Endocrinol Lett 34: 287-293, 2013

Sutton MA, Ito HT, Cressy P, Kempf C, Woo JC, Schuman EM: Miniature neurotransmission stabilizes synaptic function via tonic suppression of local dendritic protein synthesis. Cell 125: 785-799, 2006

Sutton MA, Taylor AM, Ito HT, Pham A, Schuman EM: Postsynaptic decoding of neural activity: eEF2 as a biochemical sensor coupling miniature synaptic transmission to local protein synthesis. Neuron 2007, 55: 648-661.

Tarrés-Gatius M, Miquel-Rio L, Campa L, Artigas F, Castañé A: Involvement of NMDA receptors containing the GluN2C subunit in the psychotomimetic and antidepressant-like effects of ketamine. Transl Psychiatry 10: 427-020-01110-y, 2020

Traynelis SF, Wollmuth LP, McBain CJ, Menniti FS, Vance KM, Ogden KK, Hansen KB, Yuan H, Myers SJ, Dingledine R: Glutamate receptor ion channels: structure, regulation, and function. Pharmacol Rev 62: 405-496, 2010

Valentine GW, Mason GF, Gomez R, Fasula M, Watzl J, Pittman B, Krystal JH, Sanacora G: The antidepressant effect of ketamine is not associated with changes in occipital amino acid neurotransmitter content as measured by [(1)H]-MRS. Psychiatry Res 191: 122-127, 2011

Vollenweider FX, Leenders KL, Scharfetter C, Antonini A, Maguire P, Missimer J, Angst J: Metabolic hyperfrontality and psychopathology in the ketamine model of psychosis using positron emission tomography (PET) and [18F]fluorodeoxyglucose (FDG). Eur Neuropsychopharmacol 7: 9-24, 1997

Yamaguchi JI, Toki H, Qu Y, Yang C, Koike H, Hashimoto K, Mizuno-Yasuhira A, Chaki S: (2R,6R)-Hydroxynorketamine is not essential for the antidepressant actions of (R)-ketamine in mice. Neuropsychopharmacology 43: 1900-1907, 2018

Yang C, Qu Y, Abe M, Nozawa D, Chaki S, Hashimoto K: (R)-Ketamine Shows Greater Potency and Longer Lasting Antidepressant Effects Than Its Metabolite (2R,6R)-Hydroxynorketamine. Biol Psychiatry 82: e43-e44, 2017

Yang C, Ren Q, Qu Y, Zhang JC, Ma M, Dong C, Hashimoto K: Mechanistic Target of Rapamycin-Independent Antidepressant Effects of (R)-Ketamine in a Social Defeat Stress Model. Biol Psychiatry 83: 18-28, 2018

Yang C, Shirayama Y, Zhang JC, Ren Q, Yao W, Ma M, Dong C, Hashimoto K: R-ketamine: a rapid-onset and sustained antidepressant without psychotomimetic side effects. Transl Psychiatry 5: e632, 2015

Zanos P, Highland JN, Liu X, Troppoli TA, Georgiou P, Lovett J, Morris PJ, Stewart BW, Thomas CJ, Thompson SM, Moaddel R, Gould TD: (R)-Ketamine exerts antidepressant actions partly via conversion to (2R,6R)-hydroxynorketamine, while causing adverse effects at sub-anaesthetic doses. Br J Pharmacol 176: 2573-2592, 2019

Zanos P, Moaddel R, Morris PJ, Georgiou P, Fischell J, Elmer GI, Alkondon M, Yuan P, Pribut HJ, Singh NS, Dossou KS, Fang Y, Huang XP, Mayo CL, Wainer IW, Albuquerque EX, Thompson SM, Thomas CJ, Zarate CA,Jr, Gould TD: NMDAR inhibition-independent antidepressant actions of ketamine metabolites. Nature 533: 481-486, 2016

Zanos P, Moaddel R, Morris PJ, Riggs LM, Highland JN, Georgiou P, Pereira EFR, Albuquerque EX, Thomas CJ, Zarate CA,Jr, Gould TD: Ketamine and Ketamine Metabolite Pharmacology: Insights into Therapeutic Mechanisms. Pharmacol Rev 70: 621-660, 2018

Zarate CA,Jr, Brutsche NE, Ibrahim L, Franco-Chaves J, Diazgranados N, Cravchik A, Selter J, Marquardt CA, Liberty V, Luckenbaugh DA: Replication of ketamine's antidepressant efficacy in bipolar depression: a randomized controlled add-on trial. Biol Psychiatry 71: 939-946, 2012

Zarate CA,Jr, Mathews D, Ibrahim L, Chaves JF, Marquardt C, Ukoh I, Jolkovsky L, Brutsche NE, Smith MA, Luckenbaugh DA: A randomized trial of a low-trapping nonselective N-methyl-D-aspartate channel blocker in major depression. Biol Psychiatry 74: 257-264, 2013

Zarate CA,Jr, Singh JB, Carlson PJ, Brutsche NE, Ameli R, Luckenbaugh DA, Charney DS, Manji HK: A randomized trial of an N-methyl-D-aspartate antagonist in treatment-resistant major depression. Arch Gen Psychiatry 63: 856-864, 2006

Zarate CA,Jr, Singh JB, Quiroz JA, De Jesus G, Denicoff KK, Luckenbaugh DA, Manji HK, Charney DS: A double-blind, placebo-controlled study of memantine in the treatment of major depression. Am J Psychiatry 163: 153-155, 2006

Zhang K, Xu T, Yuan Z, Wei Z, Yamaki VN, Huang M, Huganir RL, Cai X: Essential roles of AMPA receptor GluA1 phosphorylation and presynaptic HCN channels in fast-acting antidepressant responses of ketamine. Sci Signal 9: ra123, 2016

Zhou W, Wang N, Yang C, Li XM, Zhou ZQ, Yang JJ: Ketamine-induced antidepressant effects are associated with AMPA receptors-mediated upregulation of mTOR and BDNF in rat hippocampus and prefrontal cortex. Eur Psychiatry 29: 419-423, 2014